NASA Contractor Report 191178

An Analysis Code for the Rapid Engineering Estimation of Momentum and Energy Losses (REMEL)

Lawrence J. De Chant
Sverdrup Technology, Inc.
Lewis Research Center Group
Brook Park, Ohio

November 1994

Prepared for
Lewis Research Center
Under Contract NAS3–25266

National Aeronautics and
Space Administration

AN ANALYSIS CODE FOR THE RAPID ENGINEERING ESTIMATION OF MOMENTUM AND ENERGY LOSSES (REMEL)

Lawrence J. De Chant
Sverdrup Technology, Inc.
Lewis Research Center Group
Brook Park, Ohio 44142

SUMMARY

Nonideal behavior (principally viscous and heat transfer losses in aeropropulsion systems at the preliminary design level) has traditionally been modeled by defining efficiency, which is a comparison between actual and isentropic processes, and subsequent specification by empirical or heuristic methods. With the increasing complexity of aeropropulsion system designs, the reliability of these more traditional methods is uncertain. Computational fluid dynamics (CFD) and experimental methods can provide this information but are expensive in terms of human resources, cost, and time. This report discusses an alternative to empirical and CFD methods by applying classical analytical techniques and a simplified flow model to provide rapid engineering estimates of these losses.

This analysis is based on steady, quasi-one-dimensional governing equations including viscous and heat transfer terms (estimated by Reynold's analogy). Closure to these equations is provided by both classical and newly developed analytical integral solutions to compressible, turbulent boundary layer flow. Basic flows modeled after this methodology include flat plate, conical external, and fully developed internal flows. Geometry is modeled by specification of two-dimensional and axisymmetric piecewise linear elements with the resulting nonlinear differential equations system integrated by a Runge-Kutta method. Additionally, boundary layer thickness, profiles, and blockage effects may be estimated for external flow problems. Normal and oblique shocks may also be superimposed for two-dimensional external problems.

A preliminary verification of REMEL has been compared with full Navier-Stokes (FNS) and CFD boundary layer computations for several high-speed inlet and forebody designs. Requiring little computational effort, current methods compare quite well with the more complex method results. Further, the solutions compare very well with simple degenerate and asymptotic results such as Fanno flow, isentropic variable area flow, and a newly developed, combined variable area duct with friction flow solution. These solution comparisons may offer an alternative to traditional and CFD-intense methods for the rapid estimation of viscous and heat transfer losses in aeropropulsion systems.

INTRODUCTION

Preliminary design studies of aeropropulsion systems require a relatively large and complex design space, which consists of parametric representations of the system components, (e.g., geometry, operating conditions, and characteristics for a wide envelope of design and off-design operating conditions). For propulsion cycles within this design space, operation is typically modeled by using a cycle analysis tool such as the Navy/NASA Engine Program (NNEP) (ref. 1), which is based on one-dimensional gas dynamic relationships that offer flexibility and accuracy concerning nonideal multidimensional component behavior of inlets and nozzles. Efficiency factors are defined to represent other nonideal conditions and losses (viscosity, heat transfer, and other entropy production mechanisms), which then necessitate efficiency modeling. For more extensive and technically innovative designs, the traditional approach becomes less viable.

Alternatives to this approach involve the use of experimental models and computational fluid dynamics (CFD) tools to describe the basic flow, thereby quantifying the loss mechanisms. Although experiments are capable of producing the most reliable simulations, they are very expensive and time consuming. Further, a relatively limited range of parameters, such as geometry or operating conditions, may be analyzed at any one time. To a lesser extent, CFD computations have similar limitations. Both experimental measurements and CFD simulations represent both high fidelity and potentially, realistic analyses.

An option to experimental and CFD methods involves trading fidelity for ease of use and computational efficiency. Reported herein is a relatively simple flow model coupled to classical analytical solutions that describe loss mechanisms caused by viscous effects and heat transfer. As required, new models for frictional losses were developed. Although this analysis has inherent limitations, it offers an alternative (within its scope) to other more accurate but expensive techniques. The appendixes provide summarized derivations of the methodology (REMEL).

SYMBOLS

A	cross-sectional area
B	inner law constant, B = 5.5
b	channel width
C_f	skin friction coefficient
C_h	Stanton number
C_p	constant pressure specific heat
C_v	constant volume specific heat
const	constant
D	diameter
Err	error
H	total enthalpy
h	enthalpy, channel height
K	Karman constant = 0.4
k	inner law constant, k = 0.4
M	Mach number
$\dot{m}$	mass flow rate
Pr	Prandtl number
p	static pressure
q	heat flux, (energy/time/area)
$\dot{q}$	heat addition, (energy/mass)
R	ideal gas constant, rad
Re_d	Reynolds number based on diameter

Re_h	Reynolds number based on channel height
Re_x	Reynolds number based on streamwise distance, x
r	recovery factor
S	surface area
T	temperature
T_0	total temperature
u	streamwise velocity
v^*	friction velocity
x	streamwise coordinate
y	cross-stream coordinate
α	effective cone angle
γ	specific heat ratio, C_p/C_v
Δ	difference operator
δ	boundary layer thickness
θ	Karman momentum layer thickness
λ	Darcy friction factor, $\lambda \equiv 4C_f$
μ	absolute viscosity, integrating factor
ν	kinematic viscosity
ξ	integration dummy variable
ρ	density
τ	shear stress
ϕ	cone half angle
ψ	exact differential
ω	empirical constant, viscosity power law (0.67 for air)

Subscripts:

analy	analytically based (closed form), solution/integration
ave	average conditions
aw	adiabatic wall
axi	axisymmetric
dif	diffuser
incomp	incompressible flow
inner	inner diameter (conical annulus)
num	numerical solution/integration
plate	flat plate

rel	relative
s	wall "slip" (turbulent)
sep	separation
stream	streamtube
w	wall condition
2D	two-dimensional (rectangular) cross-section
0	initial streamwise location, or constant value
1,2	streamwise location
∞	free-stream condition

Superscript:

+	law of the wall
*	sonic valve or predictor-corrector level: Euler
**	predictor corrector level: backward Euler
***	predictor corrector level: midpoint rule

ANALYSIS

The goal of this analysis is to develop a simple, efficient modeling methodology while maintaining adequate physics that will estimate loss mechanisms for compressible, turbulent, internal, and external flow fields. These losses include wall-bounded shear stresses and heat transfer effects. Quasi-one-dimensional relationships have been chosen because they provide a relatively simple system of governing equations but are sufficiently powerful to model the interaction between loss mechanisms and bulk flow.

Anderson (ref. 2) notes that it is essentially assumed for this approximation that the flow variables may be described by the streamwise coordinate only. Physically, this assumption demands that rates of streamwise variation be small and shear layers and other cross-stream effects may be modeled by very thin regions. Although this assumption may not be completely satisfied, this level of formulation has historically provided a very powerful tool for first-order flow analysis.

The fundamental conservation equations for this flow (fig. 1) are

$$\frac{d}{dx}(\rho u A) = 0 \tag{1}$$

$$\rho u \frac{du}{dx} + \frac{dp}{dx} = -\frac{\tau_w}{A}\frac{dS}{dx} \tag{2}$$

and

$$\frac{dh}{dx} + u\frac{du}{dx} = \frac{\dot{q}}{A}\frac{dS}{dx} \tag{3}$$

Introducing the relationship where $p = \rho RT$

$$\frac{dp}{dx} = RT\frac{d\rho}{dx} + \rho R\frac{dT}{dx} \tag{4}$$

and the Mach number relationship

$$M^2 = \frac{u^2}{\gamma RT} \quad \text{and} \quad M\frac{dM}{dx} = \frac{u}{\gamma RT}\frac{du}{dx} - \frac{u^2}{2\gamma RT^2}\frac{dT}{dx} \tag{5}$$

Although it is implicit in relationships (1) to (5), the calorically perfect gas assumption is

$$C_p = \frac{\gamma R}{\gamma - 1} \text{ and } C_v = \frac{R}{\gamma - 1} \tag{6}$$

These relationships provide closure for the five unknowns:

$$\rho, u, p, T, M$$

It will be convenient to recast the momentum and energy equation source terms, which must be specified in a more convenient form. The momentum equation

$$C_f \equiv \frac{\tau_w}{\frac{1}{2}\rho u^2} \tag{7}$$

and the energy equation

$$\dot{q} = \gamma RTQ_0 \quad \text{and} \quad Q_0 = \frac{q_w}{\dot{m}\gamma RT} \tag{8}$$

The wall heat flux is computed via Reynold's Analogy (ref. 3):

$$q_w = \rho u C_p(T_{aw} - T_w)\frac{C_f}{2Pr} \quad \text{and} \quad C_h = \frac{C_f}{2Pr^{2/3}} \tag{9}$$

where the Stanton number C_h is introduced. Clearly, the computation of viscous effects and heat transfer will depends on the model chosen for the skin friction coefficient (see appendix B for details).

The estimation of losses caused by viscous interactions is a classical problem of considerable interest (refs. 3 and 4). Classical and recently developed methods characterized by reasonable simplicity and adequate fidelity are available and have been applied in this analysis (refs. 5 to 7).

The skin friction closure analyses consider a relatively diverse set of flows and require identification of a local turbulence closure hypothesis, integration to yield a velocity profile, and introduction of this profile in integral forms of the governing equations. This procedure yields either a differential or an algebraic relationship for the skin friction. A compressible form of Prandtl's mixing length hypothesis is chosen as an initial turbulence closure:

$$\tau_w = \rho_w \frac{\rho}{\rho_w} k^2 y^2 \left(\frac{du}{dy}\right)^2 \tag{10}$$

The density and temperature may be related to the velocity field via the Crocco-Busemman approximate energy integral and state. Integration of relationships (1) to (5) yields Van Driest's effective velocity relationship (ref. 3) which is essentially a compressible law of the wall extension:

$$\frac{u_{ave}}{av^*} \arcsin\left(a \frac{u}{u_{ave}}\right) = \frac{1}{k} \ln y^+ + B \tag{11}$$

where a is defined as

$$a^2 = r \frac{\gamma - 1}{2} M_{ave}^2 \frac{T_{ave}}{T_w} \tag{12}$$

Note that the previous relationships have been derived for adiabatic flow, while in general, analogous relationships may be derived for more general heat-transfer conditions. These profiles may then be substituted into the relevant governing integral equations. For a fully developed flow, these may be as simple as the definition of the average

$$u_{ave} \equiv \frac{2}{R^2} \int_0^R u(y)(R - y)\, dy \tag{13}$$

and may be somewhat more complicated for flat plate flow (Karman momentum integral)

$$\frac{d\theta}{dx} = \frac{C_f}{2} \quad \text{and} \quad \theta = \int_0^\infty \frac{\rho}{\rho_\infty} \frac{u}{u_\infty} \left(1 - \frac{u}{u_\infty}\right) dy \tag{14}$$

Substitution of the previously derived profiles into the integral relationships yields implicit skin friction formulas. Consider, for example, the implicit relationship for fully developed, compressible, turbulent, adiabatic pipe flow

$$\frac{1}{\sqrt{\lambda}} \arcsin \frac{(1 - a^2)^{1/2}}{a} = 2.03 \log \left(Re_d \sqrt{\lambda}\right) - 0.9130 + 1.0176 \log (1 - a^2)(1 + 2\omega) \tag{15}$$

where λ refers to the Darcy friction factor and is related to the skin friction by

$$\lambda \equiv 4C_f \tag{16}$$

Analogous relationships are available for two-dimensional flows, flat plate flows, and conical flows. In summary, these relationships provide a relatively rigorously derived closure to a major source of loss or entropy production in propulsion systems while maintaining adequate simplicity and computational efficiency.

To complete the analysis, the geometrical parameters, cross-sectional area A(x), and surface area S(x) must be specified. A class of geometry specifications that is simple and consistent with the level of analysis is available. Broadly dividing them into axisymmetric and two-dimensional geometry classes, the required relationships for cross-sectional area may be written (fig. 2)

$$\frac{dA_{axi}}{dx} = \frac{\pi}{2} D(x) \frac{dD(x)}{dx} \tag{17}$$

and

$$\frac{dA_{2D}}{dx} = h(x) \frac{db(x)}{dx} + b(x) \frac{dh(x)}{dx} \tag{18}$$

and the surface area

$$\frac{dS_{axi}}{dx} = \pi D(x) \left[1 + \frac{1}{2} \left(\frac{dD(x)}{dx} \right)^2 \right]^{1/2} \tag{19}$$

$$\frac{dS_{2D}}{dx} = 2 \left[h(x) + b(x) \right] \tag{20}$$

Other geometries are available to describe some practical cases; appendix A provides details of an analysis of a conical annulus for which the inner body diameter $D_{inner}(x)$ must be specified. Note that geometrically complex systems may be modeled by employing several of these locally linear sections. Functional continuity limitations caused by the piecewise linear nature of these elements has not presented a significant problem in the flows modeled to this point.

The reduction of the above system to a single nonlinear differential equation is straightforward but tedious. This system reduction is described in detail in appendix C. The resultant differential equation (quoted from ref. 8) is

$$-\frac{C_f}{2} \frac{1}{A} dS = -\frac{1}{\gamma M^2} [1 - M^2] \left[\frac{\frac{\gamma - 1}{2} (Q_0 - M dM)}{1 + \frac{\gamma - 1}{2} M^2} - \frac{1}{\gamma M^2} \frac{dA}{A} + \frac{1}{\gamma M^2} Q_0 \right] \tag{21}$$

where the relationship has been rewritten:

$$Q_0 = \frac{1}{\gamma - 1} \left[1 + \frac{\gamma - 1}{2} M^2 - \frac{T_w}{T} \right] C_h \frac{dS}{A} \tag{22}$$

Equation (21) is not defined for any steady, compressible analysis, where the Mach number is equal to 1. This is a result of the term

$$1 - M^2 \rightarrow 0 \tag{23}$$

thus causing a singular relationship physically representing the transition between subsonic and supersonic flow, and correspondingly, the transition from elliptic to hyperbolic governing equations. The most expedient solution is to formulate and analyze the unsteady hyperbolic problem or possibly to solve the steady, small perturbation, transonic flow problem.

The initial value problem, equation (15), is a complex nonlinear first-order differential equation. Although for special cases it is integrable in closed form (see ref. 9 and appendix D), a general solution requires numerical integration. Place equation (21) in standard form:

$$\frac{dM}{dx} = \left[\frac{C_f}{2}\frac{1}{A}\frac{dS}{dx} - \frac{1}{A\gamma M^2}\frac{dA}{dx} + \frac{1}{\gamma M^2}\left(1 + \frac{\gamma - 1}{2}M^2 - \frac{T_w}{T}\right)\frac{C_h}{A}\frac{dS}{dx}\right]\left[\frac{\gamma M^3\left(1 + \frac{\gamma - 1}{2}M^2\right)}{(1 - M^2)}\right] \qquad (24)$$

$$-\frac{1}{2}M\left(1 + \frac{\gamma - 1}{2}M^2 - \frac{T_w}{T}\right)\frac{C_h}{A}\frac{dS}{dx}$$

This equation may be solved by any applicable integration scheme for initial value problems. It is possible to note a clear singularity at the transonic point, a good choice being the classical fourth-order Runge-Kutta method (ref. 10).

Quantities other than the Mach number are of interest: temperature, velocity, pressure, and total pressure. To obtain these quantities, the related differential equations (appendix C) for temperature and pressure are considered:

$$\frac{dT}{dx} = \frac{T\left(1 + \frac{\gamma - 1}{2}M^2 - \frac{T_w}{T}\right)C_h\frac{1}{A}\frac{dS}{dx} - (\gamma - 1)M\frac{dM}{dx}}{1 + \frac{\gamma - 1}{2}M^2} \qquad (25)$$

and

$$\frac{dp}{dx} = -\gamma M^2 p\left[\frac{1}{2}\frac{C_f}{A}\frac{dS}{dx} + \frac{\frac{1}{2}\left(1 + \frac{\gamma - 1}{2}M^2 - \frac{T_w}{T}\right)C_h\frac{1}{A}\frac{dS}{dx} + \frac{1}{M}\frac{dM}{dx}}{1 + \frac{\gamma - 1}{2}M^2}\right] \qquad (26)$$

With the Mach number specified, these differential equations are numerically integrated to yield the temperature and pressure. Other quantities of interest immediately follow from their definitions, which are algebraic relationships.

Equation (26) was strongly weighted toward internal flows that are modeled easily because of their well-defined geometrical constraints. On the other hand, modern high-speed inlet systems are characterized by both internal and external compression systems, making the models that approximate external flows to be of considerable use. Hence, the particular problem of adiabatic, two-dimensional external flow over a flat semi-infinite plate is worth considering. The external flow has a constant pressure field $p(x) = p_\infty$. This additional constraint is used to compute the streamtube cross-sectional area. Following the solution methodology in appendix E, the relationship is written

$$\frac{dy_{stream}}{dx} = \frac{C_f}{2}\left[1 + (\gamma - 1)M^2\right] \tag{27}$$

This differential equation describes the location of the bounding streamtube for a given mass flow rate. Note that this relationship is in terms of the local Mach number, which requires simultaneous integration of the Mach number differential equation and the cross-sectional-area differential equation. The coupling is not as problematic as it might seem, because the predictor-corrector structure of the Runge-Kutta integration permits equation decoupling at any intermediate integration step, since operations are explicit at any step. Here, the implied given mass flow rate is constrained by the size and location of the cowl. The mass flow rate will need to be computed by an iterative method involving the following steps (fig. 3):

(1) Estimate the starting location of the streamtube cross-sectional area:

$$A(0)_0 = \frac{\dot{m}_{cowl,0}}{\rho_\infty u_\infty} \tag{28}$$

(2) Integrate to compute the cross-sectional area A(x) and the local flow conditions (e.g., M(x), p(x), T(x)) using equations (24) to (26) and numerical technique.

(3) Compute the actual capture

$$\dot{m}_{cowl,1} = \rho(x_{cowl})u(x_{cowl})A_{cowl} \tag{29}$$

(4) Repeat step 1

$$A(0)_1 = \frac{\dot{m}_{cowl,1}}{\rho_\infty u_\infty} \tag{30}$$

Thus, the mass flow rate definition is consistent with viscous effects (displacement) on the external body.

Other factors describing the flow, such as profile shape estimates and boundary layer thicknesses (especially for external flows) are of interest. Although the analysis was designed to ignore local profiles (the basis of the quasi-one-dimensional assumption) by introducing some classical empirical assumptions for profile definition (e.g., 1/7th power law), reasonable estimates are available. Consider the adiabatic external flow over a flat semi-infinite plate. The momentum equation (Karman integral form) is written

$$\frac{C_f}{2} = \frac{d\theta}{dx} \quad \text{and} \quad \theta = \int_0^\infty \frac{\rho}{\rho_\infty}\frac{u}{u_\infty}\left(1 - \frac{u}{u_\infty}\right)dy \tag{31}$$

where $\delta(x)$ is the boundary layer thickness. Now introducing (from eq. (4))

$$\frac{\rho}{\rho_\infty} = \frac{1}{1 + \frac{\gamma - 1}{2}M_\infty^2\left[1 - \left(\frac{u}{u_\infty}\right)^2\right]} \tag{32}$$

The relationship may be written

$$C_f(x) = \frac{d}{dx}\int_0^{\delta(x)} \frac{\frac{u}{u_\infty}\left(1 - \frac{u}{u_\infty}\right)}{1 + \frac{\gamma - 1}{2}M_\infty^2\left[1 - \left(\frac{u}{u_\infty}\right)^2\right]}\,dy \tag{33}$$

The empirical closure to this relationship is provided by the power law profile

$$\frac{u}{u_\infty} = \left[\frac{y}{\delta(x)}\right]^{1/n} \quad \text{and} \quad 6 \le n \le 9 \tag{34}$$

Because the skin friction coefficient $C_f(x)$ is a known parameter at any specified streamwise location, these relationships provide an algebraic relationship for the boundary layer thickness $\delta(x)$ and, thereby, the local velocity, density, and temperature profiles (appendix F). Given a simple linear skin friction distribution, the boundary layer thickness is written

$$\delta(x) = \frac{1}{2I_0}\left[\frac{\Delta C_f}{2}x^2 + C_{f0}x\right] + \delta(0) \tag{35}$$

where the term I_0 represents the pure number

$$I_0 \equiv \int_0^1 \frac{w^{1/n}(1 - w^{1/n})}{1 + \frac{\gamma - 1}{2}M_\infty^2(1 - w^{2/n})}\,dw \tag{36}$$

This integral cannot be evaluated in closed form by elementary means; therefore, a trapezoid rule numerical integration scheme is employed. Relaxation of the linear skin friction assumption is possible (appendix F).

The average flow conditions for any point in the flow field are a related profile-dependent parameter. This type of parameter is often used when a design requires boundary layer control, such as bleed or boundary layer diversion. The local profile is known from the previous analysis; therefore the integral average may be computed. The reduction of a multidimensional flow field to a single set of parameters is not a unique process. Appendix G presents an analysis that attempts to provide this type of physically satisfactory reduction. The physical basis of this methodology is to develop a locally consistent one-dimensionally consistent approximation. When a simple canonical example is considered, the system is written

$$f(a_{ave},b_{ave}) = \frac{1}{y_2 - y_1}\int_{y_1}^{y_2} f\,[a(y),b(y)]\,dy \equiv RHS_1 \tag{37}$$

and

$$g(a_{ave},b_{ave}) = \frac{1}{y_2 - y_1}\int_{y_1}^{y_2} g\,[a(y),b(y)]\,dy \equiv RHS_2 \tag{38}$$

Because the right-hand terms RHS_1 and RHS_2 are known, the previous relationships define a nonlinear system in terms of the two variables a_{ave} and b_{ave} and the terms f and g

$$\begin{bmatrix} f(a_{ave},b_{ave}) \\ g(a_{ave},b_{ave}) \end{bmatrix} = \begin{bmatrix} RHS_1 \\ RHS_2 \end{bmatrix} \tag{39}$$

This system may be either analytically or numerically inverted to yield the locally consistent one-dimensional approximations. This methodology may also be applied to yield local values for the quantities u_{ave} and T_{ave} (appendix G).

Several other loss mechanisms, including shock and subsonic diffuser losses, must be modeled to provide realistic simulations. Although shock losses are often analyzed within the framework of an inlet analysis package or within the cycle analysis code itself, it is necessary to provide changes in the local flow properties caused by shock phenomena. To provide this capability, normal and oblique shocks may be specified at internal and external locations. Normal shock location and strength are user specified. The actual physical location of these shocks is a function of the pressure field, but computation of the normal shock location would probably involve more iteration than would be reasonable for this type of preliminary design analysis.

External oblique shocks (for which a location is better defined) are modeled by the superposition of classical oblique shocks on the quasi-one-dimensional analysis. To convert these inherently two-dimensional flow structures into this report's one-dimensional framework, an approximate rotation is required. Through this rotation, shock strength (the magnitude of postshock properties) is maintained but not shock geometry. Although approximate by their nature, the above strategies provide flexible and accurate models for loss estimation and property changes caused by these flow irreversibilities.

In contrast to the first-principle modeling strategies employed to model shock losses, no analytically based model is available to model losses in adverse pressure gradient flows (i.e., subsonic diffuser flows) because of the highly complex nature of these flows (including separation and potential flow reversal). These same difficulties are found in external adverse pressure gradient flows. To provide a reasonable model for internal subsonic diffuser flow, an empirical relationship from the experimental work of Squire is applied (ref. 11). The model and potential first-principle methods are described in appendix H. The work of Squire provides an empirically based effective skin friction which is written

$$C_{f,dif} = f(\alpha)C_{f,plate} \tag{40}$$

where $f(\alpha)$ is the empirically derived weighting factor. The analytically based alternative to this empirical closer is not as well developed or tested. This analysis is based on the observation that at the point of separation, the wall shear stress τ_w is small compared to the pressure gradient. Employing this observation combined with a mixing length hypothesis yields the local velocity field (in the law of the wall variables)

$$u^+ = 2\frac{\alpha^{1/2}}{k}y^{+1/2} + u_s \tag{41}$$

Equation (41) may be used to estimate skin friction values for adverse pressure gradient flows. The inherently local basis of this derivation limits the applicability of the results.

These relationships provide the analytical basis for viscous heat transfer loss analysis. Although the model is inherently local, it provides a simple but complete computational tool. A large portion of this analysis' physical

basis is contained within the modeling of the skin friction coefficient C_f. The available closure analyses for this term are summarized and detailed in appendix B.

RESULTS AND DISCUSSION

The goal of this analysis was to describe several complex, nonlinear fluid dynamics problems with a simple system of nonlinear equations. To evaluate the model's success, the theoretical correctness of the analysis and the ability to estimate flow-field losses and other flow-field phenomena were verified. Theoretical correctness or consistency was assessed by generating a series of degenerate or asymptotic cases for which closed form integrations are available. The ability of the model to predict flow parameters was measured by comparing it to experimental measurements or state-of-the-art CFD simulations.

The theoretical consistency of the model is mandatory and not subject to interpretation. Numerous classical analytical, quasi-one-dimensional flow solutions with and without loss mechanisms are available (refs. 2, 8, and 12). Shapiro (ref. 8) provides a very comprehensive discussion of these solutions. A more extensive approach which provides analytical solutions to many generalized one-dimensional flow problems is applied by Young (ref. 9).

Considering the following classical problems

(1) One-dimensional flow with friction (Fanno flow)—a simple degenerate case that becomes immediately available by assuming $C_h = 0$, $T_w = T$. The geometry is described by

$$A(x) = \frac{\pi}{4} D^2 = \text{const} \quad \text{and} \quad \frac{dS(x)}{dx} = \pi D = \text{const} \tag{42}$$

Substitution of these relationships into equation (14) with algebraic simplification yields

$$4C_f \frac{dx}{D} = \frac{2}{\gamma M^2} \frac{(1 - M^2)\frac{dM}{M}}{\left(1 + \frac{\gamma - 1}{2} M^2\right)} \tag{43}$$

which is exactly the governing equation, in terms of the Mach number, for Fanno flow (ref. 2).

(2) Isentropic throughflow variable area ducts—a degenerate flow problem that is a very small isentropic, and demands the sources of irreversibility (e.g., friction and heat transfer). It is justifiable to assume in equation (14) that $C_f = C_h = 0$ yielding with algebraic simplification

$$-\frac{dA}{A} = \frac{[1 - M^2]}{M\left(1 + \frac{\gamma - 1}{2} M^2\right)} dM \tag{44}$$

Because this relationship is not traditionally derived in differential form but is instead performed in integral form, the development is shown in greater detail. Integrating and evaluating at stations 1 and 2, the equation is written

$$\frac{A_1}{A_2} = \left(\frac{M_2}{M_1}\right)\left(\frac{1 + \frac{\gamma - 1}{2}M_2^2}{1 + \frac{\gamma - 1}{2}M_1^2}\right)^{1/2(1+\gamma/1-\gamma)} \tag{45}$$

By further restricting the problem with the sonic values $A_1 = A^*$ and $M_1 = 1$, the new relationship is written

$$\left(\frac{A}{A^*}\right) = \frac{1}{M^2}\left[\frac{2}{\gamma + 1}\left(1 + \frac{\gamma + 1}{2}M^2\right)\right]^{\gamma+1/\gamma-1} \tag{46}$$

which may be recognized as the classical area Mach number relation (Anderson, ref. 2).

(3) Combined variable-area duct with friction analysis—a flow problem that has a varying cross-sectional area with friction present. Analyses 1 and 2 have been elementary in that they have only considered variation with respect to individual effects. This problem is a subset of a general problem solved by Young (ref. 9). These closed-form solutions are restricted in applicability. For example, closed-form (explicit functional) integration requires that the varying terms be artificially related (appendix D). The governing equation (14) reduces to

$$\frac{dA}{A} - \gamma M^2 \frac{C_f(x)}{2A} dS = \frac{(M^2 - 1)}{M\left(1 + \frac{\gamma - 1}{2}M^2\right)} dM \tag{47}$$

To integrate this equation, the reasonable assumptions are introduced (fig. 4)

$$C_f = C_{f0} = \text{const} \qquad A(x) = (H_1 x + H_0)b \qquad dS(x) = b\,dx \qquad b = 2L_{width} = \text{const} \tag{48}$$

where the definitions have been imposed

$$H_1 \equiv \tan\alpha \qquad \text{and} \qquad H_0 \equiv h_0 \tag{49}$$

Under these assumptions, the previous differential equation is integrated to yield (appendix D)

$$\left(\frac{H_0}{H_1 x + H_0}\right) = \frac{M}{M_0}\left(\frac{2H_1 - \gamma C_{f0}M^2}{2H_1 - \gamma C_{f0}M_0^2}\right)^{2H_1 - \gamma C_{f0}/2(\gamma C_{f0} + (\gamma - 1)H_1)} \left(\frac{1 + \frac{\gamma - 1}{2}M^2}{1 + \frac{\gamma - 1}{2}M_0^2}\right)^{-1/2((\gamma+1H_1)/\gamma C_{f0} + (\gamma - 1)H_1)} \tag{50}$$

This formidable, nonlinear algebraic equation is the closed form result for this flow and may be solved to yield the Mach number at any duct location. Appendix D briefly discusses an inversion by the secant method, an elementary root-finding technique. Since the intent of this derivation is to use the solution to help verify the numerical solution, the following specific cases are considered.

The two-dimensional supersonic duct flow is described by the following parameters: H_0 = initial channel half height; H_1 = tan α channel half angle, x = streamwise distance, C_{f0} = constant skin friction coefficient, and

M_0 = initial Mach number. Starting with the simple case of a frictionless variable area ($C_{f0} = 0$, $H_0 = 1.0$, $H_1 = 0.1$, $M_0 = 1.5$, $x = 1$),

$$M_{analy}(x) = 1.65179 \qquad M_{num}(x) = 1.65179 \qquad Err_{rel} = 0.0 \text{ percent}$$

where Err_{rel} is the relative error. These results compare very favorably. Similarly, the simple case of constant cross-sectional area with friction ($C_{f0} = 0.1$, $H_0 = 1.0$, $H_1 = 0.0$, $M_0 = 1.5$, $x = 1.0$) shows similarly good results:

$$M_{analy}(x) = 1.47292 \qquad M_{num}(x) = 1.47286 \qquad Err_{rel} = 0.004 \text{ percent}$$

Both cases are examples of the simple flows discussed in the first two sections of this report. Now, consider a case that combines variable area with friction ($C_{f0} = 0.01$, $H_0 = 1.0$, $H_1 = 0.1$, $M_0 = 1.5$, $x = 1.0$):

$$M_{analy}(x) = 1.62735 \qquad M_{num}(x) = 1.62760 \qquad Err_{rel} = 0.015 \text{ percent}$$

This result also compares quite well because it combines several effects are combined. The final example is the subsonic flow with a variable area duct and friction ($C_{f0} = 0.01$, $H_0 = 1.0$, $H_1 = 0.01$, $M_0 = 0.50$, $x = 10.0$):

$$M_{analy}(x) = 0.44869 \qquad M_{num}(x) = 0.44869 \qquad Err_{rel} = 0.0 \text{ percent}$$

Although it appears as though a subsonic diffuser problem was described, this is a contrived problem for which a simple, constant skin friction result is imposed. Greater physical significance could be introduced by defining an average, effective skin friction value of appropriate magnitude for this flow, but for the purposes of verifying the analytical correctness of this method, this was not attempted.

In summary, a simple flow that combined two important effects simultaneously, which could be described by a closed-form analytical solution, was used to validate the numerical solution method. Closed-form solutions of this type are typically unavailable, therefore, other verification methods discussed in subsequent sections were necessary.

Mach 2.5 Supersonic Throughflow Fan Inlet Model

Although the previous analytical comparisons have provided confidence with respect to the accuracy and consistency of the derivation and the numerical integration technique, they have not furnished any independent information concerning their ability to predict complex flows losses. Experimental results and CFD (full Navier Stokes (FNS) and boundary layer) results will be used to perform this more independent verification.

The supersonic through-flow fan inlet model is an innovative propulsion concept for high-speed flight applications. In this model, the supersonic free-stream flow is accelerated by the fan while the flow regime is maintained. As indicated by Barnhart (ref. 13), a benefit of this fan is its ability to operate with a relatively short, lightweight inlet; thus, the prediction of viscous losses in the inlet portion of this flow will be critical. The base inlet is an axisymmetric, conical centerbody with a 12.5° half-angle (fig. 5). The external flow portion then terminates in an annular section.

The modeling includes an inviscid bow shock, a viscous external conical flow, and an annular internal flow field. The choice of a viscous closure model is critical. The external skin friction portion was computed using Van Driest's method (ref. 3) with appropriate modification for the conical nature of the flow field. The internal portion of the flow field is modeled using the fully developed internal method (appendix B and fig. 6).

The results of this modeling are presented in figure 6, where the total pressure recovery is compared with an FNS simulation (ref. 14). Comparing the results for the fan face total pressure recovery reveals that the relative error is on the order of 2 percent, which is well within the 10 percent relative error considered reasonable for a preliminary design tool. Apparently, the simple integral method is providing results that are as accurate as those of the Navier-Stokes simulation.

Estimated CPU requirements are shown to emphasize the savings in computational time. With respect to computational speed, the integral analysis is superior (on the order of 1:10 000). Further, in a flow that is non-ideal (e.g., adverse pressure gradient, separating, shock-boundary-layer interactions), an FNS simulation may provide the only available solution method. A final potential limitation of a Navier-Stokes analyses is the strong dependence of solution results on grid characteristics as demonstrated by figure 6. This limitation is minimized because an FNS simulation may provide considerable flow field detail. It seems to the author that computating a detailed flow field, and averaging to yield a single performance parameter are inherently inefficient and that REMEL may be preferable when integrated information is desired.

External Forebody Boundary Layer Analysis

To test the quasi-one-dimensional loss analysis, an external problem was chosen for which well-documented CFD boundary layer results (STAN5, ref. 15) and a compressible, turbulent boundary layer analysis, are available for comparison. The physical problem is supersonic flow over a long (110 ft) external forebody. This forebody is modeled as a long two-dimensional flat plate, which is realistic for a vehicle with a large radius of curvature. Figure 7 presents a satisfactory comparison of STAN5 and the quasi-one-dimensional methodology. Another comparison is available if the incompressible limit to this flow (M approaching zero) is considered in that classical, semiempirical, boundary layer thickness estimates are available (appendix G). For this case the boundary layer thickness is

$$\delta_{\text{incomp,analy}}(110') = 1.19' \qquad \delta_{\text{incomp,1D}}(110') = 1.174' \tag{51}$$

with an error of 1.7 percent, which is acceptable. Although limited in scope, this external flow tests the adequacy of the model and helps provide confidence in the use of the code and the modeling technique.

CONCLUSIONS

A model was developed to provide rapid engineering estimates of viscous and heat transfer losses in aeropropulsion systems. This method was intended as an alternative to traditional empirical and costly CFD methodologies. A simple quasi-one-dimensional flow model with viscous and heat transfer terms included (integrated numerically) provided the basis for this model. Closure to this system for several basic flows (flat plate, conical, and internal fully developed) is provided by both classical and newly developed compressible, turbulent skin friction analyses. Further, boundary layer thickness, profile, and viscous blockage effects may be estimated. Geometry is modeled by piecewise, discrete linear elements.

A preliminary verification of this analysis and model was performed by comparison to FNS and finite difference-based boundary layer results. Although minimal computational effort was required, the comparison was very favorable. Comparison was also made to several classical, degenerate analytical solutions and a newly developed analytical solution for flow with friction in variable area ducts. These comparisons help to prove that this simple model may provide an alternative to other methods for the estimation of viscous and heat transfer losses in propulsion systems.

ACKNOWLEDGMENTS

The author would like to thank Mr. Paul Barnhart, Dr. John K. Lytle, and Mr. Leo Burkardt for their technical support and helpful suggestions throughout all phases of this project. This research was sponsored by the NASA Lewis Research Center, Cleveland, Ohio, under contract NAS3–25266.

APPENDIX A

A PRELIMINARY USER'S GUIDE TO THE RAPID ENGINEERING ESTIMATES OF MOMENTUM AND ENERGY LOSS (REMEL) CODE

The main text and appendixes of this report have provided a detailed theoretical description of an analysis based on quasi-one-dimensional methods coupled to integral closure formulations. This methodology is used to provide theoretically based estimates of momentum and energy losses; however, it is equally important to provide the actual user with a simple, practical description of REMEL's operation.

Input Variable List

For the purpose of discussion, it is generally convenient to divide variables into three types (fig. 12)

(1) Interval variables—defined along a duct or plate section (e.g., skin friction) between two station variables

(2) Station variables—defined at specific streamwise locations (e.g., area or position)

(3) Control variables—used to provide logical control via on and off switches for necessary features (e.g., choosing internal versus external flow). A control variable may either be associated with an interval or a station.

The variables with name, type, purpose, and associated units contained within the FORTRAN NAMELIST input are

CFV (interval); first guess for skin friction iteration

AIV (station); cross-sectional area, ft^2

ANV (station); diameter of annulus, inner body, ft

DIV (station); diameter of pipe, outer body, ft

TWV (interval); wall temperature/average temperature ratio, used for heat transfer computations

TTV (interval); physical wall temperature, R

CHV (interval); Stanton number, first guess, used for heat transfer computation

CPV (interval); pressure coefficient, NOT used for normal computations

XIV (station); streamwise location, ft

XV (station); streamwise location, ft

RMV (station 1 only); Mach number

PV (station 1 only); static pressure, psi

TV (station 1 only); static temperature, R

RHV (station 1 only); density, slug/ft^3

UV (station 1 only); velocity, ft/s

BLV (station); boundary layer bleed, percentage of main flow

ARBLV (station); area ratio of bleed port, NORMALLY = 1

NDIFFV (interval, control variable), diffuser flag; NDIFF = 0, no diffuser; NDIFF = 1, diffuser present

ISHCKV (station, control variable), normal shock flag; ISHCKV = 0, no normal shock; ISHCKV = 1, normal shock present

IOBLIQ (station, control variable); oblique shock flag, two-dimensional only; IOBLIQ = 0, no oblique shock; IOBLIQ = 1, oblique shock present

IPRSIT (interval, control variable); flag to specify which external flow interval is to be used in capture stream tube computations, two-dimensional only, IPRSIT = 0, ignore possible capture computation in this interval; IPSIT = 1, perform possible capture computation in this interval

ICOWL (station, control variable); flag to indicate which station represents the cowl (beginning of internal inlet), needed for external streamtube capture computation, two-dimensional only; ICOWL = 0, station is not cowl; ICOWL = 1, station is cowl

ICAP (control variable); external stream tube computation flag, two-dimensional only, ICAP = 0, ignore external capture streamtube computation; ICAP = 1 perform external capture streamtube computation

DELTV (station); ramp angle, degrees; if present, see OBLIQ, two-dimensional only

NPROFL (interval, control variable); indicates within which interval a profile computation is to be performed; NPROFL = 0, no profile computation is to be performed within this interval; NPROFL = 1, profile computation to be performed within this interval

PROLOC (interval); physical streamwise location (referenced from station 1) within specified interval, ft, see NPROFL

YMXAVE (interval); upper bound for averaging computation, ft, two-dimensional only

YMNAVE (interval); lower bound for averaging computation, ft, two-dimensional only

PEXP (general variable); power law exponent to be used in profile computation, $7 \leftarrow \text{PEXP} \leftarrow 9$

NCONV (interval, control variable); boundary layer type; NCONV = 0, compressible, turbulent, flat plate (refs. 5 and 6) also required for diffuser and external conical analyses (see Mach 2.5 Supersonic Throughflow Fan Inlet Model); NCONV = 1, compressible, turbulent, internal, fully-developed, axisymmetric flow (ref. 7); NCONV = 2, compressible, turbulent, internal, fully-developed, two-dimensional flow (ref. 7)

NCON1V (interval, control variable); flag indicating conical duct versus conical annulus for axisymmetric problems; NCON1V = 0, conical duct; NCON1V = 1, conical annulus

NCONEV (interval, control variable); flag indicating internal versus external flow field, required for boundary layer computations; NCONEV = 0, internal flow; NCONEV = 1, external flow

NCONCV (interval, control variable); flag indicating geometry type, axisymmetric or two-dimensional; NCONCV = 0, axisymmetric only; NCONCV = 1, two-dimensional only

NNOZV (control variable); simplified nozzle computation; currently under development

NVISC (interval, control variable); flag to control boundary layer iteration; NVISC = 0, perform iteration to tolerance; NVISC = 1, no iteration (use initial guess); for CFV = 0, inviscid flow is recovered

RLXV (station); flow path width, ft, two-dimensional only

RLYV (station); flow path height, ft, two-dimensional only

GAMMV (interval); specific heat ratio

NINTER (general variable); interval number required

APPENDIX B

SKIN FRICTION CLOSURE RELATIONSHIPS

The quasi-one-dimensional analyses described in the main text provides a methodology for the computation of bulk aerodynamic losses such as total pressure. This analysis requires specification of the local viscous and heat transfer losses which are the most important source of entropy generation (loss). These losses are modeled by the specification of a skin friction coefficient and Stanton number, typically related to the skin friction coefficient by Reynold's Analogy.

Although computation of the skin friction is a fundamental problem, simple closed-form relationships that would be of an appropriate complexity level are not readily available for a wide range of compressible, turbulent flows with arbitrary conditions. Special cases for which relatively simple external flow field solutions are available include

- Compressible, turbulent flow over a flat plate (ref. 5)
- Compressible, turbulent flow over a cone (ref. 6) and for internal flow fields
- Compressible, turbulent flow in fully developed pipes and channels (ref. 7)

The strategy followed will extend these simple flows to more complex ones. For example, an external flow field in a moderate-pressure gradient may be modeled using the simple flat plate solution. Similarly, an accelerating nozzle flow can be modeled using the fully developed skin friction relationships. Certain processes such as subsonic diffusion may not be modeled by these techniques because of their fundamental characteristics.

The discussion may begin by considering the relatively simple case of fully developed flow in channels and pipes. For convenience, the adiabatic case will be considered only, although De Chant and Tattar (ref. 7) have extended this methodology to include heat transfer and roughness effects. Consider the governing equations for turbulent flow. Starting with a compressible, mixing length hypothesis

$$\tau_w = \rho_w \frac{\rho}{\rho_w} k^2 y^2 \left(\frac{du}{dy}\right)^2 \tag{B1}$$

and the density relationship, which is a combination of the Crocco-Busemman relationships and state

$$\frac{\rho_w}{\rho} = \frac{T}{T_w} = 1 - r\frac{\gamma - 1}{2} M_{ave}^2 \frac{T_{ave}}{T_w} \left(\frac{u}{u_{ave}}\right)^2 \tag{B2}$$

where r represents the turbulent recovery factor and is approximately r = 1. Eliminating the density relationship and integrating

$$\left(\frac{\tau_w}{\rho_w}\right)^{1/2} \frac{1}{k} \ln y + \text{const} = \frac{u_{ave}}{a} \arcsin\left(\frac{au}{u_{ave}}\right) \tag{B3}$$

Demanding that in the limit $M_{ave} = 0$ the classical law of the wall is recovered, the constant is specified, and the velocity solution may be written

$$\frac{u}{u_{ave}} = \frac{1}{a} \sin\left[\frac{v^* a}{u_{ave}}\left(\frac{1}{k} \ln y^+ + B\right)\right] \tag{B4}$$

where

$$a^2 \equiv r\frac{\gamma - 1}{2} M_{ave}^2 \frac{T_{ave}}{T_w} \tag{B5}$$

$$v^* \equiv \left(\frac{\tau_w}{\rho_w}\right)^{1/2} \quad \text{and} \quad y^+ \equiv \frac{yv^*}{\nu_w} \tag{B6}$$

and the constants $k = 0.4$, $B = 5.50$. This is the Van Driest "effective velocity" (ref. 3) for adiabatic flow.

Although the derivation is semiempirical, it represents an enormous step forward in the analysis of turbulent compressible flow, providing a compressible inner law formula.

To apply this relationship, the skin friction coefficient definition

$$\tau_w = \frac{1}{2}\rho_{ave} u_{ave}^2 \tag{B7}$$

and the Reynolds number definition are combined

$$\frac{Rv^*}{\nu} = \frac{\sqrt{2}}{4} Re_d \sqrt{C_f}\,(1 - a^2)^{1/2(1+2\omega)} \tag{B8}$$

introducing the power law relationship for the absolute viscosity

$$\frac{\mu}{\mu_w} = \left(\frac{T}{T_w}\right)^{\omega} \quad \text{and} \quad \omega \approx 0.76 \tag{B9}$$

To obtain the desired skin friction relationship, the effective velocity relationship is rewritten

$$\frac{u_{ave}}{av^*} \arcsin\left(a\frac{u}{u_{ave}}\right) = \frac{1}{k} \ln y^+ + B \tag{B10}$$

Averaging both sides of the relationship (across the pipe or channel), the right side may be readily computed

$$\int_0^R \left[\frac{1}{K}\ln\left(\frac{yv^*}{\nu_w}\right) + B\right](R - y)dy = \frac{1}{K}\ln\left(\frac{Rv^*}{\nu_w}\right) + 1.75 \tag{B11}$$

However, the left side is much more complex. Accepting the simple approximation

$$\int_0^R \arcsin\left(a\frac{u}{u_{ave}}\right)(R - y)dy \approx \arcsin a \tag{B12}$$

the effective velocity relationship may be written

$$\frac{\sqrt{2}}{\sqrt{C_f}}\frac{\arcsin a}{a}(1 - a^2)^{1/2} = \frac{1}{k}\ln\left(\frac{Rv^*}{\nu_w}\right) + \text{const} = u^+_{ave_{incomp}} \tag{B13}$$

where the constant has been generalized to include the two-dimensional case

const = 1.75 (axisymmetric tube) and const = 3.0 (two-dimensional channel)

Finally, collecting terms for the axisymmetric case introducing the Darcy Friction factor $\lambda = 4C_f$ for ease of comparison, the skin friction relationship is written

$$\frac{1}{\sqrt{\lambda}}\frac{\arcsin a}{a}(1 - a^2)^{1/2} = 2.03\ \log\left(Re_d\sqrt{\lambda}\right) - 0.9130 + 1.0176\ \log(1 - a^2)(1 + 2\omega) \tag{B14}$$

and the equivalent relationship for two-dimensional channels

$$\frac{1}{\sqrt{\lambda}}\frac{\arcsin a}{a}(1 - a^2)^{1/2} = 2.0325\ \log\left(Re_h\sqrt{\lambda}\right) + 0.142 + 1.0176\ \log(1 - a^2)(1 + 2\omega) \tag{B15}$$

Confidence in the validity of these relationships may be estimated by considering the previous equations in the incompressible limit $a^2 = 0$. Considering the axisymmetric pipe flow in this limit, Prandtl's formula (ref. 3) is recovered

$$\frac{1}{\sqrt{\lambda}} = 2.0\ \log\left(Re_d\sqrt{\lambda}\right) - 0.8 \tag{B16}$$

where a slight adjustment of the constants was introduced following Prandtl. Analogously, the two-dimensional relationship degenerates to

$$\frac{1}{\sqrt{\lambda}} = 2.035\ \log\left(Re_h\sqrt{\lambda}\right) + 0.142 \tag{B17}$$

which may also be found in White (ref. 3). Further comparison to experimental work may be found in De Chant and Tattar (ref. 7). Although these relationships are implicit in the skin friction, they are readily solved by fixed-point iterative methods.

Similarly, Van Driest obtained a relationship for flow over a flat plate using a Karman momentum integral

$$\frac{d\theta}{dx} = \frac{C_f}{2} \quad \text{and} \quad \theta = \int_0^\infty \frac{\rho}{\rho_\infty}\frac{u}{u_\infty}\left(1 - \frac{u}{u_\infty}\right)dy \tag{B18}$$

and his equivalent velocity. To maintain simplicity, only the relationship for adiabatic flow is presented (ref. 4) and the reader is referred to Van Driest's original paper (ref. 5) or White's presentation (ref. 3). This relationship is

$$\frac{0.242}{\sqrt{C_f}}(1 - a^2)^{1/2}\frac{\arcsin a}{a} = \log(Re_x C_f) + \frac{1 + 2\omega}{2}\log(1 - a^2) \tag{B19}$$

Note the obvious similarities between this solution and the previous internal flow solution. These similarities are a result of the internal solutions using the Van Driest equivalent velocity in their formulation.

Another external flow of considerable interest consists of supersonic flow over a cone (fig. 8 and ref. 3). Consider the Karman integral relationship for this flow

$$\frac{d\theta}{dx} + \frac{\theta}{r_0}\frac{dr_0}{dx} = \frac{C_f}{2} \quad \text{and} \quad r_0 = r_0(x) \tag{B20}$$

where

$$r_0 = x \sin \phi \tag{B21}$$

Assuming a power law relationship for the skin friction

$$C_f \approx \theta^{-m} \quad \text{and} \quad \frac{1}{8} \le \theta \le \frac{1}{4} \tag{B22}$$

this classical Bernoulli equation may be solved to yield

$$\frac{C_{f,cone}}{C_{f,plate}} = (m + 2)^{m/(1+m)} \tag{B23}$$

or, as White points out

$$Re_{x,cone} = (2 + m)Re_{x,plate} \tag{B24}$$

which implies that the flat plate relationship given previously is used, but the local Reynolds number is modified.

An alternative analysis to the above empirical analysis was also developed, which is especially useful in estimating the level of approximation in computing external flow skin friction over axisymmetric bodies (fig. 9) using flat plate methods. This analysis also uses the Karman integral relationship, placed in nondimensional form for convenience

$$\frac{1}{Re_x'}\frac{d}{dRe_x'}(Re_\theta Re_x') = \frac{C_f(x)}{2} \tag{B25}$$

where the modified Reynolds number is defined by

$$Re_x' \equiv \frac{\rho_\infty u_\infty \dfrac{(r_0 - \tan\phi x)}{\tan\phi}}{\mu_\infty} \tag{B26}$$

and ϕ is the conical body half angle (fig. 9).

Following Van Driest (ref. 5), the right side of the above equation is frozen and integrated to yield

$$Re_\theta = C_f\frac{Re_x'}{2} + \frac{const}{Re_x'} \tag{B27}$$

introducing a Van Driest's flat plate relationship for Re_θ

$$Re_\theta = \frac{1}{KE}\frac{1}{(1 - a^2)^{(1+2w)/2}} \exp\left(\frac{k}{a}\frac{\sqrt{2}}{\sqrt{C_f}}(1- a^2)^{1/2} \arcsin a\right) \tag{B28}$$

where k = 0.4, E = free constant, and a is defined

$$1 - a^2 = \frac{1}{1 + \dfrac{\gamma - 1}{2}M^2} = \frac{T_\infty}{T_w} \tag{B29}$$

To evaluate these integration constants, it is required that the analysis recover the flat plate case for Re_x', approaching infinity. In this limit, the dependent term of the Reynolds number via L'Hospitals' Rule becomes

$$C_f\frac{Re_x'}{2} + \frac{const}{Re_x'} \rightarrow C_f Re_x' \tag{B30}$$

In this limit, Van Driest's relationship for adiabatic flow over a flat plate must be recovered, thus fixing the constant E. The other constant is determined by noting that as Re_x' decreases, the second term becomes unbounded, thus, this constant must be zero. Under these conditions, the solution may be written

$$0.242(1 - a^2)^{1/2} \frac{\arcsin a}{a} \frac{1}{\sqrt{C_f}} = \frac{1 + 2w}{2} \log (1 - a^2) + 0.41 + \log\left[C_f \frac{\left(\frac{Re_d}{2 \tan \phi} - Re_x\right)}{2}\right] \quad \text{(B31)}$$

By examining this relationship, a couple of statements are possible

(1) As the body becomes more slender, x increasing, the skin friction grows dramatically. This trend is confirmed by White (ref. 3).

(2) A gently tapering cone shows less skin friction than a strongly varying conical body.

Considering a specific case, $Re_x = 3.0 \times 10^6$; $Re_d = 3.0 \times 10^6$ with a 5° cone angle yields $C_f = 0.00252$; for comparison a flat plate value at $Re_x = 3.0 \times 10^6$; $C_{f,plate} = 0.00295$. For this large diameter problem, there is little difference. Now consider the same problem for a more narrow body, $Re_d = 7.5 \times 10^5$, which yields a skin friction $C_f = 0.003827$, which is a difference of approximately 30 percent.

Although this analysis is applicable to conical aft bodies, it is not viable for aft bodies with separated flow. Further, this solution is not valid for $Re_d < 1.0 \times 10^3$, for which the inner turbulence law is strongly modified. In spite of these limitations, this analysis provides a useful approximation for external flows over axisymmetric ones for which curvature effects may not be wholly neglected.

In summary, the above relationships provide a series of analytically based skin friction estimates for a range of elementary internal and external flows. Although these relationships are semiempirical and not completely arbitrary, they may be extended to a broader class of flows.

APPENDIX C

DERIVATION OF GOVERNING DIFFERENTIAL EQUATIONS

A summarized discussion (see Analysis) was presented for the reduction of the governing equations to a single differential equation in terms of the average Mach number. This discussion attempts to more fully describe that reduction, starting with the governing equations

$$d(\rho u A) = 0 \tag{C1}$$

$$\frac{dp}{\rho u^2} + \frac{du}{u} + \frac{C_f}{2}\frac{dS}{A} = 0 \tag{C2}$$

$$dh + udu = d\dot{q} \tag{C3}$$

$$dp = RTd\rho + \rho RdT \tag{C4}$$

$$MdM = \frac{udu}{\gamma R t} - \frac{u^2}{2\gamma RT^2}dT \tag{C5}$$

beginning by eliminating pressure through state

$$\frac{dp}{\rho u^2} = \frac{RTd\rho}{\rho u^2} + \frac{RdT}{u^2} \tag{C6}$$

and by energy

$$RdT = \frac{\gamma - 1}{\gamma}(\dot{q} - udu) \tag{C7}$$

but, by the definition of the Mach number

$$\frac{dp}{\rho u^2} = -\frac{du}{u}\left[\frac{1}{\gamma M^2} + \frac{\gamma - 1}{\gamma}\right] - \frac{dA}{A}\frac{1}{\gamma M^2} + \dot{q}\frac{\gamma - 1}{\gamma u^2} \tag{C8}$$

similarly

$$\frac{du}{u} = \frac{1}{2}\frac{dT}{T} + \frac{dM}{M} \tag{C9}$$

From the energy equation, the temperature may be eliminated

$$\frac{dT}{T} = (\gamma - 1)\frac{\left[\frac{\dot{q}}{\gamma RT} - MdM\right]}{\left[1 + \frac{\gamma - 1}{2}M^2\right]} \tag{C10}$$

Substituting into the governing equation, the relationship may be written

$$-\frac{1}{2}C_f\frac{dS}{A} = \left[\frac{\frac{\gamma - 1}{2}\left(\frac{\dot{q}}{\gamma RT} - MdM\right)}{\left[1 + \frac{\gamma - 1}{2}M^2\right]} + \frac{dM}{M}\right]\left[1 - \left(\frac{1}{\gamma M^2} + \frac{\gamma - 1}{\gamma}\right)\right] - \frac{dA}{A}\frac{1}{\gamma M^2} + q\frac{\gamma - 1}{\gamma u^2} \tag{C11}$$

The heat transfer term must now be considered. The term, q, represents heating rate per unit mass. Since the flow is not reacting (or has another internal heating phenomena associated with it) it is justifiable to assume that the only heating is through the boundaries. Thus

$$\frac{\dot{q}}{\gamma RT} = \frac{q_w dS}{\dot{m}\gamma RT} \equiv Q_0 dS \tag{C12}$$

and introducing the Stanton number C_h the relationship is written

$$q_w = \rho u \underline{\underline{c}}_p (T_{aw} - T_w)C_h \quad \text{and} \quad \frac{T_{aw}}{T} = 1 + \frac{\gamma - 1}{2}M^2 \tag{C13}$$

Substituting yields

$$\frac{\dot{q}}{\gamma RT} = \frac{1}{\gamma - 1}\left[1 + \frac{\gamma - 1}{2}M^2 - \frac{T_w}{T}\right]C_h\frac{dS}{A} \tag{C14}$$

As an aside, it may be noted that via Reynold's Analogy, the Stanton number may be estimated

$$C_h = \frac{C_f}{2Pr^{2/3}} \tag{C15}$$

With the heat transfer term computed, the governing Mach number differential equation may immediately be written

$$-\frac{C_f}{2}\frac{1}{A}dS = -\frac{1}{\gamma M^2}[1 - M^2]\left[\frac{\frac{\gamma - 1}{2}(Q_0 - MdM)}{1 + \frac{\gamma - 1}{2}M^2}\right] - \frac{1}{\gamma M^2}\frac{dA}{A} + \frac{1}{\gamma M^2}Q_0 \tag{C16}$$

The additional relationships for temperature and pressure have similar derivations. Considering the energy equation

$$\frac{dh}{\gamma RT} + \frac{udu}{\gamma RT} = \frac{1}{\gamma - 1}\left[1 + \frac{\gamma - 1}{2}M^2 - \frac{T_w}{T}\right]C_h\frac{dS}{A} \tag{C17}$$

and introducing the definition of Mach number

$$\frac{udu}{\gamma RT} = \frac{dT}{T}\frac{M^2}{2} + MdM \tag{C18}$$

the equation is written

$$\frac{dT}{T}\left[1 + \frac{\gamma - 1}{2}M^2\right] + (\gamma - 1)MdM = \left[1 + \frac{\gamma - 1}{2}M^2 - \frac{T_w}{T}\right]C_h\frac{dS}{A} \tag{C19}$$

Finally, the above relationship is solved for the temperature derivative to yield

$$\frac{dT}{dx} = \frac{T\left[1 + \frac{\gamma - 1}{2}M^2 - \frac{T_w}{T}\right]C_h\frac{1}{A}\frac{dS}{dx} - (\gamma - 1)\frac{MdM}{dx}}{1 + \frac{\gamma - 1}{2}M^2} \tag{C20}$$

Similarly, the pressure differential equation may be considered. Applying momentum, state, and the Mach number definition yields

$$dp = -\gamma M^2 p\left[\frac{1}{2}C_f\frac{dS}{A} + \frac{1}{2}\frac{dT}{T} + \frac{dM}{M}\right] \tag{C21}$$

but by the energy equation, this reduces to

$$\frac{dT}{T} = (\gamma - 1)\frac{\left[\frac{\dot{q}}{\gamma RT} - MdM\right]}{\left[1 + \frac{\gamma - 1}{2}M^2\right]} \tag{C22}$$

Substituting yields the pressure differential equation

$$\frac{dp}{dx} = -\gamma M^2 p\left[\frac{1}{2}\frac{C_f}{A}\frac{dS}{dx} + \frac{\frac{1}{2}\left(1 + \frac{\gamma - 1}{2}M^2 - \frac{T_w}{T}\right)C_h\frac{1}{A}\frac{dS}{dx} + \frac{1}{M}\frac{dM}{dx}}{1 + \frac{\gamma - 1}{2}M^2}\right] \tag{C23}$$

Thus, a more thorough derivation of the fundamental differential equations describing the quasi-one-dimensional flow has been presented.

APPENDIX D

AN EXACT SOLUTION TO VARIABLE AREA DUCT FLOW WITH FRICTION

To help verify the accuracy of the basic analysis, several classical degenerate analytical solutions to the governing differential equations are considered. Most of these analytical solutions involve variation in a single parameter. One very practical problem involves compressible flow with friction in a variable area duct. As stated previously, this solution is a somewhat simplified variation of the class of solutions discussed by Young (ref. 9). The success of both Young's technique and the aforementioned depend on a semi-artificially simple relationship between the variable terms. Examples of these terms include

$$\frac{1}{A}\frac{dA}{dx} \qquad \frac{C_f}{2A}\frac{dS}{dx} \qquad \frac{1}{T_0}\frac{dT_0}{dx} \qquad \cdots \tag{D1}$$

It is typically required that the above terms be proportional to one another, which somewhat limits the application of this technique. This constraint may be written

$$\frac{1}{A}\frac{dA}{dx} \propto \frac{C_f}{2A}\frac{dS}{dx} \propto \frac{1}{T_0}\frac{dT_0}{dx} \qquad \cdots \tag{D2}$$

Despite the inherent limitations, these integrations and the chosen case are of considerable interest. Thus, the details of this solution are provided. Consider the differential equation

$$\frac{2dA}{A} - \gamma M^2 \frac{C_f(x)\,dS}{A} + \frac{(1+\gamma M^2)}{A} C_h(x)\left(\frac{T_w}{T_0} - 1\right) = \frac{(M^2-1)}{\left(1 + \frac{\gamma-1}{2}M^2\right)}\frac{dM^2}{M^2} \tag{D3}$$

This relationship continues to retain the heat transfer term denoted by the Stanton number C_h and the wall temperature to the total temperature ratio. Retention of the heat transfer term makes closed form integration more difficult and restrictive. To see this, consider a two-dimensional duct with constant skin friction. The geometry is written

$$A(x) = h(x)b \qquad \text{and} \qquad \frac{dS}{dx} \approx b \tag{D4}$$

$$h(x) = \tan \alpha x + h_0 \qquad \text{and} \qquad b \equiv 2L_{width}$$

and defining

$$H_1 \equiv \tan \alpha \qquad \text{and} \qquad H_0 \equiv h_0 \tag{D5}$$

where α denotes the half angle of the two-dimensional duct. Writing the previous differential equation

$$\frac{\tan \alpha}{h(x)} - \frac{2\gamma M^2 C_{f0}}{h(x)} + \frac{2C_h(x)\,(1+\gamma M^2)}{h(x)}\left(\frac{T_w}{T_0} - 1\right) = \frac{M^2-1}{M^2\left(1 + \frac{\gamma-1}{2}M^2\right)}\frac{dM^2}{dx} \tag{D6}$$

For a separable solution to exist, it is required that the heat transfer terms follow

$$C_h(x)\left(\frac{T_w}{T_0} - 1\right) = \text{const} \tag{D7}$$

but from the energy equation

$$\dot{m}C_p \frac{dT_0}{dx} = q_w \frac{dS}{dx} \tag{D8}$$

and the definition of the Stanton number

$$q_w(x) \equiv C_h(x)\rho u C_p(T_w - T_0) \tag{D9}$$

yields the differential equation

$$\frac{1}{T_0}\frac{dT_0}{dx} = \frac{C_h\left(\frac{T_w}{T_0} - 1\right)}{A}\frac{dS}{dx} \tag{D10}$$

This relationship may be integrated to yield

$$\frac{T_0}{T_{01}} = e^{C_h(T_w/T_0 - 1)\int_0^x (1/A)(dS/dx)d\xi} \tag{D11}$$

For the specific two-dimensional case, the equation is obtained

$$\frac{T_0}{T_{01}} = \left(\frac{\tan \alpha x}{h_0} + 1\right)^{C_h\left|T_w/T_0 - 1\right|/(\tan \alpha)} \tag{D12}$$

The above relationship is a complex transcendental equation in terms of the total temperature T_0. Similarly, the heat transfer flux $q_w(x)$ computed using the above relationships is quite complex. This indicates that artificial imposition of a heat flux with these characteristics is probably physically unrealistic. Therefore, it is possible to note that care is required in applying assumptions that are mathematically convenient, but physically unrealistic.

As indicated by the title of this appendix, the principal interest here is the adiabatic problem, and therefore, it is possible to neglect the heat transfer terms completely. Thus, the previously analyzed differential equation is recovered

$$\frac{dA}{A} - \gamma M^2 \frac{C_f(x)}{2A} dS = \frac{(M^2 - 1)}{M\left(1 + \frac{\gamma - 1}{2}M^2\right)} dM \tag{D13}$$

By inspection, it is evident that the above relationship is separable with the assumption of constant skin friction C_f. It is probably instructive to analyze this problem by using a slightly different methodology with the hope that it may be possible to relax this restriction.

The solution technique chosen is to convert the governing equation to an exact differential equation by the use of an integrating factor (ref. 16). Summarizing the technique considers the general first order linear or non-linear equation

$$M(x,y)dx + N(x,y)dy = 0 \tag{D14}$$

To better define the notion of an exact differential equation, consider the function

$$\psi(x,y) = 0 \tag{D15}$$

which may be differentiated to yield

$$\frac{\partial \psi}{\partial x} dx + \frac{\partial \psi}{\partial y} dy = 0 \tag{D16}$$

but equating the terms in this relationship to previously defined general differential equation yields

$$\frac{\partial \psi}{\partial x} = M(x,y) \quad \text{and} \quad \frac{\partial \psi}{\partial y} = N(x,y) \tag{D17}$$

which at least implicitly solves the differential equation. Specification of the function ψ is the key to this solution method. By considering these functions with reasonable continuity requirements, it is possible to introduce the constraints

$$\frac{\partial M}{\partial y} = \frac{\partial N}{\partial x} \tag{D18}$$

Thus, with the above relationship and the previous definitions, it is possible to partially integrate to obtain the function ψ.

Only a relatively restricted class of differential equations will be exact; therefore, it would be very useful to introduce a function that preconditions the differential equation to be exact. This preconditioning function may be termed an integrating factor. Consider the equation

$$\mu(x,y)[M(x,y)\,dx + N(x,y)\,dy] = 0 \tag{D19}$$

where $\mu(x,y)$ is the integrating factor. The continuity requirements for this equation demand that

$$\frac{\partial(\mu M)}{\partial y} = \frac{\partial(\mu N)}{\partial x} \tag{D20}$$

or

$$M\frac{\partial \mu}{\partial y} - N\frac{\partial \mu}{\partial x} + \left(\frac{\partial M}{\partial y} - \frac{\partial N}{\partial x}\right)\mu = 0 \tag{D21}$$

The above relationship for μ is more complex than the original differential equation, since it is now a partial differential equation. To avoid this situation, the most reasonable way to proceed is to assume $\mu = \mu(y)$ only. This will reduce the above partial differential equation to an ordinary differential equation. This simplification will suffer a considerable loss in generality of applicability of this technique.

At this point, it is possible to consider the Mach number equation. Placing it in standard variables

$$M(x,y) \equiv \frac{2H_1 - \gamma C_f y^2}{2(H_1 x + H_0)} \quad \text{and} \quad N(x,y) \equiv \frac{(1 - y^2)}{y\left(1 + \frac{\gamma - 1}{2}y^2\right)} \tag{D22}$$

where $y = M$ and $H_1 = \tan \alpha$. The relationship for the integrating factor $\mu = \mu(y)$ becomes

$$\frac{d\mu}{dy} = \frac{N_x - M_y}{M}\mu = \frac{2\gamma C_f y}{2H_1 - \gamma C_f y^2} \tag{D23}$$

This differential equation may be integrated to yield

$$\mu(y) = \frac{1}{2H_1 - \gamma C_f y^2} \tag{D24}$$

The constant of integration may be ignored since any integrating factor μ is acceptable. Several comments concerning this integration are in order. The primary observation that can be made is that the assumption concerning the structure of the integrating factor $\mu = \mu(y)$ unsurprisingly leads to the same restrictions as would separability. It is possible to use the integrating factor structure to compute the partial differential equation required for the integrating factor when this restriction is released. Consider

$$\frac{2H_1 - \gamma C_f(x) y^2}{2(H_1 x + H_0)}\mu_y - \frac{1 - y^2}{y\left(1 + \frac{\gamma - 1}{2}y^2\right)}\mu_x - \frac{\gamma C_f(x) y}{H_1 x + H_0}\mu = 0 \tag{D25}$$

For supersonic flow, this partial differential equation should have real characteristics which are defined by the ordinary differential equations

$$\frac{dx}{-\frac{1 - y^2}{y\left(1 + \frac{\gamma - 1}{2}y^2\right)}} = \frac{dy}{\frac{2H_1 - \gamma C_f(x) y^2}{2(H_1 x + H_0)}} = \frac{d\mu}{\frac{\gamma C_f(x) y}{H_1 x + H_0}} \tag{D26}$$

Although solvable in principle, the above relationship is very complex. It is fairly clear that the previous simplifying assumptions are necessary in most cases. It does not seem unreasonable to state that a general analytical

solution of the governing equations is probably unavailable. This gives insight into the virtual necessity of a numerical integration technique.

Returning to the simplified constant skin friction adiabatic flow in a linearly varying duct (fig. 4), the integrating factor may be applied. This yields the two relationships

$$\psi_x(x,y) = \mu M(x,y) \qquad \text{and} \qquad \psi_y(x,y) = \mu N(x,y) \tag{D27}$$

integrating the first

$$\psi(x,y) = \frac{1}{2H_1} \ln (H_1 x + H_0) + h(y) \tag{D28}$$

Differentiating with respect to y yields

$$h'(y) = \psi_y(x,y) = \mu N(x,y) = \frac{(1 - y^2)}{y\left(1 + \frac{\gamma - 1}{2} y^2\right)} \frac{1}{(2H_1 - \gamma C_{f0} y^2)} \tag{D29}$$

This may be integrated to yield the unknown function of integration

$$h(y) = \int \frac{1 - y^2}{y\left(1 + \frac{\gamma - 1}{2} y^2\right)(2H_1 - \gamma C_{f0} y^2)} dy \tag{D30}$$

Although tedious, this relationship may be integrated by a partial fraction technique. Eliminating the integration constant and simplifying the previously noted equation is obtained

$$\left(\frac{H_0}{H_1 x + H_0}\right) = \frac{M}{M_0} \left(\frac{2H_1 - \gamma C_{f0} M^2}{2H_1 - \gamma C_{f0} M_0^2}\right)^{2H_1 - \gamma C_{f0}/2(\gamma C_{f0} + (\gamma - 1)H_1)} \left(\frac{1 + \frac{\gamma - 1}{2} M^2}{1 + \frac{\gamma - 1}{2} M_0^2}\right)^{-1/2[(\gamma + 1H_1/\gamma C_{f0} + (\gamma - 1)H_1]} \tag{D31}$$

This nonlinear algebraic relationship is the closed-form solution for this flow. A solution for the Mach number must be obtained numerically, but a secant method might be a good choice, considering the complexity of the relationship. Before proceeding with the numerical procedure, it is instructive to consider the limiting cases of the flow

(1) isentropic, variable area flow

(2) constant area flow with friction (Fanno flow)

Considering the first case with $C_f = 0$ it is possible to obtain

$$\frac{H_0}{H_1 x + H_0} = \left[\frac{M}{M_0}\right]\left[\frac{1 + \frac{\gamma - 1}{2}M^2}{1 + \frac{\gamma - 1}{2}M_0^2}\right]^{1/2(\gamma+1/1-\gamma)} \tag{D32}$$

the expected Mach number/area relationship. In the second case $H_1 = 0$ the trivial relationship $1 = 1$ is obtained. Although this is clearly correct, it provides no useful information. Young (ref. 9) describes a similar situation. This degeneracy is attributed to the singular behavior caused by the nonlinear nature of the governing equations. Quite simply, a nontrivial limit does not exist because of the logarithmic/exponential form of the solution. In spite of this limitation, the above solution is viable for small values of area change.

Thus, this indepth appendix seeks to assess the general availability of analytical integrations for the governing quasi-one-dimensional equations. A nonsimple flow, namely variable area duct flow with friction is analyzed in detail. The analytical solutions are used to compare or validate to previously described numerical procedures. Further, these type of solutions are both useful and interesting.

APPENDIX E

EXTERNAL STREAMTUBE DIFFERENTIAL EQUATION DERIVATION AND SOLUTION METHODOLOGY

The quasi-one-dimensional flow modeling approach applied in this report is an easily implemented modeling methodology for internal flows because of their explicitly defined boundary conditions. External flow fields play an equally important part of an integrated propulsion system model. Therefore, an extension of classical quasi-one-dimensional flow methods to external flow problems is necessary.

At this point, the one basic modeling difference between internal and external flows (at least at the boundary layer level of modeling fidelity) is worth emphasizing. Geometry is specified and the pressure field is to be computed in internal flows, whereas in external flows, geometry is computed and the pressure field is specified by the free stream flow field (fig. 10). This fundamental difference may be exploited for the classic example problem of flat plate flow. This analysis begins by considering the pressure field differential equation derived previously in appendix C

$$\frac{dp}{dx} = -\gamma M^2 p \left[\frac{\frac{1}{2}\frac{C_f}{A}\frac{dS}{dx} + \frac{\frac{1}{2}\left(1 + \frac{\gamma - 1}{2}M^2 - \frac{T_w}{T}\right)C_h\frac{1}{A}\frac{dS}{dx} + \frac{1}{M}\frac{dM}{dx}}{1 + \frac{\gamma - 1}{2}M^2} \right] \tag{E1}$$

Presuming adiabatic flow and the classical flat plate assumption $dp/dx \ll 1$, it is immediately possible that

$$\frac{1}{2}\frac{C_f}{A}\frac{dS}{dx} + \frac{\frac{1}{M}\frac{dM}{dx}}{1 + \frac{\gamma - 1}{2}M^2} = 0 \tag{E2}$$

The term dM/dx may be eliminated through the previously derived Mach number differential equation, for which adiabatic flow may be written

$$\frac{dM}{dx} = \left[\frac{C_f}{2}\frac{1}{A}\frac{dS}{dx} - \frac{1}{\gamma M^2}\frac{1}{A}\frac{dA}{dx} \right] \frac{\gamma M^3 \left(1 + \frac{\gamma - 1}{2}\right)M^2}{1 - M^2} \tag{E3}$$

Solving for dA/dx

$$\frac{dA}{dx} = \frac{C_f}{2}[1 + (\gamma - 1)M^2] \tag{E4}$$

which, for two-dimensional flow

$$dS = b\ dx \quad \text{and} \quad dA = b\ dy \tag{E5}$$

yields the desired governing relationship

$$\frac{dy_{stream}}{dx} = \frac{C_f}{2}[1 + (\gamma - 1)M^2] \tag{E6}$$

This equation provides the geometry of the streamtube given the previous specifications. An initial condition $y_{stream}(0)$ is required. This initial streamtube location is computed via the previously explained capture-streamtube methodology.

Although the Mach number relationship and the streamtube differential equation represent a system of two coupled first-order differentials, their solution is perhaps not as problematic as it might appear. In fact, the predictor-corrector nature of the Runge-Kutta integration scheme actually decouple these relationships. This may be demonstrated by considering the canonical problem

$$\frac{dM}{dx} = f(x,M,y) \quad \text{and} \quad \frac{dy}{dx} = g(x,M,y) \tag{E7}$$

The following are the various prediction correction levels for the Runge-Kutta scheme (ref. 10).

Euler predictor, half step

$$M^*_{n+1/2} = M_n + \frac{h}{2} f(x_n, M_n, y_n) \tag{E8}$$

$$y^*_{n+1/2} = y_n + \frac{h}{2} g(x_n, M_n, y_n) \tag{E9}$$

Backward Euler corrector, half step

$$M^{**}_{n+1/2} = M_n + \frac{h}{2} f(x_{n+1/2}, M^*_{n+1/2}, y^*_{n+1/2}) \tag{E10}$$

$$y^{**}_{n+1/2} = y_n + \frac{h}{2} g(x_{n+1/2}, M^*_{n+1/2}, y^*_{n+1/2}) \tag{E11}$$

Midpoint Rule predictor, full step

$$M^{***}_{n+1} = M_n + hf(x_{n+1/2}, M^{**}_{n+1/2}, y^{**}_{n+1/2}) \tag{E12}$$

$$y^{***}_{n+1} = y_n + hg(x_{n+1/2}, M^{**}_{n+1/2}, y^{**}_{n+1/2}) \tag{E13}$$

Simpson's Rule corrector, full step

$$M_{n+1} = M_n + \frac{h}{6}[f(x_n, M_n, y_n) + 2f(x_{n+1/2}, M^{*}_{n+1/2}, y^{*}_{n+1/2}) + 2f(x_{n+1/2}, M^{**}_{n+1/2}, y^{**}_{n+1/2}) + f(x_{n+1}, M^{***}_{n+1}, y^{***}_{n+1})] \tag{E14}$$

$$y_{n+1} = y_n + \frac{h}{6}[g(x_n, M_n, y_n) + 2g(x_{n+1/2}, M^{*}_{n+1/2}, y^{*}_{n+1/2}) + 2g(x_{n+1/2}, M^{**}_{n+1/2}, y^{**}_{n+1/2}) + g(x_{n+1}, M^{***}_{n+1}, y^{***}_{n+1})] \tag{E15}$$

Commenting on the above cascade of relationships, it is apparent that at any predictor or corrector level, the relationships are completely explicit. Further, at any level, they are also decoupled. Thus, a vector problem, such as the one of interest, will be integrable in a relatively simple fashion.

The preceding discussion has sought to describe a physically realistic extension of the quasi-one-dimensional methodology which is easily set up for internal flows to an external problem. Additionally, as a result of the explicit structure of the predictor-corrector Runge-Kutta method, the integration is shown to be relatively convenient.

APPENDIX F

APPROXIMATION OF EXTERNAL PROFILES ON TWO-DIMENSIONAL SURFACES

Although this analysis was not intended to provide detailed profile information for external flow problems, this type of information is often of considerable interest. An approximate analysis was introduced in the text to estimate flow field profiles for elementary external flow problems. This appendix describes this analysis in significantly greater detail. By repeating the governing equation for a Karman Integral flat-plate flow

$$\frac{C_f}{2} = \frac{d\theta}{dx} \quad \text{and} \quad \theta = \int_0^\infty \frac{\rho}{\rho_\infty}\frac{u}{u_\infty}\left(1 - \frac{u}{u_\infty}\right)dy \tag{F1}$$

From Crocco's law

$$\frac{T}{T_\infty} = 1 + \frac{\gamma - 1}{2}M_\infty^2\left[1 - \left(\frac{u}{u_\infty}\right)^2\right] \tag{F2}$$

and by state and the boundary layer assumption

$$\frac{\rho}{\rho_\infty} = \frac{1}{1 + \frac{\gamma - 1}{2}M_\infty^2\left[1 - \left(\frac{u}{u_\infty}\right)^2\right]} \tag{F3}$$

Finally, applying a power law velocity assumption

$$\frac{u}{u_\infty} = \left(\frac{y}{\delta}\right)^{1/n} \tag{F4}$$

substituting into the Karman integral and separating variables

$$\frac{1}{2}C_f(x)\,dx = d[\delta(x)]\int_0^1 \frac{w^{1/n}(1 - w^{1/n})}{1 + \frac{\gamma - 1}{2}M_\infty^2(1 - w^{2/n})}\,dw \tag{F5}$$

Since the preceding analyses provide the capability of estimating the skin friction $C_f(x)$, the above is the fundamental relationship for the boundary layer thickness. It may be noted that the integral portion of the above equation, defined by I_0 is merely a number, not a function of the streamwise variable x although the complexity of the integral may necessitate numerical integration.

To proceed (integrate with respect to x), a function for the skin friction relationship must be proposed. Typically, it will be desirable to evaluate at only two locations in any geometric element. Thus, curve fit relationships based on two known skin friction values are introduced. For example

$$C_f(x) = \Delta C_f x + C_{f0} \qquad \Delta C_f \equiv \frac{C_{f2} - C_{f1}}{x_2 - x_1} \qquad C_{f0} = \frac{C_{f1}x_2 - C_{f2}x_1}{x_2 - x_1} \tag{F6}$$

which, when substituted into the previous relationship and integrated with respect to x

$$\delta(x) = \frac{1}{2I_0}\left[\frac{\Delta C_f}{2} x^2 + C_{f0}x\right] + \delta(0) \tag{F7}$$

Alternatively, a power function is available for use, which yields

$$C_f(x) = a\left(\frac{x}{x_1}\right)^b \qquad a = C_{f1} \qquad b = \frac{\ln\left(\frac{C_{f2}}{C_{f1}}\right)}{\ln\left(\frac{x_2}{x_1}\right)} \tag{F8}$$

and correspondingly

$$\delta(x) = \frac{a}{2I_0(b + 1)}\left(\frac{x}{x_1}\right)^{b+1} + \delta(0) \tag{F9}$$

Experience indicates that linear and polar law methods are approximately equally accurate, although a power law form certainly has considerable historical precedence. With specification of the boundary layer thickness, all other thermodynamic and fluid dynamic flow profiles are available. Thus summarizing, this appendix has presented a simple methodology to predict flow profiles and boundary layer thicknesses over external bodies.

APPENDIX G

EXTERNAL FLOW FIELD AVERAGING

The basis of the quasi-one-dimensional viscous loss analysis hinges on the assumption that a flow field may be described by a one-dimensional or "averaged" flow field. This is a very good assumption for internal and many external flow fields. However, there are problems that may make it necessary to actually analyze a flow field profile. Further, it is often helpful to be able to describe a portion of this profile by a set of averaged quantities. As a common example of where this type of information might be of use, consider a boundary layer diverter system on the external forebody of an integrated propulsion/vehicle concept (fig. 11). This diverter system consists of a bleed port and duct system used to remove the highly disturbed and decelerated air from the lower part of the boundary layer, permitting cleaner, higher recovery air to be available to the internal inlet/ engine system.

The modeling of this problem consists of an external boundary layer modeling with profile information, selection of a certain component of the profile to be removed, and computation of one-dimensional properties in this element (averaging). Thus, an algorithm derived to recover one-dimensional properties for an element of an external flow is developed.

As mentioned in the text, the process of averaging or "one-dimensionalization" is not unique. In this analysis, a process that yields conservative quantities, such as mass, momentum, and total enthalpy, fluxes in their respective one-dimensional forms is selected. Since external flows are of the greatest importance, the development presented here is limited to simple power law profiles. Thus, considering the relationships governing the conservative quantities

$$\left(\frac{\rho_{ave}}{\rho_\infty}\right)\left(\frac{u_{ave}}{u_\infty}\right) = \frac{1}{y_2 - y_1}\int_{y_1}^{y_2}\left(\frac{\rho}{\rho_\infty}\right)\left(\frac{u}{u_\infty}\right)dy \tag{G1}$$

$$\frac{p_{ave}}{\rho_\infty u_\infty^2} + \left(\frac{\rho_{ave}}{\rho_\infty}\right)\left(\frac{u_{ave}}{u_\infty}\right)^2 = \frac{1}{y_2 - y_1}\int_{y_1}^{y_2}\frac{p}{\rho_\infty u_\infty^2}dy + \frac{1}{y_2 - y_1}\int_{y_1}^{y_2}\left(\frac{\rho}{\rho_\infty}\right)\left(\frac{u}{u_\infty}\right)^2 dy \tag{G2}$$

and

$$\frac{T_{ave}}{T_\infty} + \frac{\gamma - 1}{2}M_\infty^2\left(\frac{u_{ave}}{u_\infty}\right)^2 = \frac{1}{y_2 - y_1}\int_{y_1}^{y_2}\left(\frac{T}{T_\infty}\right)dy + \frac{\gamma - 1}{2}\frac{1}{y_2 - y_1}M_\infty^2\int_{y_1}^{y_2}\left(\frac{u}{u_\infty}\right)^2 dy \tag{G3}$$

Now, by the boundary layer approximation

$$\frac{dp}{dy} << 1 \quad \text{and} \quad p_{ave} = p_\infty = p(y) = \text{const} \tag{G4}$$

and the state relationship

$$\frac{\rho}{\rho_\infty} = \frac{T_\infty}{T} \tag{G5}$$

yields the relationships

$$\frac{\rho}{\rho_\infty} = \frac{1}{1 + \frac{\gamma - 1}{2} M_\infty^2 \left[1 - \left(\frac{u}{u_\infty}\right)^2\right]} \tag{G6}$$

and

$$\frac{T}{T_\infty} = 1 + \frac{\gamma - 1}{2} M^2 \left[1 - \left(\frac{u}{u_\infty}\right)^2\right] \tag{G7}$$

Finally, introducing the hypothesis for the profile description

$$\frac{u}{u_\infty} = \left(\frac{y}{\delta}\right)^{1/n} \tag{G8}$$

The above equations may be combined to yield working relationships. It is possible to simplify by noting that the pressure field is not profile-dependent, and thus cancels, as does the total enthalpy-averaging relationship with the adiabatic flow assumption. These relationships reduce to

$$\left(\frac{\rho_{ave}}{\rho_\infty}\right)\left(\frac{u_{ave}}{u_\infty}\right) = \frac{1}{w_2 - w_1} \int_{w_1}^{w_2} \frac{w^{1/n}}{1 + \frac{\gamma - 1}{2} M_\infty^2 \left[1 - \left(\frac{u}{u_\infty}\right)^{2/n}\right]} dw \equiv RHS_1 \tag{G9}$$

and

$$\left(\frac{\rho_{ave}}{\rho_\infty}\right)\left(\frac{u_{ave}}{u_\infty}\right)^2 = \frac{1}{w_2 - w_1} \int_{w_1}^{w_2} \frac{w^{2/n}}{1 + \frac{\gamma - 1}{2} M_\infty^2 \left[1 - \left(\frac{u}{u_\infty}\right)^{2/n}\right]} dw \equiv RHS_2 \tag{G10}$$

where

$$w \equiv \frac{y}{\delta} \qquad w_1 \equiv \frac{y_1}{\delta} \qquad w_2 \equiv \frac{y_2}{\delta} \tag{G11}$$

The boundary layer thickness is computed via the algorithm described in appendix F. With this thickness known and the parameters describing the segment of the profile of interest y_1 and y_2 the terms denoted RHS_1 and RHS_2 are pure numbers which are generally easy to calculate. In general, these computations will require numerical estimation, and a trapezoid rule integration scheme is used in the analysis.

Given the above information, it is now possible to recover the averages

$$\frac{u_{ave}}{u_\infty} = \frac{RHS_2}{RHS_1} \tag{G12}$$

and

$$\frac{\rho_{ave}}{\rho_\infty} = \frac{RHS_1}{\left(\frac{u_{ave}}{u_\infty}\right)} \tag{G13}$$

Similarly, the total enthalpy definition

$$\frac{T_{ave}}{T_\infty} = 1 - \frac{\gamma - 1}{2} M_\infty^2 \left[1 - \left(\frac{u_{ave}}{u_\infty}\right)^2\right] \tag{G14}$$

The remaining average values are available by state and definition.

Although equations (G12 to G14) are still too complex to obtain closed-form integrations, a simple asymptotic end member (namely incompressible flow) may be profitably examined. This examination permits the free-stream Mach number M to approach zero. This yields for a full-width interval, $w_1 = 0$, $w_2 = 1$

$$\frac{u_{ave,incomp}}{u_\infty} = \frac{n + 1}{n + 2} \approx \frac{8}{9} \quad \text{and} \quad n = 7 \tag{G15}$$

It is of interest to compare this value to the more conventional definition of the average

$$\frac{u_{ave}}{u_\infty} = \int_0^1 w^{1/n}\, dw \tag{G16}$$

which, for this example, yields

$$\frac{u_{ave,incomp}}{u_\infty} = \frac{n}{n + 1} \approx \frac{7}{8} \quad \text{and} \quad n = 7 \tag{G18}$$

which is a difference of approximately 1.5 percent. For higher Mach number flows, significantly greater differences might be expected.

Thus, summarizing in terms of one-dimensionalization, a conservative averaging process was described, permitting a portion of a profile over an external body and converts it into a set of simple parameters. This process has application in the design of bleed and diverter systems for high-speed vehicles.

APPENDIX H

DIFFUSER FLOW CORRELATION AND ANALYSIS

The analytical prediction of flow fields and losses in subsonic diffusers is a difficult modeling problem. This stems from the fact that the flow within a diffuser is characterized by a strong adverse pressure gradient ($dp/dx > 0$) which strongly influences the formation of the boundary layer and may, in fact, cause flow reversal. Further, classical parabolic-boundary layer equations are no longer valid in the separation region, where the flow field becomes elliptic. Formally, the only way to analyze problems of this type are to employ full Navier-Stokes (FNS) analyses. Given these difficulties, an empirical methodology, which is actually applied, will be described, followed by a brief comment on analytical models that may be useful in this flow regime.

The basic modeling methodology involves modeling the flow via the previously described quasi-one-dimensional relationships for a duct or conical pipe, except that the effective skin friction parameter is computed via the relationship

$$C_{f,dif} = f(\alpha)C_{f,plate} \tag{H1}$$

where α is the effective cone angle (degrees) and f is the empirical relationship

$$f(\alpha) \equiv 1.01379 + 0.001269\alpha + 0.027466\alpha^2 \tag{H2}$$

The effective diffuser angle for nonconical shapes is computed via a hydraulic diameter concept and may be written

$$\alpha = 2 \arctan\left[\frac{2(A_2P_1 - A_1P_2)}{P_1P_2(x_2 - x_1)}\right] \tag{H3}$$

where P_1P_2 denote the local perimeter. Thus, since the flat plate skin friction is easily available, via Van Driest's relationship (appendix A), the effective skin friction and losses may be easily estimated for this flow.

Although the above methodology will provide the required prediction, its empirical basis may be limited in its applicability. Further, this type of coarse empiricism is somewhat incompatible with this analysis. To begin to motivate a more analytically based analysis, a derivation of the law of the wall function in the region near a separation point is developed. Consider the stress closure Prandtl's mixing length hypothesis

$$\frac{\tau_w}{\rho} + \frac{1}{\rho}\frac{dp}{dx}y = k^2y^2\left(\frac{du}{dy}\right)^2 \tag{H4}$$

Near the stagnation point, the wall shear stress is very small, thus it is possible to write in the dimensionless law of the wall variables

$$\alpha^+y^+ = k^2y^{+2}\left(\frac{du^+}{dy^+}\right)^2 \quad \text{and} \quad \alpha^+ \equiv \frac{\nu}{\tau_w v^*}\frac{dp}{dx} \tag{H5}$$

which may be integrated to yield

$$u^+ = 2\frac{\alpha^{+1/2}}{k}y^{+1/2} + u_s \qquad \text{and} \qquad u_s \approx 0 \tag{H6}$$

Similar relationships have been developed by Townsend (ref. 17) and Spalding (ref. 18). Applying the mass conservation relationship for a two-dimensional channel

$$Re_h = \int_0^{h^+} u^+(y^+)dy^+ \tag{H7}$$

and the definitions

$$h^+ = \frac{\sqrt{2}}{2}Re_h C_f^{1/2} \tag{H8}$$

and

$$\alpha^+ = 2\sqrt{2}\,\frac{1}{C_f^{3/2}}\frac{1}{Re_h}\left(\frac{dp^*}{dx}\right) \qquad \text{and} \qquad \frac{dp^*}{dx} \equiv \frac{h}{\rho_{ave}u_{ave}^2}\frac{dp}{dx} \tag{H9}$$

Substitution, integration, and simplification yields

$$C_{f,sep} = 0.6814\left(\frac{dp^*}{dx}\right)^{-2/3} \tag{H10}$$

The above result is interesting, in that it is not a function of the Reynolds number because the flow near the separation point is dominated by the free-stream flow field pressure gradient. Further, as the pressure gradient becomes more severe, the above model predicts a reducing skin friction. This trend is correct for the local skin friction, but the overall effect of separation is a larger effective skin friction coefficient. Thus, although the above may represent a theoretically plausible analysis, the practical result is still not directly applicable to the quasi-one-dimensional analysis described here. Further, research in this area would certainly be desirable.

APPENDIX I

EXAMPLE PROBLEMS

Several examples are provided, including the FORTRAN NAMELIST inputs and selected portions of the output to help illustrate the simple features of the REMEL code and its ability to simulate more complex features.

Mach 2.5 Supersonic Conical Inlet

The physical problem is described in more detail in the text. The actual geometry and flow fields are modeled using two intervals corresponding to the internal and external inlets, NINTER = 2. The external streamtube and axisymmetric geometry are unknown, therefore, ICAP = 0. The external flow field and boundary layer are modeled (appendix A) using a flat plate skin friction (NCONV = 0), and annular (NCON1V = 1), and external (NCONEV = 1) flows. The internal flow is modeled as a compressible, turbulent axisymmetric duct flow, thus, NCONV = 1, NCON1V = 1, and NCONEV = 0. Finally, the initial conditions are assumed to be approximately free stream, since the bow-shock recovery is approximately 0.9955. Input files and selected portions of the output are provided.

Variable Area Duct with Constant Skin Friction

This problem provides a simple example that was used to verify the REMEL code. A linearly varying (AIV(1) = 2.0 AIV(2) = 2.2), two-dimensional (NCONCV = 1) duct with unit width and constant value skin (NVISCV = 1) friction (CFV = 0.01) are modeled. Initial conditions were arbitrarily chosen with the Mach number set to 1.5 (RMV = 1.5). Again, input files and a portion of the output is provided.

Multiple Ramp External/Internal Forebody

Figure 13 shows a model for a multiple ramp, two-dimensional external forebody. Because of the length of the forebody, viscous displacement may not be neglected, thus a capture streamtube computation is performed and the inputs and portions of the output are provided.

In summary, this appendix has described the actual operation of the REMEL code and the input variables with the FORTRAN NAMELIST input files. Further, several example input and files. It is hoped that this type of information and the extensive theoretical background provided in this report will make the REMEL code and analysis a practical tool for preliminary design analysis.

MACH 2.5 SUPERSONIC CONICAL INLET

Input

```
,
&input
 cfv=.005d0,.005d0,.005d0,.005d0,.005d0
 aiv=10.06d0,10.06d0,11.0589d0,0.0d0,0.0d0
 anv=0.0d0,2.d0,3.6d0,0.0d0,0.d0
 div=3.580,4.1d0,5.2d0,0.0d0,0.d0
 twv=1.d0,1.d0,1.d0,1.d0,1.d0
 ttv=390.d0,390.d0,390.d0,390.d0,390.d0
 chv=0.d0,0.d0,0.d0,0.d0,0.d0
 cpv=0.d0,0.d0,0.d0,0.d0,0.d0
 xiv=0.d0,4.00d0,8.16d0,000.0d0,000.d0
 xv=0.d0,4.0d0,8.16d0,000.0d0,000.d0
 rmv=2.5d0
 pv=1.69199d0
 tv=390.0d0
 rhv=.3639d-3
 uv=2420.25d0
 blv=0.d0,0.00d0,0.00d0,0.d0,0.d0
 arblv=1.d0,1.d0,1.d0,1.d0,1.d0
 ndiffv=0,0,0,0,0
 ishckv=0,0,0,0,0
 iobliq=0,0,0,0,0
 iprsit=0,0,0,0,0
 icowl=0,0,0,0,0
 icap=0
 deltv=0.d0,0.d0,0.d0,0.d0,0.d0
 nconv=0,1,0,0,0
 nconlv=1,1,0,0,0
 nconev=1,0,0,0,0
 nconcv=0,0,0,0,0
 nnozv=0,0,0,0,0
 nviscv=0,0,0,0,0
 rlxv=0.d0,0.d0,0.d0,0.d0,0.d0
 rlyv=.0d0,.0d0,.0d0,.0d0,.0d0
 gammv=1.4d0,1.4d0,1.4d0,1.4d0,1.4d0
 patmo=.09d0
 ninter=2
&end
```

```
NCOUNT=          1
REYNOLDS NUM INLET=  2187499.99999999953
CF AT INLET= 0.243511653201405832E-02
MACH NUMBER INLET=  2.50000000000000000
MASS FLOW RATE INLET(LBM/S)=  285.296298329699994
REYNOLDS NUM EXIT=  28163899.6882536970
CF AT EXIT= 0.156959903040475226E-02
MACH NUMBER EXIT=  2.46927612058021273
MASS FLOW RATE EXIT=  285.296298293933319

NCOUNT=          2
REYNOLDS NUM INLET=  2187499.99999999953
CF AT INLET= 0.243511653201405832E-02
MACH NUMBER INLET=  2.50000000000000000
MASS FLOW RATE INLET(LBM/S)=  285.296298329699994
REYNOLDS NUM EXIT=  28339087.2728763670
CF AT EXIT= 0.156270318238634445E-02
MACH NUMBER EXIT=  2.48761747430185465
MASS FLOW RATE EXIT=  285.296298209389022

NCOUNT=          3
REYNOLDS NUM INLET=  2187499.99999999953
CF AT INLET= 0.243511653201405832E-02
MACH NUMBER INLET=  2.50000000000000000
MASS FLOW RATE INLET(LBM/S)=  285.296298329699994
REYNOLDS NUM EXIT=  28339290.6124872118
CF AT EXIT= 0.156269521757371746E-02
MACH NUMBER EXIT=  2.48763870525716602
MASS FLOW RATE EXIT=  285.296298208663814

**********************************************

INTERVAL NUMBER=          1

PRINT OUT INPUT DATA
CROSS SECTION AREA
INLET AREA=  10.060000000000001
EXIT AREA=  10.060000000000001
DIAMETER(OUTER)
INLET DIAMETER=  3.58000000000000007
EXIT DIAMETER=  4.10000000000000009
ANNULUS DIAMETER(INNER)
INLET ANNULUS DIAMETER= 0.00000000000000000E+00
EXIT ANNULUS DIAMETER=  2.00000000000000000

INITIAL CONDITIONS
MACH NUMBER=  2.50000000000000000
PRESSURE=  1.69199000000000011
TEMPERATURE=  390.000000000000000
DENSITY= 0.363900000000000009E-03
VELOCITY=  2420.25000000000000
```

X POSITION	MACH NUMBER	PRESSURE	P02/P01	ETA KINETIC
0.00000	2.50000	1.69199	1.00000	1.00000
0.04000	2.49985	1.69215	0.99986	0.99997
0.08000	2.49970	1.69231	0.99972	0.99994
0.12000	2.49955	1.69247	0.99958	0.99990
0.16000	2.49940	1.69262	0.99944	0.99987
0.20000	2.49925	1.69278	0.99930	0.99984
0.24000	2.49910	1.69294	0.99916	0.99981
0.28000	2.49896	1.69309	0.99903	0.99978
0.32000	2.49881	1.69325	0.99889	0.99975
0.36000	2.49866	1.69340	0.99875	0.99971
0.40000	2.49852	1.69355	0.99862	0.99968
0.44000	2.49837	1.69371	0.99848	0.99965
0.48000	2.49823	1.69386	0.99835	0.99962
0.52000	2.49808	1.69401	0.99821	0.99959
0.56000	2.49794	1.69416	0.99808	0.99956
0.60000	2.49779	1.69431	0.99794	0.99953
0.64000	2.49765	1.69447	0.99781	0.99950
0.68000	2.49751	1.69461	0.99768	0.99947
0.72000	2.49737	1.69476	0.99755	0.99944
0.76000	2.49723	1.69491	0.99742	0.99941
0.80000	2.49709	1.69506	0.99728	0.99938
0.84000	2.49695	1.69521	0.99715	0.99935
0.88000	2.49681	1.69536	0.99703	0.99932
0.92000	2.49667	1.69550	0.99690	0.99929
0.96000	2.49653	1.69565	0.99677	0.99926
1.00000	2.49639	1.69579	0.99664	0.99923
1.04000	2.49626	1.69594	0.99651	0.99920
1.08000	2.49612	1.69608	0.99639	0.99917
1.12000	2.49598	1.69623	0.99626	0.99914
1.16000	2.49585	1.69637	0.99613	0.99911
1.20000	2.49571	1.69651	0.99601	0.99909
1.24000	2.49558	1.69665	0.99588	0.99906
1.28000	2.49545	1.69680	0.99576	0.99903
1.32000	2.49531	1.69694	0.99564	0.99900
1.36000	2.49518	1.69708	0.99551	0.99897
1.40000	2.49505	1.69722	0.99539	0.99894
1.44000	2.49492	1.69735	0.99527	0.99891
1.48000	2.49478	1.69749	0.99515	0.99889
1.52000	2.49465	1.69763	0.99502	0.99886
1.56000	2.49452	1.69777	0.99490	0.99883
1.60000	2.49439	1.69791	0.99478	0.99880
1.64000	2.49427	1.69804	0.99466	0.99878
1.68000	2.49414	1.69818	0.99455	0.99875
1.72000	2.49401	1.69831	0.99443	0.99872
1.76000	2.49388	1.69845	0.99431	0.99869
1.80000	2.49376	1.69858	0.99419	0.99867
1.84000	2.49363	1.69871	0.99407	0.99864
1.88000	2.49351	1.69885	0.99396	0.99861
1.92000	2.49338	1.69898	0.99384	0.99859
1.96000	2.49326	1.69911	0.99373	0.99856
2.00000	2.49313	1.69924	0.99361	0.99853
2.04000	2.49301	1.69937	0.99350	0.99851
2.08000	2.49289	1.69950	0.99338	0.99848
2.12000	2.49276	1.69963	0.99327	0.99846
2.16000	2.49264	1.69976	0.99316	0.99843
2.20000	2.49252	1.69989	0.99305	0.99840
2.24000	2.49240	1.70002	0.99294	0.99838
2.28000	2.49228	1.70015	0.99282	0.99835
2.32000	2.49216	1.70027	0.99271	0.99833

2.36000	2.49204	1.70040	0.99260	0.99830
2.40000	2.49192	1.70052	0.99249	0.99828
2.44000	2.49181	1.70065	0.99238	0.99825
2.48000	2.49169	1.70077	0.99228	0.99823
2.52000	2.49157	1.70090	0.99217	0.99820
2.56000	2.49146	1.70102	0.99206	0.99818
2.60000	2.49134	1.70114	0.99195	0.99815
2.64000	2.49123	1.70126	0.99185	0.99813
2.68000	2.49111	1.70139	0.99174	0.99810
2.72000	2.49100	1.70151	0.99164	0.99808
2.76000	2.49088	1.70163	0.99153	0.99805
2.80000	2.49077	1.70175	0.99143	0.99803
2.84000	2.49066	1.70187	0.99132	0.99801
2.88000	2.49055	1.70198	0.99122	0.99798
2.92000	2.49044	1.70210	0.99112	0.99796
2.96000	2.49032	1.70222	0.99102	0.99793
3.00000	2.49021	1.70234	0.99091	0.99791
3.04000	2.49010	1.70245	0.99081	0.99789
3.08000	2.49000	1.70257	0.99071	0.99786
3.12000	2.48989	1.70268	0.99061	0.99784
3.16000	2.48978	1.70280	0.99051	0.99782
3.20000	2.48967	1.70291	0.99041	0.99779
3.24000	2.48957	1.70303	0.99031	0.99777
3.28000	2.48946	1.70314	0.99022	0.99775
3.32000	2.48935	1.70325	0.99012	0.99773
3.36000	2.48925	1.70336	0.99002	0.99770
3.40000	2.48914	1.70348	0.98992	0.99768
3.44000	2.48904	1.70359	0.98983	0.99766
3.48000	2.48894	1.70370	0.98973	0.99764
3.52000	2.48883	1.70381	0.98964	0.99762
3.56000	2.48873	1.70391	0.98954	0.99759
3.60000	2.48863	1.70402	0.98945	0.99757
3.64000	2.48853	1.70413	0.98936	0.99755
3.68000	2.48843	1.70424	0.98926	0.99753
3.72000	2.48833	1.70435	0.98917	0.99751
3.76000	2.48823	1.70445	0.98908	0.99749
3.80000	2.48813	1.70456	0.98899	0.99746
3.84000	2.48803	1.70466	0.98890	0.99744
3.88000	2.48793	1.70477	0.98881	0.99742
3.92000	2.48783	1.70487	0.98872	0.99740
3.96000	2.48774	1.70497	0.98863	0.99738
4.00000	2.48764	1.70508	0.98854	0.99736

X POSITION	TEMPERATURE	DENSITY	VELCTY
0.00000	390.00000	0.0003639	2420.25000
0.04000	390.02617	0.0003639	2420.18505
0.08000	390.05224	0.0003639	2420.12032
0.12000	390.07822	0.0003639	2420.05584
0.16000	390.10410	0.0003639	2419.99158
0.20000	390.12989	0.0003639	2419.92756
0.24000	390.15558	0.0003640	2419.86378
0.28000	390.18118	0.0003640	2419.80022
0.32000	390.20668	0.0003640	2419.73690
0.36000	390.23209	0.0003640	2419.67381
0.40000	390.25740	0.0003640	2419.61096
0.44000	390.28262	0.0003640	2419.54834
0.48000	390.30775	0.0003640	2419.48595
0.52000	390.33278	0.0003640	2419.42380
0.56000	390.35772	0.0003640	2419.36188

0.60000	390.38256	0.0003640	2419.30019
0.64000	390.40730	0.0003641	2419.23874
0.68000	390.43196	0.0003641	2419.17752
0.72000	390.45651	0.0003641	2419.11653
0.76000	390.48098	0.0003641	2419.05577
0.80000	390.50534	0.0003641	2418.99525
0.84000	390.52962	0.0003641	2418.93497
0.88000	390.55380	0.0003641	2418.87491
0.92000	390.57788	0.0003641	2418.81509
0.96000	390.60187	0.0003641	2418.75550
1.00000	390.62577	0.0003641	2418.69615
1.04000	390.64957	0.0003641	2418.63703
1.08000	390.67328	0.0003642	2418.57814
1.12000	390.69689	0.0003642	2418.51949
1.16000	390.72041	0.0003642	2418.46107
1.20000	390.74383	0.0003642	2418.40288
1.24000	390.76716	0.0003642	2418.34493
1.28000	390.79039	0.0003642	2418.28720
1.32000	390.81353	0.0003642	2418.22972
1.36000	390.83658	0.0003642	2418.17246
1.40000	390.85953	0.0003642	2418.11544
1.44000	390.88239	0.0003642	2418.05865
1.48000	390.90515	0.0003642	2418.00210
1.52000	390.92782	0.0003642	2417.94578
1.56000	390.95039	0.0003643	2417.88969
1.60000	390.97287	0.0003643	2417.83384
1.64000	390.99525	0.0003643	2417.77821
1.68000	391.01754	0.0003643	2417.72283
1.72000	391.03974	0.0003643	2417.66767
1.76000	391.06184	0.0003643	2417.61275
1.80000	391.08385	0.0003643	2417.55806
1.84000	391.10576	0.0003643	2417.50361
1.88000	391.12758	0.0003643	2417.44938
1.92000	391.14930	0.0003643	2417.39540
1.96000	391.17093	0.0003643	2417.34164
2.00000	391.19247	0.0003643	2417.28812
2.04000	391.21391	0.0003644	2417.23483
2.08000	391.23525	0.0003644	2417.18177
2.12000	391.25651	0.0003644	2417.12895
2.16000	391.27766	0.0003644	2417.07636
2.20000	391.29873	0.0003644	2417.02401
2.24000	391.31970	0.0003644	2416.97188
2.28000	391.34057	0.0003644	2416.92000
2.32000	391.36135	0.0003644	2416.86834
2.36000	391.38204	0.0003644	2416.81692
2.40000	391.40263	0.0003644	2416.76573
2.44000	391.42313	0.0003644	2416.71477
2.48000	391.44353	0.0003644	2416.66405
2.52000	391.46384	0.0003644	2416.61356
2.56000	391.48406	0.0003645	2416.56330
2.60000	391.50418	0.0003645	2416.51328
2.64000	391.52421	0.0003645	2416.46349
2.68000	391.54414	0.0003645	2416.41393
2.72000	391.56398	0.0003645	2416.36461
2.76000	391.58372	0.0003645	2416.31551
2.80000	391.60337	0.0003645	2416.26666
2.84000	391.62293	0.0003645	2416.21803
2.88000	391.64239	0.0003645	2416.16964
2.92000	391.66176	0.0003645	2416.12148
2.96000	391.68103	0.0003645	2416.07356

```
    3.00000      391.70021        0.0003645     2416.02587
    3.04000      391.71930        0.0003645     2415.97841
    3.08000      391.73829        0.0003646     2415.93119
    3.12000      391.75718        0.0003646     2415.88419
    3.16000      391.77599        0.0003646     2415.83743
    3.20000      391.79469        0.0003646     2415.79091
    3.24000      391.81331        0.0003646     2415.74462
    3.28000      391.83183        0.0003646     2415.69856
    3.32000      391.85025        0.0003646     2415.65273
    3.36000      391.86859        0.0003646     2415.60714
    3.40000      391.88682        0.0003646     2415.56178
    3.44000      391.90497        0.0003646     2415.51665
    3.48000      391.92302        0.0003646     2415.47176
    3.52000      391.94097        0.0003646     2415.42710
    3.56000      391.95884        0.0003646     2415.38267
    3.60000      391.97660        0.0003646     2415.33848
    3.64000      391.99428        0.0003646     2415.29452
    3.68000      392.01186        0.0003647     2415.25079
    3.72000      392.02934        0.0003647     2415.20730
    3.76000      392.04673        0.0003647     2415.16404
    3.80000      392.06403        0.0003647     2415.12101
    3.84000      392.08123        0.0003647     2415.07821
    3.88000      392.09834        0.0003647     2415.03565
    3.92000      392.11536        0.0003647     2414.99332
    3.96000      392.13228        0.0003647     2414.95123
    4.00000      392.14911        0.0003647     2414.90937
PRESSURE ERROR= 0.773423717629298773E-02

NCOUNT=          1
REYNOLDS NUM INLET=  6278617.83875040361
CF AT INLET= 0.149084455092967283E-02
MACH NUMBER INLET=  2.48763870525716602
MASS FLOW RATE INLET(LBM/S)=  285.296298208663814
REYNOLDS NUM EXIT=  4292881.01663589478
CF AT EXIT= 0.160250492736515151E-02
MACH NUMBER EXIT=  2.44746023471743768
MASS FLOW RATE EXIT=  285.296332954555169

NCOUNT=          2
REYNOLDS NUM INLET=  6278617.83875040361
CF AT INLET= 0.149084455092967283E-02
MACH NUMBER INLET=  2.48763870525716602
MASS FLOW RATE INLET(LBM/S)=  285.296298208663814
REYNOLDS NUM EXIT=  4399879.67962897150
CF AT EXIT= 0.157228395956136098E-02
MACH NUMBER EXIT=  2.52029755358157770
MASS FLOW RATE EXIT=  285.296299423526364

NCOUNT=          3
REYNOLDS NUM INLET=  6278617.83875040361
CF AT INLET= 0.149084455092967283E-02
MACH NUMBER INLET=  2.48763870525716602
MASS FLOW RATE INLET(LBM/S)=  285.296298208663814
REYNOLDS NUM EXIT=  4400846.40356329549
CF AT EXIT= 0.157201616258644309E-02
MACH NUMBER EXIT=  2.52094857446618126
MASS FLOW RATE EXIT=  285.296299260349883

NCOUNT=          4
REYNOLDS NUM INLET=  6278617.83875040361
```

CF AT INLET= 0.14908445092967283E-02
MACH NUMBER INLET= 2.48763870525716602
MASS FLOW RATE INLET(LBM/S)= 285.296298208663814
REYNOLDS NUM EXIT= 4400854.97277871310
CF AT EXIT= 0.15720137892142435 8E-02
MACH NUMBER EXIT= 2.52095434468284907
MASS FLOW RATE EXIT= 285.296299258915951

****

INTERVAL NUMBER= 2

PRINT OUT INPUT DATA
CROSS SECTION AREA
INLET AREA= 10.060000000000001
EXIT AREA= 11.058900000000000
DIAMETER(OUTER)
INLET DIAMETER= 4.10000000000000009
EXIT DIAMETER= 5.19999999999999996
ANNULUS DIAMETER(INNER)
INLET ANNULUS DIAMETER= 2.00000000000000000
EXIT ANNULUS DIAMETER= 3.60000000000000009

INITIAL CONDITIONS
MACH NUMBER= 2.48763870525716602
PRESSURE= 1.70507625195991608
TEMPERATURE= 392.149105097107906
DENSITY= 0.364704773810158077E-03
VELOCITY= 2414.90936744580210

X POSITION	MACH NUMBER	PRESSURE	P02/P01	ETA KINETIC
4.00000	2.48764	1.70508	1.00000	1.00000
4.04160	2.48802	1.70298	0.99936	0.99985
4.08320	2.48839	1.70090	0.99872	0.99970
4.12480	2.48877	1.69881	0.99808	0.99956
4.16640	2.48914	1.69674	0.99744	0.99941
4.20800	2.48952	1.69466	0.99680	0.99926
4.24960	2.48989	1.69260	0.99617	0.99911
4.29120	2.49026	1.69054	0.99553	0.99897
4.33280	2.49063	1.68848	0.99489	0.99882
4.37440	2.49100	1.68643	0.99426	0.99867
4.41600	2.49137	1.68438	0.99362	0.99852
4.45760	2.49174	1.68234	0.99299	0.99837
4.49920	2.49211	1.68031	0.99235	0.99823
4.54080	2.49248	1.67828	0.99172	0.99808
4.58240	2.49284	1.67625	0.99108	0.99793
4.62400	2.49321	1.67423	0.99045	0.99778
4.66560	2.49357	1.67221	0.98982	0.99763
4.70720	2.49393	1.67020	0.98919	0.99749
4.74880	2.49429	1.66820	0.98856	0.99734
4.79040	2.49465	1.66620	0.98792	0.99719
4.83200	2.49501	1.66420	0.98729	0.99704
4.87360	2.49537	1.66221	0.98666	0.99689
4.91520	2.49573	1.66023	0.98603	0.99675
4.95680	2.49609	1.65825	0.98540	0.99660
4.99840	2.49644	1.65627	0.98478	0.99645
5.04000	2.49680	1.65430	0.98415	0.99630
5.08160	2.49715	1.65233	0.98352	0.99615
5.12320	2.49751	1.65037	0.98289	0.99601

5.16480	2.49786	1.64842	0.98227	0.99586
5.20640	2.49821	1.64647	0.98164	0.99571
5.24800	2.49856	1.64452	0.98101	0.99556
5.28960	2.49891	1.64258	0.98039	0.99541
5.33120	2.49926	1.64064	0.97976	0.99527
5.37280	2.49961	1.63871	0.97914	0.99512
5.41440	2.49995	1.63678	0.97852	0.99497
5.45600	2.50030	1.63486	0.97789	0.99482
5.49760	2.50064	1.63294	0.97727	0.99467
5.53920	2.50099	1.63103	0.97665	0.99453
5.58080	2.50133	1.62912	0.97603	0.99438
5.62240	2.50167	1.62722	0.97541	0.99423
5.66400	2.50202	1.62532	0.97478	0.99408
5.70560	2.50236	1.62342	0.97416	0.99393
5.74720	2.50270	1.62153	0.97354	0.99379
5.78880	2.50303	1.61965	0.97293	0.99364
5.83040	2.50337	1.61777	0.97231	0.99349
5.87200	2.50371	1.61589	0.97169	0.99334
5.91360	2.50405	1.61402	0.97107	0.99319
5.95520	2.50438	1.61215	0.97045	0.99305
5.99680	2.50472	1.61029	0.96984	0.99290
6.03840	2.50505	1.60843	0.96922	0.99275
6.08000	2.50538	1.60658	0.96860	0.99260
6.12160	2.50571	1.60473	0.96799	0.99245
6.16320	2.50605	1.60288	0.96737	0.99231
6.20480	2.50638	1.60104	0.96676	0.99216
6.24640	2.50670	1.59920	0.96615	0.99201
6.28800	2.50703	1.59737	0.96553	0.99186
6.32960	2.50736	1.59555	0.96492	0.99171
6.37120	2.50769	1.59372	0.96431	0.99157
6.41280	2.50801	1.59190	0.96369	0.99142
6.45440	2.50834	1.59009	0.96308	0.99127
6.49600	2.50866	1.58828	0.96247	0.99112
6.53760	2.50899	1.58648	0.96186	0.99097
6.57920	2.50931	1.58467	0.96125	0.99083
6.62080	2.50963	1.58288	0.96064	0.99068
6.66240	2.50995	1.58108	0.96003	0.99053
6.70400	2.51027	1.57930	0.95942	0.99038
6.74560	2.51059	1.57751	0.95881	0.99023
6.78720	2.51091	1.57573	0.95821	0.99008
6.82880	2.51123	1.57396	0.95760	0.98994
6.87040	2.51154	1.57219	0.95699	0.98979
6.91200	2.51186	1.57042	0.95639	0.98964
6.95360	2.51217	1.56866	0.95578	0.98949
6.99520	2.51249	1.56690	0.95518	0.98934
7.03680	2.51280	1.56514	0.95457	0.98920
7.07840	2.51311	1.56339	0.95397	0.98905
7.12000	2.51342	1.56164	0.95336	0.98890
7.16160	2.51374	1.55990	0.95276	0.98875
7.20320	2.51405	1.55816	0.95216	0.98860
7.24480	2.51435	1.55643	0.95155	0.98845
7.28640	2.51466	1.55470	0.95095	0.98831
7.32800	2.51497	1.55297	0.95035	0.98816
7.36960	2.51528	1.55125	0.94975	0.98801
7.41120	2.51558	1.54953	0.94915	0.98786
7.45280	2.51589	1.54782	0.94855	0.98771
7.49440	2.51619	1.54611	0.94795	0.98757
7.53600	2.51650	1.54440	0.94735	0.98742
7.57760	2.51680	1.54270	0.94675	0.98727
7.61920	2.51710	1.54100	0.94615	0.98712

7.66080	2.51740	1.53931	0.94555	0.98697
7.70240	2.51770	1.53762	0.94496	0.98682
7.74400	2.51800	1.53593	0.94436	0.98668
7.78560	2.51830	1.53425	0.94376	0.98653
7.82720	2.51860	1.53257	0.94317	0.98638
7.86880	2.51890	1.53089	0.94257	0.98623
7.91040	2.51919	1.52922	0.94198	0.98608
7.95200	2.51949	1.52756	0.94138	0.98593
7.99360	2.51978	1.52589	0.94079	0.98579
8.03520	2.52008	1.52423	0.94020	0.98564
8.07680	2.52037	1.52258	0.93960	0.98549
8.11840	2.52066	1.52093	0.93901	0.98534
8.16000	2.52095	1.51928	0.93842	0.98519

X POSITION	TEMPERATURE	DENSITY	VELCTY
4.00000	392.14911	0.0003647	2414.90937
4.04160	392.08323	0.0003643	2415.07326
4.08320	392.01753	0.0003639	2415.23669
4.12480	391.95201	0.0003635	2415.39965
4.16640	391.88667	0.0003632	2415.56216
4.20800	391.82152	0.0003628	2415.72420
4.24960	391.75654	0.0003624	2415.88579
4.29120	391.69174	0.0003620	2416.04692
4.33280	391.62712	0.0003616	2416.20760
4.37440	391.56268	0.0003613	2416.36783
4.41600	391.49842	0.0003609	2416.52760
4.45760	391.43433	0.0003605	2416.68692
4.49920	391.37043	0.0003601	2416.84579
4.54080	391.30669	0.0003597	2417.00421
4.58240	391.24314	0.0003594	2417.16218
4.62400	391.17975	0.0003590	2417.31971
4.66560	391.11655	0.0003586	2417.47680
4.70720	391.05351	0.0003582	2417.63344
4.74880	390.99066	0.0003579	2417.78964
4.79040	390.92797	0.0003575	2417.94539
4.83200	390.86546	0.0003571	2418.10071
4.87360	390.80312	0.0003568	2418.25559
4.91520	390.74095	0.0003564	2418.41003
4.95680	390.67896	0.0003560	2418.56404
4.99840	390.61713	0.0003557	2418.71761
5.04000	390.55548	0.0003553	2418.87074
5.08160	390.49399	0.0003549	2419.02345
5.12320	390.43268	0.0003546	2419.17572
5.16480	390.37153	0.0003542	2419.32756
5.20640	390.31056	0.0003538	2419.47898
5.24800	390.24975	0.0003535	2419.62997
5.28960	390.18911	0.0003531	2419.78053
5.33120	390.12864	0.0003527	2419.93066
5.37280	390.06833	0.0003524	2420.08037
5.41440	390.00819	0.0003520	2420.22966
5.45600	389.94822	0.0003517	2420.37853
5.49760	389.88841	0.0003513	2420.52698
5.53920	389.82877	0.0003509	2420.67501
5.58080	389.76929	0.0003506	2420.82261
5.62240	389.70998	0.0003502	2420.96981
5.66400	389.65083	0.0003499	2421.11658
5.70560	389.59185	0.0003495	2421.26295
5.74720	389.53303	0.0003492	2421.40889
5.78880	389.47437	0.0003488	2421.55443

5.83040	389.41587	0.0003485	2421.69955
5.87200	389.35754	0.0003481	2421.84427
5.91360	389.29936	0.0003478	2421.98857
5.95520	389.24135	0.0003474	2422.13247
5.99680	389.18350	0.0003471	2422.27596
6.03840	389.12581	0.0003467	2422.41905
6.08000	389.06827	0.0003464	2422.56173
6.12160	389.01090	0.0003460	2422.70400
6.16320	388.95369	0.0003457	2422.84588
6.20480	388.89663	0.0003453	2422.98735
6.24640	388.83973	0.0003450	2423.12843
6.28800	388.78299	0.0003446	2423.26910
6.32960	388.72641	0.0003443	2423.40938
6.37120	388.66999	0.0003439	2423.54926
6.41280	388.61372	0.0003436	2423.68874
6.45440	388.55760	0.0003433	2423.82783
6.49600	388.50165	0.0003429	2423.96652
6.53760	388.44584	0.0003426	2424.10483
6.57920	388.39020	0.0003422	2424.24274
6.62080	388.33470	0.0003419	2424.38026
6.66240	388.27936	0.0003416	2424.51739
6.70400	388.22418	0.0003412	2424.65413
6.74560	388.16915	0.0003409	2424.79049
6.78720	388.11427	0.0003405	2424.92646
6.82880	388.05954	0.0003402	2425.06204
6.87040	388.00496	0.0003399	2425.19724
6.91200	387.95054	0.0003395	2425.33205
6.95360	387.89627	0.0003392	2425.46649
6.99520	387.84215	0.0003389	2425.60054
7.03680	387.78818	0.0003385	2425.73421
7.07840	387.73436	0.0003382	2425.86751
7.12000	387.68068	0.0003379	2426.00042
7.16160	387.62716	0.0003375	2426.13296
7.20320	387.57379	0.0003372	2426.26512
7.24480	387.52057	0.0003369	2426.39691
7.28640	387.46749	0.0003366	2426.52832
7.32800	387.41456	0.0003362	2426.65936
7.36960	387.36178	0.0003359	2426.79003
7.41120	387.30915	0.0003356	2426.92033
7.45280	387.25666	0.0003353	2427.05025
7.49440	387.20432	0.0003349	2427.17981
7.53600	387.15213	0.0003346	2427.30900
7.57760	387.10008	0.0003343	2427.43782
7.61920	387.04818	0.0003340	2427.56628
7.66080	386.99642	0.0003336	2427.69437
7.70240	386.94480	0.0003333	2427.82209
7.74400	386.89333	0.0003330	2427.94945
7.78560	386.84201	0.0003327	2428.07645
7.82720	386.79083	0.0003323	2428.20309
7.86880	386.73979	0.0003320	2428.32937
7.91040	386.68889	0.0003317	2428.45529
7.95200	386.63814	0.0003314	2428.58085
7.99360	386.58752	0.0003311	2428.70605
8.03520	386.53705	0.0003308	2428.83089
8.07680	386.48672	0.0003304	2428.95538
8.11840	386.43653	0.0003301	2429.07951
8.16000	386.38649	0.0003298	2429.20329

PRESSURE ERROR= 0.108967128294555918
SOLUTION COMPLETED

VARIABLE AREA DUCT WITH CONSTANT SKIN FRICTION

Input

```
,
&input
 cfv=.010d0,.010d0,.000d0,.000d0,.005d0,
 aiv=2.00d0,2.200d0,0.00d0,0.0000d0,.0000d0,
 anv=0.d0,0.d0,0.0d0,0.0d0,0.d0,
 div=0.0d0,0.0d0,0.0d0,0.0d0,0.d0,
 twv=1.d0,1.d0,1.d0,1.d0,1.d0,
 ttv=390.d0,390.d0,390.d0,390.d0,390.d0,
 chv=0.d0,0.d0,0.d0,0.d0,0.d0,
 cpv=0.d0,0.d0,0.d0,0.d0,0.d0,
 xiv=.01d0,1.000d0,0.000d0,0.000d0,0.000d0,
 xv=.01d0,1.000d0,0.000d0,0.000d0,0.000d0,
 rmv=1.50d0,
 pv=3.46760,
 tv=394.08d0,
 rhv=7.3820d-4,
 uv=1167.76d0,
 blv=0.d0,0.00d0,0.00d0,0.d0,0.d0,
 arblv=1.d0,1.d0,1.d0,1.d0,1.d0,
 ndiffv=0,0,0,0,0,
 ishckv=0,0,0,0,0,
 iobliq=0,0,0,0,0,
 iprsit=0,0,0,0,0,
 icowl=0,0,0,0,0,
 icap=0,
 deltv=0.0,00.d0,00.d0,0.d0,0.d0,
 nprofl=0,0,0,0,0,
 proloc=0.d0,0.d0,0.d0,0.d0,0.d0,
 ymxave=0.0d0,0.d0,0.d0,0.d0,0.d0,
 ymnave=0.0d0,0.d0,0.d0,0.d0,0.d0,
 pexp=7.d0,
 nconv=2,2,0,0,0,
 nconlv=0,0,0,0,0,
 nconev=0,0,0,0,0,
 nconcv=1,1,0,0,0,
 nnozv=0,0,0,0,0,
 nviscv=1,1,0,0,0,
 rlxv=.000d0,.000d0,0.000d0,0.000d0,0.000d0,
 rlyv=1.00000d0,1.000d0,0.000d0,.000d0,.0000d0,
 gammv=1.4d0,1.4d0,1.4d0,1.4d0,1.4d0,
 patmo=.09d0,
 ninter=1,
&end
```

```
NCOUNT=          1
REYNOLDS NUM INLET=  1457736.08520740340
CF AT INLET= 0.10000000000000002E-01
MACH NUMBER INLET=  1.50000000000000000
MASS FLOW RATE INLET(LBM/S)=  55.5154038207999925
REYNOLDS NUM EXIT=  1380296.29687077436
CF AT EXIT= 0.10000000000000002E-01
MACH NUMBER EXIT=  1.62759939837821022
MASS FLOW RATE EXIT=  55.5154041540652514

NCOUNT=          2
REYNOLDS NUM INLET=  1457736.08520740340
CF AT INLET= 0.10000000000000002E-01
MACH NUMBER INLET=  1.50000000000000000
MASS FLOW RATE INLET(LBM/S)=  55.5154038207999925
REYNOLDS NUM EXIT=  1380296.29687077436
CF AT EXIT= 0.10000000000000002E-01
MACH NUMBER EXIT=  1.62759939837821022
MASS FLOW RATE EXIT=  55.5154041540652514

NCOUNT=          3
REYNOLDS NUM INLET=  1457736.08520740340
CF AT INLET= 0.10000000000000002E-01
MACH NUMBER INLET=  1.50000000000000000
MASS FLOW RATE INLET(LBM/S)=  55.5154038207999925
REYNOLDS NUM EXIT=  1380296.29687077436
CF AT EXIT= 0.10000000000000002E-01
MACH NUMBER EXIT=  1.62759939837821022
MASS FLOW RATE EXIT=  55.5154041540652514

NCOUNT=          4
REYNOLDS NUM INLET=  1457736.08520740340
CF AT INLET= 0.10000000000000002E-01
MACH NUMBER INLET=  1.50000000000000000
MASS FLOW RATE INLET(LBM/S)=  55.5154038207999925
REYNOLDS NUM EXIT=  1380296.29687077436
CF AT EXIT= 0.10000000000000002E-01
MACH NUMBER EXIT=  1.62759939837821022
MASS FLOW RATE EXIT=  55.5154041540652514

NCOUNT=          5
REYNOLDS NUM INLET=  1457736.08520740340
CF AT INLET= 0.10000000000000002E-01
MACH NUMBER INLET=  1.50000000000000000
MASS FLOW RATE INLET(LBM/S)=  55.5154038207999925
REYNOLDS NUM EXIT=  1380296.29687077436
CF AT EXIT= 0.10000000000000002E-01
MACH NUMBER EXIT=  1.62759939837821022
MASS FLOW RATE EXIT=  55.5154041540652514

NCOUNT=          6
REYNOLDS NUM INLET=  1457736.08520740340
CF AT INLET= 0.10000000000000002E-01
```

```
MACH NUMBER INLET=  1.50000000000000000
MASS FLOW RATE INLET(LBM/S)=  55.5154038207999925
REYNOLDS NUM EXIT=  1380296.29687077436
CF AT EXIT= 0.10000000000000002E-01
MACH NUMBER EXIT=  1.62759939837821022
MASS FLOW RATE EXIT=  55.5154041540652514

NCOUNT=          7
REYNOLDS NUM INLET=  1457736.08520740340
CF AT INLET= 0.10000000000000002E-01
MACH NUMBER INLET=  1.50000000000000000
MASS FLOW RATE INLET(LBM/S)=  55.5154038207999925
REYNOLDS NUM EXIT=  1380296.29687077436
CF AT EXIT= 0.10000000000000002E-01
MACH NUMBER EXIT=  1.62759939837821022
MASS FLOW RATE EXIT=  55.5154041540652514

NCOUNT=          8
REYNOLDS NUM INLET=  1457736.08520740340
CF AT INLET= 0.10000000000000002E-01
MACH NUMBER INLET=  1.50000000000000000
MASS FLOW RATE INLET(LBM/S)=  55.5154038207999925
REYNOLDS NUM EXIT=  1380296.29687077436
CF AT EXIT= 0.10000000000000002E-01
MACH NUMBER EXIT=  1.62759939837821022
MASS FLOW RATE EXIT=  55.5154041540652514

NCOUNT=          9
REYNOLDS NUM INLET=  1457736.08520740340
CF AT INLET= 0.10000000000000002E-01
MACH NUMBER INLET=  1.50000000000000000
MASS FLOW RATE INLET(LBM/S)=  55.5154038207999925
REYNOLDS NUM EXIT=  1380296.29687077436
CF AT EXIT= 0.10000000000000002E-01
MACH NUMBER EXIT=  1.62759939837821022
MASS FLOW RATE EXIT=  55.5154041540652514

NCOUNT=         10
REYNOLDS NUM INLET=  1457736.08520740340
CF AT INLET= 0.10000000000000002E-01
MACH NUMBER INLET=  1.50000000000000000
MASS FLOW RATE INLET(LBM/S)=  55.5154038207999925
REYNOLDS NUM EXIT=  1380296.29687077436
CF AT EXIT= 0.10000000000000002E-01
MACH NUMBER EXIT=  1.62759939837821022
MASS FLOW RATE EXIT=  55.5154041540652514

**********************************************

INTERVAL NUMBER=          1

PRINT OUT INPUT DATA
CROSS SECTION AREA
INLET AREA=  2.00000000000000000
EXIT AREA=  2.19999999999999996
CHANNEL DIMENSIONS
INLET CHANNEL HEIGHT=  1.00000000000000000
EXIT CHANNEL HEIGHT=  1.00000000000000000
INLET CHANNEL WIDTH= 0.00000000000000000E+00
EXIT CHANNEL WIDTH= 0.00000000000000000E+00
```

INITIAL CONDITIONS
MACH NUMBER= 1.5000000000000000
PRESSURE= 3.4676000000000002
TEMPERATURE= 394.079999999999984
DENSITY= 0.738200000000000000E-03
VELOCITY= 1167.75999999999999

X POSITION	MACH NUMBER	PRESSURE	P02/P01	ETA KINETIC
0.01000	1.50000	3.46760	1.00000	1.00000
0.01990	1.50147	3.45970	0.99984	0.99990
0.02980	1.50293	3.45184	0.99969	0.99980
0.03970	1.50438	3.44403	0.99953	0.99970
0.04960	1.50584	3.43624	0.99938	0.99960
0.05950	1.50728	3.42850	0.99922	0.99950
0.06940	1.50873	3.42079	0.99906	0.99940
0.07930	1.51016	3.41312	0.99891	0.99930
0.08920	1.51160	3.40549	0.99875	0.99920
0.09910	1.51303	3.39790	0.99859	0.99911
0.10900	1.51445	3.39034	0.99843	0.99901
0.11890	1.51587	3.38281	0.99828	0.99891
0.12880	1.51729	3.37532	0.99812	0.99881
0.13870	1.51870	3.36787	0.99796	0.99870
0.14860	1.52010	3.36045	0.99781	0.99860
0.15850	1.52151	3.35307	0.99765	0.99850
0.16840	1.52290	3.34572	0.99749	0.99840
0.17830	1.52430	3.33841	0.99733	0.99830
0.18820	1.52569	3.33113	0.99717	0.99820
0.19810	1.52707	3.32388	0.99702	0.99810
0.20800	1.52845	3.31667	0.99686	0.99800
0.21790	1.52983	3.30949	0.99670	0.99790
0.22780	1.53120	3.30234	0.99654	0.99780
0.23770	1.53257	3.29522	0.99638	0.99770
0.24760	1.53394	3.28814	0.99622	0.99760
0.25750	1.53530	3.28109	0.99607	0.99750
0.26740	1.53666	3.27407	0.99591	0.99739
0.27730	1.53801	3.26708	0.99575	0.99729
0.28720	1.53936	3.26013	0.99559	0.99719
0.29710	1.54070	3.25320	0.99543	0.99709
0.30700	1.54204	3.24631	0.99527	0.99699
0.31690	1.54338	3.23944	0.99511	0.99689
0.32680	1.54471	3.23261	0.99495	0.99678
0.33670	1.54604	3.22580	0.99479	0.99668
0.34660	1.54737	3.21903	0.99463	0.99658
0.35650	1.54869	3.21229	0.99447	0.99648
0.36640	1.55001	3.20557	0.99431	0.99638
0.37630	1.55132	3.19889	0.99415	0.99627
0.38620	1.55263	3.19223	0.99399	0.99617
0.39610	1.55394	3.18560	0.99383	0.99607
0.40600	1.55524	3.17900	0.99367	0.99597
0.41590	1.55654	3.17243	0.99351	0.99586
0.42580	1.55784	3.16589	0.99335	0.99576
0.43570	1.55913	3.15937	0.99319	0.99566
0.44560	1.56042	3.15289	0.99303	0.99556
0.45550	1.56171	3.14643	0.99287	0.99545
0.46540	1.56299	3.13999	0.99271	0.99535
0.47530	1.56427	3.13359	0.99255	0.99525
0.48520	1.56555	3.12721	0.99239	0.99514
0.49510	1.56682	3.12086	0.99223	0.99504

0.50500	1.56809	3.11453	0.99207	0.99494
0.51490	1.56935	3.10823	0.99191	0.99483
0.52480	1.57061	3.10196	0.99175	0.99473
0.53470	1.57187	3.09571	0.99158	0.99463
0.54460	1.57313	3.08949	0.99142	0.99452
0.55450	1.57438	3.08330	0.99126	0.99442
0.56440	1.57563	3.07713	0.99110	0.99432
0.57430	1.57687	3.07098	0.99094	0.99421
0.58420	1.57811	3.06486	0.99078	0.99411
0.59410	1.57935	3.05877	0.99062	0.99401
0.60400	1.58059	3.05270	0.99045	0.99390
0.61390	1.58182	3.04665	0.99029	0.99380
0.62380	1.58305	3.04063	0.99013	0.99369
0.63370	1.58428	3.03464	0.98997	0.99359
0.64360	1.58550	3.02866	0.98981	0.99348
0.65350	1.58672	3.02272	0.98964	0.99338
0.66340	1.58794	3.01679	0.98948	0.99328
0.67330	1.58915	3.01089	0.98932	0.99317
0.68320	1.59036	3.00501	0.98916	0.99307
0.69310	1.59157	2.99916	0.98899	0.99296
0.70300	1.59277	2.99333	0.98883	0.99286
0.71290	1.59398	2.98752	0.98867	0.99275
0.72280	1.59518	2.98173	0.98851	0.99265
0.73270	1.59637	2.97597	0.98834	0.99254
0.74260	1.59756	2.97023	0.98818	0.99244
0.75250	1.59875	2.96451	0.98802	0.99233
0.76240	1.59994	2.95881	0.98786	0.99223
0.77230	1.60113	2.95314	0.98769	0.99212
0.78220	1.60231	2.94749	0.98753	0.99202
0.79210	1.60348	2.94186	0.98737	0.99191
0.80200	1.60466	2.93625	0.98720	0.99181
0.81190	1.60583	2.93066	0.98704	0.99170
0.82180	1.60700	2.92510	0.98688	0.99160
0.83170	1.60817	2.91955	0.98671	0.99149
0.84160	1.60933	2.91403	0.98655	0.99139
0.85150	1.61050	2.90853	0.98639	0.99128
0.86140	1.61166	2.90305	0.98622	0.99118
0.87130	1.61281	2.89758	0.98606	0.99107
0.88120	1.61397	2.89214	0.98590	0.99096
0.89110	1.61512	2.88672	0.98573	0.99086
0.90100	1.61626	2.88133	0.98557	0.99075
0.91090	1.61741	2.87595	0.98541	0.99065
0.92080	1.61855	2.87059	0.98524	0.99054
0.93070	1.61969	2.86525	0.98508	0.99043
0.94060	1.62083	2.85993	0.98492	0.99033
0.95050	1.62196	2.85463	0.98475	0.99022
0.96040	1.62310	2.84935	0.98459	0.99012
0.97030	1.62423	2.84409	0.98442	0.99001
0.98020	1.62535	2.83885	0.98426	0.98990
0.99010	1.62648	2.83363	0.98410	0.98980
1.00000	1.62760	2.82842	0.98393	0.98969

X POSITION	TEMPERATURE	DENSITY	VELCTY
0.01000	394.08000	0.0007382	1167.76000
0.01990	393.84093	0.0007370	1168.54689
0.02980	393.60269	0.0007357	1169.33048
0.03970	393.36529	0.0007345	1170.11081
0.04960	393.12872	0.0007333	1170.88790
0.05950	392.89297	0.0007321	1171.66179

0.06940	392.65803	0.0007309	1172.43250
0.07930	392.42390	0.0007297	1173.20005
0.08920	392.19057	0.0007285	1173.96447
0.09910	391.95804	0.0007273	1174.72579
0.10900	391.72630	0.0007261	1175.48404
0.11890	391.49534	0.0007249	1176.23923
0.12880	391.26516	0.0007237	1176.99140
0.13870	391.03575	0.0007226	1177.74057
0.14860	390.80710	0.0007214	1178.48677
0.15850	390.57922	0.0007202	1179.23001
0.16840	390.35209	0.0007191	1179.97032
0.17830	390.12572	0.0007179	1180.70772
0.18820	389.90008	0.0007167	1181.44225
0.19810	389.67519	0.0007156	1182.17391
0.20800	389.45103	0.0007145	1182.90274
0.21790	389.22760	0.0007133	1183.62876
0.22780	389.00489	0.0007122	1184.35198
0.23770	388.78289	0.0007111	1185.07243
0.24760	388.56161	0.0007099	1185.79013
0.25750	388.34104	0.0007088	1186.50510
0.26740	388.12118	0.0007077	1187.21737
0.27730	387.90201	0.0007066	1187.92695
0.28720	387.68353	0.0007055	1188.63386
0.29710	387.46574	0.0007044	1189.33813
0.30700	387.24864	0.0007033	1190.03976
0.31690	387.03221	0.0007022	1190.73880
0.32680	386.81646	0.0007011	1191.43524
0.33670	386.60139	0.0007000	1192.12912
0.34660	386.38697	0.0006989	1192.82045
0.35650	386.17322	0.0006978	1193.50925
0.36640	385.96012	0.0006968	1194.19553
0.37630	385.74768	0.0006957	1194.87932
0.38620	385.53588	0.0006946	1195.56064
0.39610	385.32473	0.0006936	1196.23949
0.40600	385.11422	0.0006925	1196.91591
0.41590	384.90435	0.0006915	1197.58991
0.42580	384.69510	0.0006904	1198.26149
0.43570	384.48649	0.0006894	1198.93069
0.44560	384.27849	0.0006883	1199.59752
0.45550	384.07112	0.0006873	1200.26199
0.46540	383.86436	0.0006862	1200.92413
0.47530	383.65822	0.0006852	1201.58394
0.48520	383.45268	0.0006842	1202.24144
0.49510	383.24775	0.0006832	1202.89666
0.50500	383.04341	0.0006821	1203.54960
0.51490	382.83968	0.0006811	1204.20028
0.52480	382.63653	0.0006801	1204.84871
0.53470	382.43398	0.0006791	1205.49492
0.54460	382.23201	0.0006781	1206.13891
0.55450	382.03063	0.0006771	1206.78071
0.56440	381.82982	0.0006761	1207.42032
0.57430	381.62959	0.0006751	1208.05776
0.58420	381.42993	0.0006741	1208.69305
0.59410	381.23083	0.0006731	1209.32620
0.60400	381.03231	0.0006721	1209.95722
0.61390	380.83434	0.0006711	1210.58613
0.62380	380.63693	0.0006702	1211.21293
0.63370	380.44008	0.0006692	1211.83766
0.64360	380.24378	0.0006682	1212.46031
0.65350	380.04803	0.0006672	1213.08090

0.66340	379.85282	0.0006663	1213.69945
0.67330	379.65816	0.0006653	1214.31597
0.68320	379.46403	0.0006644	1214.93047
0.69310	379.27045	0.0006634	1215.54296
0.70300	379.07739	0.0006625	1216.15346
0.71290	378.88486	0.0006615	1216.76197
0.72280	378.69286	0.0006606	1217.36852
0.73270	378.50139	0.0006596	1217.97312
0.74260	378.31043	0.0006587	1218.57577
0.75250	378.12000	0.0006577	1219.17649
0.76240	377.93008	0.0006568	1219.77528
0.77230	377.74067	0.0006559	1220.37217
0.78220	377.55177	0.0006549	1220.96717
0.79210	377.36337	0.0006540	1221.56028
0.80200	377.17549	0.0006531	1222.15152
0.81190	376.98810	0.0006522	1222.74089
0.82180	376.80121	0.0006513	1223.32842
0.83170	376.61481	0.0006504	1223.91410
0.84160	376.42891	0.0006494	1224.49796
0.85150	376.24350	0.0006485	1225.08000
0.86140	376.05858	0.0006476	1225.66024
0.87130	375.87414	0.0006467	1226.23868
0.88120	375.69019	0.0006458	1226.81533
0.89110	375.50671	0.0006449	1227.39021
0.90100	375.32371	0.0006440	1227.96333
0.91090	375.14119	0.0006432	1228.53469
0.92080	374.95914	0.0006423	1229.10432
0.93070	374.77756	0.0006414	1229.67220
0.94060	374.59644	0.0006405	1230.23837
0.95050	374.41579	0.0006396	1230.80282
0.96040	374.23561	0.0006387	1231.36557
0.97030	374.05588	0.0006379	1231.92662
0.98020	373.87661	0.0006370	1232.48599
0.99010	373.69780	0.0006361	1233.04369
1.00000	373.51944	0.0006353	1233.59973

PRESSURE ERROR= 0.184328171105900815
SOLUTION COMPLETED

MULTIPLE RAMP EXTERNAL/INTERNAL FOREBODY

Input

```
^
 &input
  cfv=.005d0,.005d0,.005d0,.005d0,.005d0
  aiv=61.66d0,61.66d0,61.66d0,26.83d0,0.0d0
  anv=0.d0,0.d0,0.0d0,0.0d0,0.d0
  div=0.0d0,0.0d0,0.0d0,0.0d0,0.d0
  twv=1.d0,1.d0,1.d0,1.d0,1.d0
  ttv=390.d0,390.d0,390.d0,390.d0,390.d0
  chv=0.d0,0.d0,0.d0,0.d0,0.d0
  cpv=0.d0,0.d0,0.d0,0.d0,0.d0
  xiv=1.d0,48.5d0,70.33d0,83.33d0,0.d0
  xv=1.d0,48.5d0,70.33d0,83.33d0,0.d0
  rmv=3.d0
  pv=1.692d0
  tv=390.0d0
  rhv=.3639d-3
  uv=2904.3d0
  blv=0.d0,0.00d0,0.00d0,0.d0,0.d0
  arblv=1.d0,1.d0,1.d0,1.d0,1.d0
  ndiffv=0,0,0,0,0
  ishckv=0,0,0,0,0
  iobliq=0,1,1,0,0
  iprsit=1,1,1,1,0
  icowl=0,0,0,1,0
  icap=1
  deltv=0.d0,3.5d0,8.4d0,0.d0,0.d0
  nprofl=0,0,1,0,0
  proloc=0.d0,0.d0,83.33d0,0.d0,0.d0
  ymxave=0.d0,0.d0,1.5d0,0.d0,0.d0
  ymnave=0.0d0,0.d0,.7d0,0.d0,0.d0
  pexp=7.d0
  nconv=0,0,0,0,0
  nconlv=0,0,0,0,0
  nconev=1,1,1,1,0
  nconcv=1,1,1,1,1
  nnozv=0,0,0,0,0
  nviscv=0,0,0,0,0
  rlxv=38.33d0,38.33d0,38.33d0,38.33d0,0.d0
  rlyv=2.0d0,2.0d0,2.0d0,0.7d0,2.0d0
  gammv=1.4d0,1.4d0,1.4d0,1.4d0,1.4d0
  patmo=.09d0
  ninter=3
 &end
```

```
PRESSURE ERROR= 0.155917264258482742E-06

OBLIQUE SHOCK HAS BEEN FORMED
SHOCK ANGLE=  23.1133850423633582
MACH NUMBER=  2.67823709894495710
TOTAL PRESSURE RATIO= 0.998345940258362763
STATIC PRESSURE RATIO=  1.28824151812254595
STATIC TEMPERATURE RATIO=  1.07555645273820022
POST SHOCK PRESSURE=  2.17970430880976185
POST SHOCK TEMP=  448.534728454446110
POST SHOCK DENSITY= 0.407612798717579665E-03
POST SHOCK VELOCITY=  2780.57731618572228
POST SHOCK AREA=  57.4968715072469507
POST SHOCK STREAMTUBE HEIGHT=  1.50004882617393553

PRESSURE ERROR= 0.208195749021870195E-08

OBLIQUE SHOCK HAS BEEN FORMED
SHOCK ANGLE=  29.0127846812868384
MACH NUMBER=  2.26740549161464511
TOTAL PRESSURE RATIO= 0.983250679585674206
STATIC PRESSURE RATIO=  1.73394139055847929
STATIC TEMPERATURE RATIO=  1.17595708719497916
POST SHOCK PRESSURE=  3.77947951235519164
POST SHOCK TEMP=  538.400496421680543
POST SHOCK DENSITY= 0.588806841771031446E-03
POST SHOCK VELOCITY=  2579.10982918136153
POST SHOCK AREA=  42.9125494871498745
POST SHOCK STREAMTUBE HEIGHT=  1.11955516533132982

PRESSURE ERROR= 0.467183088741065742E-09

*********************************************
FLOW ERROR= 0.386040790769471343
NCAP=           2
*********************************************

PRESSURE ERROR= 0.429481654863069223E-06

OBLIQUE SHOCK HAS BEEN FORMED
SHOCK ANGLE=  23.7995876132075814
MACH NUMBER=  2.5981701562709844 7
TOTAL PRESSURE RATIO= 0.998467941201814896
STATIC PRESSURE RATIO=  1.28002554220260367
STATIC TEMPERATURE RATIO=  1.07355462168303806
POST SHOCK PRESSURE=  2.16580228723405521
POST SHOCK TEMP=  464.660976258493633
POST SHOCK DENSITY= 0.390956926094784601E-03
POST SHOCK VELOCITY=  2745.51364744851446
POST SHOCK AREA=  37.2746793715892366
POST SHOCK STREAMTUBE HEIGHT= 0.972467502519938368

PRESSURE ERROR= 0.589783690715393710E-08
```

```
 OBLIQUE SHOCK HAS BEEN FORMED
 SHOCK ANGLE=  30.0444444608582657
 MACH NUMBER=  2.17833356373061582
 TOTAL PRESSURE RATIO= 0.984719666726587978
 STATIC PRESSURE RATIO=  1.70506042467237284
 STATIC TEMPERATURE RATIO=  1.16982809269303356
 POST SHOCK PRESSURE=  3.69282374584802220
 POST SHOCK TEMP=  560.278359698230020
 POST SHOCK DENSITY= 0.552842007300769910E-03
 POST SHOCK VELOCITY=  2527.63420624396974
 POST SHOCK AREA=  28.6319662638908490
 POST SHOCK STREAMTUBE HEIGHT= 0.746985814346226171

 PRESSURE ERROR= 0.126752092171392371E-08

 ***********************************************
 FLOW ERROR= 0.875242811440029717E-01
 NCAP=          3
 ***********************************************

 PRESSURE ERROR= 0.519575790324777644E-06

 OBLIQUE SHOCK HAS BEEN FORMED
 SHOCK ANGLE=  23.9668966704651680
 MACH NUMBER=  2.57941442797487586
 TOTAL PRESSURE RATIO= 0.998495461508553575
 STATIC PRESSURE RATIO=  1.27812008566180202
 STATIC TEMPERATURE RATIO=  1.07308932758312059
 POST SHOCK PRESSURE=  2.16257806131597974
 POST SHOCK TEMP=  468.533080213172127
 POST SHOCK DENSITY= 0.387148728853351290E-03
 POST SHOCK VELOCITY=  2737.02756276276654
 POST SHOCK AREA=  34.4532911699253823
 POST SHOCK STREAMTUBE HEIGHT= 0.898859670491139504

 PRESSURE ERROR= 0.711198147092189756E-08

 OBLIQUE SHOCK HAS BEEN FORMED
 SHOCK ANGLE=  30.2966171031818874
 MACH NUMBER=  2.15768357785070908
 TOTAL PRESSURE RATIO= 0.985043207257049455
 STATIC PRESSURE RATIO=  1.69852657265459261
 STATIC TEMPERATURE RATIO=  1.16843585589195231
 POST SHOCK PRESSURE=  3.67319627646134039
 POST SHOCK TEMP=  565.473985627168759
 POST SHOCK DENSITY= 0.544851071239845462E-03
 POST SHOCK VELOCITY=  2515.25480818241675
 POST SHOCK AREA=  26.6396137599986673
 POST SHOCK STREAMTUBE HEIGHT= 0.695006881293990866

 PRESSURE ERROR= 0.150942487132500471E-08

 ***********************************************
 FLOW ERROR= 0.210638391525614704E-01
 NCAP=          4
 ***********************************************

 PRESSURE ERROR= 0.543084946727297784E-06

 OBLIQUE SHOCK HAS BEEN FORMED
```

```
SHOCK ANGLE=  24.007843719562927 7
MACH NUMBER=  2.5748680767341407 5
TOTAL PRESSURE RATIO= 0.99850207258714340 8
STATIC PRESSURE RATIO=  1.2776593273590888 3
STATIC TEMPERATURE RATIO=  1.0729767563328922 5
POST SHOCK PRESSURE=  2.1617984078507672 7
POST SHOCK TEMP=  469.47713086832311 5
POST SHOCK DENSITY= 0.38623093437365195 8E-03
POST SHOCK VELOCITY=  2734.9545931774665 1
POST SHOCK AREA=  33.833343003683619 8
POST SHOCK STREAMTUBE HEIGHT= 0.88268570320072053 9

PRESSURE ERROR= 0.74261702911173949 2E-08

OBLIQUE SHOCK HAS BEEN FORMED
SHOCK ANGLE=  30.358376292673611 4
MACH NUMBER=  2.1526898256177318 1
TOTAL PRESSURE RATIO= 0.98512049702580570 3
STATIC PRESSURE RATIO=  1.6969558601789696 0
STATIC TEMPERATURE RATIO=  1.1681008505673851 1
POST SHOCK PRESSURE=  3.6684764494851944 7
POST SHOCK TEMP=  566.73740347348649 5
POST SHOCK DENSITY= 0.54293790545848017 6E-03
POST SHOCK VELOCITY=  2512.2352951633188 2
POST SHOCK AREA=  26.201829028845274 6
POST SHOCK STREAMTUBE HEIGHT= 0.68358541687569207 6

PRESSURE ERROR= 0.15710347703132696 4E-08

NCOUNT=           1
REYNOLDS NUM INLET=  7881119.1782132126 4
CF AT INLET= 0.17672791024221265 7E-02
MACH NUMBER INLET=  3.0000000000000000
MASS FLOW RATE INLET(LBM/S)=  1150.7954294885607 9
REYNOLDS NUM EXIT=  300928563.03663498 2
CF AT EXIT= 0.10491545457571196 8E-02
MACH NUMBER EXIT=  2.7329408939457915 4
MASS FLOW RATE EXIT=  1150.7949829962406 1

NCOUNT=           2
REYNOLDS NUM INLET=  7881119.1782132126 4
CF AT INLET= 0.17672791024221265 7E-02
MACH NUMBER INLET=  3.0000000000000000
MASS FLOW RATE INLET(LBM/S)=  1150.7954294885607 9
REYNOLDS NUM EXIT=  301406756.57540804 1
CF AT EXIT= 0.10485679094083838 1E-02
MACH NUMBER EXIT=  2.7346703610760714 2
MASS FLOW RATE EXIT=  1150.7949794904740 8

NCOUNT=           3
REYNOLDS NUM INLET=  7881119.1782132126 4
CF AT INLET= 0.17672791024221265 7E-02
MACH NUMBER INLET=  3.0000000000000000
MASS FLOW RATE INLET(LBM/S)=  1150.7954294885607 9
REYNOLDS NUM EXIT=  301419588.83735281 2
CF AT EXIT= 0.10485521828538310 5E-02
MACH NUMBER EXIT=  2.7347167410884061 2
MASS FLOW RATE EXIT=  1150.7949793971937 4

**********************************************
```

INTERVAL NUMBER= 1

PRINT OUT INPUT DATA
CROSS SECTION AREA
INLET AREA= 33.8157268088002212
EXIT AREA= 39.2923014429942015
CHANNEL DIMENSIONS
INLET CHANNEL HEIGHT= 0.882226110326121124
EXIT CHANNEL HEIGHT= 1.02510569900845816
INLET CHANNEL WIDTH= 38.3299999999999983
EXIT CHANNEL WIDTH= 38.3299999999999983

INITIAL CONDITIONS
MACH NUMBER= 3.00000000000000000
PRESSURE= 1.69199999999999995
TEMPERATURE= 390.000000000000000
DENSITY= 0.363900000000000009E-03
VELOCITY= 2904.30000000000001

X POSITION	MACH NUMBER	PRESSURE	P02/P01	ETA KINETIC
1.00000	3.00000	1.69200	1.00000	1.00000
1.47500	2.99602	1.69200	0.99405	0.99905
1.95000	2.99208	1.69200	0.98819	0.99811
2.42500	2.98818	1.69200	0.98241	0.99718
2.90000	2.98431	1.69200	0.97672	0.99625
3.37500	2.98047	1.69200	0.97111	0.99533
3.85000	2.97667	1.69200	0.96558	0.99441
4.32500	2.97291	1.69200	0.96013	0.99350
4.80000	2.96918	1.69200	0.95476	0.99260
5.27500	2.96548	1.69200	0.94946	0.99171
5.75000	2.96182	1.69200	0.94424	0.99082
6.22500	2.95819	1.69200	0.93910	0.98994
6.70000	2.95460	1.69200	0.93402	0.98906
7.17500	2.95103	1.69200	0.92902	0.98819
7.65000	2.94750	1.69200	0.92409	0.98733
8.12500	2.94400	1.69200	0.91922	0.98647
8.60000	2.94053	1.69200	0.91442	0.98562
9.07500	2.93709	1.69200	0.90969	0.98477
9.55000	2.93368	1.69200	0.90502	0.98393
10.02500	2.93030	1.69200	0.90042	0.98310
10.50000	2.92695	1.69200	0.89588	0.98227
10.97500	2.92363	1.69200	0.89140	0.98145
11.45000	2.92034	1.69200	0.88698	0.98063
11.92500	2.91708	1.69200	0.88262	0.97982
12.40000	2.91385	1.69200	0.87832	0.97902
12.87500	2.91064	1.69200	0.87407	0.97822
13.35000	2.90747	1.69200	0.86988	0.97743
13.82500	2.90432	1.69200	0.86575	0.97664
14.30000	2.90120	1.69200	0.86167	0.97586
14.77500	2.89811	1.69200	0.85764	0.97508
15.25000	2.89504	1.69200	0.85367	0.97431
15.72500	2.89200	1.69200	0.84975	0.97355
16.20000	2.88898	1.69200	0.84588	0.97279
16.67500	2.88600	1.69200	0.84206	0.97203
17.15000	2.88304	1.69200	0.83828	0.97128
17.62500	2.88010	1.69200	0.83456	0.97054
18.10000	2.87719	1.69200	0.83088	0.96980
18.57500	2.87430	1.69200	0.82725	0.96907

19.05000	2.87144	1.69200	0.82367	0.96834
19.52500	2.86861	1.69200	0.82013	0.96762
20.00000	2.86579	1.69200	0.81664	0.96690
20.47500	2.86301	1.69200	0.81319	0.96619
20.95000	2.86024	1.69200	0.80978	0.96548
21.42500	2.85750	1.69200	0.80642	0.96478
21.90000	2.85479	1.69200	0.80310	0.96408
22.37500	2.85209	1.69200	0.79982	0.96339
22.85000	2.84942	1.69200	0.79658	0.96270
23.32500	2.84678	1.69200	0.79338	0.96202
23.80000	2.84415	1.69200	0.79022	0.96134
24.27500	2.84155	1.69200	0.78710	0.96067
24.75000	2.83897	1.69200	0.78401	0.96000
25.22500	2.83641	1.69200	0.78097	0.95934
25.70000	2.83388	1.69200	0.77796	0.95868
26.17500	2.83136	1.69200	0.77499	0.95803
26.65000	2.82887	1.69200	0.77205	0.95738
27.12500	2.82640	1.69200	0.76915	0.95674
27.60000	2.82395	1.69200	0.76628	0.95610
28.07500	2.82152	1.69200	0.76345	0.95546
28.55000	2.81911	1.69200	0.76065	0.95483
29.02500	2.81672	1.69200	0.75789	0.95421
29.50000	2.81435	1.69200	0.75516	0.95359
29.97500	2.81201	1.69200	0.75246	0.95297
30.45000	2.80968	1.69200	0.74980	0.95236
30.92500	2.80737	1.69200	0.74716	0.95175
31.40000	2.80508	1.69200	0.74456	0.95115
31.87500	2.80282	1.69200	0.74199	0.95055
32.35000	2.80057	1.69200	0.73944	0.94996
32.82500	2.79834	1.69200	0.73693	0.94937
33.30000	2.79613	1.69200	0.73445	0.94879
33.77500	2.79394	1.69200	0.73200	0.94821
34.25000	2.79177	1.69200	0.72957	0.94763
34.72500	2.78961	1.69200	0.72718	0.94706
35.20000	2.78748	1.69200	0.72481	0.94649
35.67500	2.78536	1.69200	0.72247	0.94593
36.15000	2.78326	1.69200	0.72015	0.94537
36.62500	2.78118	1.69200	0.71787	0.94481
37.10000	2.77912	1.69200	0.71561	0.94426
37.57500	2.77708	1.69200	0.71338	0.94372
38.05000	2.77505	1.69200	0.71117	0.94318
38.52500	2.77304	1.69200	0.70899	0.94264
39.00000	2.77105	1.69200	0.70683	0.94210
39.47500	2.76908	1.69200	0.70470	0.94157
39.95000	2.76712	1.69200	0.70259	0.94105
40.42500	2.76518	1.69200	0.70051	0.94053
40.90000	2.76326	1.69200	0.69845	0.94001
41.37500	2.76135	1.69200	0.69642	0.93950
41.85000	2.75946	1.69200	0.69441	0.93899
42.32500	2.75759	1.69200	0.69242	0.93848
42.80000	2.75574	1.69200	0.69045	0.93798
43.27500	2.75390	1.69200	0.68851	0.93748
43.75000	2.75207	1.69200	0.68659	0.93699
44.22500	2.75027	1.69200	0.68469	0.93650
44.70000	2.74848	1.69200	0.68282	0.93602
45.17500	2.74670	1.69200	0.68096	0.93553
45.65000	2.74494	1.69200	0.67913	0.93506
46.12500	2.74320	1.69200	0.67732	0.93458
46.60000	2.74147	1.69200	0.67552	0.93411
47.07500	2.73976	1.69200	0.67375	0.93365

47.55000	2.73806	1.69200	0.67200	0.93318
48.02500	2.73638	1.69200	0.67027	0.93272
48.50000	2.73472	1.69200	0.66856	0.93227

X POSITION	TEMPERATURE	DENSITY	VELCTY
1.00000	390.00000	0.0003639	2904.30000
1.47500	390.66557	0.0003633	2902.92289
1.95000	391.32636	0.0003627	2901.55500
2.42500	391.98242	0.0003621	2900.19629
2.90000	392.63378	0.0003615	2898.84667
3.37500	393.28048	0.0003609	2897.50608
3.85000	393.92256	0.0003603	2896.17446
4.32500	394.56006	0.0003597	2894.85175
4.80000	395.19300	0.0003591	2893.53787
5.27500	395.82143	0.0003585	2892.23278
5.75000	396.44538	0.0003580	2890.93640
6.22500	397.06489	0.0003574	2889.64869
6.70000	397.67999	0.0003569	2888.36957
7.17500	398.29071	0.0003563	2887.09899
7.65000	398.89708	0.0003558	2885.83690
8.12500	399.49915	0.0003552	2884.58323
8.60000	400.09694	0.0003547	2883.33793
9.07500	400.69048	0.0003542	2882.10095
9.55000	401.27980	0.0003537	2880.87223
10.02500	401.86494	0.0003532	2879.65171
10.50000	402.44593	0.0003526	2878.43935
10.97500	403.02279	0.0003521	2877.23509
11.45000	403.59555	0.0003516	2876.03888
11.92500	404.16425	0.0003511	2874.85067
12.40000	404.72891	0.0003507	2873.67040
12.87500	405.28957	0.0003502	2872.49804
13.35000	405.84624	0.0003497	2871.33353
13.82500	406.39896	0.0003492	2870.17682
14.30000	406.94775	0.0003487	2869.02787
14.77500	407.49265	0.0003483	2867.88662
15.25000	408.03367	0.0003478	2866.75304
15.72500	408.57084	0.0003474	2865.62707
16.20000	409.10420	0.0003469	2864.50867
16.67500	409.63375	0.0003465	2863.39780
17.15000	410.15954	0.0003460	2862.29441
17.62500	410.68158	0.0003456	2861.19846
18.10000	411.19990	0.0003451	2860.10991
18.57500	411.71453	0.0003447	2859.02871
19.05000	412.22548	0.0003443	2857.95483
19.52500	412.73278	0.0003439	2856.88821
20.00000	413.23645	0.0003434	2855.82883
20.47500	413.73653	0.0003430	2854.77664
20.95000	414.23302	0.0003426	2853.73159
21.42500	414.72595	0.0003422	2852.69367
21.90000	415.21534	0.0003418	2851.66281
22.37500	415.70122	0.0003414	2850.63899
22.85000	416.18361	0.0003410	2849.62216
23.32500	416.66252	0.0003406	2848.61230
23.80000	417.13798	0.0003402	2847.60936
24.27500	417.61001	0.0003398	2846.61331
24.75000	418.07863	0.0003395	2845.62411
25.22500	418.54386	0.0003391	2844.64172
25.70000	419.00572	0.0003387	2843.66612
26.17500	419.46423	0.0003383	2842.69726

```
  26.65000       419.91941       0.0003380       2841.73512
  27.12500       420.37128       0.0003376       2840.77965
  27.60000       420.81985       0.0003372       2839.83084
  28.07500       421.26515       0.0003369       2838.88863
  28.55000       421.70719       0.0003365       2837.95300
  29.02500       422.14599       0.0003362       2837.02393
  29.50000       422.58158       0.0003358       2836.10137
  29.97500       423.01396       0.0003355       2835.18529
  30.45000       423.44315       0.0003352       2834.27567
  30.92500       423.86918       0.0003348       2833.37247
  31.40000       424.29206       0.0003345       2832.47567
  31.87500       424.71181       0.0003342       2831.58523
  32.35000       425.12844       0.0003338       2830.70113
  32.82500       425.54197       0.0003335       2829.82333
  33.30000       425.95241       0.0003332       2828.95181
  33.77500       426.35979       0.0003329       2828.08653
  34.25000       426.76411       0.0003326       2827.22748
  34.72500       427.16540       0.0003322       2826.37462
  35.20000       427.56367       0.0003319       2825.52792
  35.67500       427.95894       0.0003316       2824.68736
  36.15000       428.35121       0.0003313       2823.85292
  36.62500       428.74051       0.0003310       2823.02455
  37.10000       429.12685       0.0003307       2822.20225
  37.57500       429.51024       0.0003304       2821.38598
  38.05000       429.89070       0.0003301       2820.57572
  38.52500       430.26825       0.0003298       2819.77143
  39.00000       430.64289       0.0003296       2818.97311
  39.47500       431.01464       0.0003293       2818.18072
  39.95000       431.38352       0.0003290       2817.39423
  40.42500       431.74953       0.0003287       2816.61363
  40.90000       432.11270       0.0003284       2815.83889
  41.37500       432.47304       0.0003282       2815.06999
  41.85000       432.83055       0.0003279       2814.30690
  42.32500       433.18525       0.0003276       2813.54960
  42.80000       433.53716       0.0003274       2812.79807
  43.27500       433.88628       0.0003271       2812.05228
  43.75000       434.23263       0.0003268       2811.31222
  44.22500       434.57623       0.0003266       2810.57786
  44.70000       434.91708       0.0003263       2809.84917
  45.17500       435.25519       0.0003261       2809.12615
  45.65000       435.59059       0.0003258       2808.40876
  46.12500       435.92327       0.0003256       2807.69699
  46.60000       436.25325       0.0003253       2806.99081
  47.07500       436.58055       0.0003251       2806.29021
  47.55000       436.90517       0.0003248       2805.59516
  48.02500       437.22713       0.0003246       2804.90565
  48.50000       437.54643       0.0003244       2804.22166
PRESSURE ERROR= 0.54308471116579315E-06

OBLIQUE SHOCK HAS BEEN FORMED
SHOCK ANGLE=  24.007844534564309
MACH NUMBER=  2.5748679864147492
TOTAL PRESSURE RATIO= 0.99850207271825001
STATIC PRESSURE RATIO=  1.2776593182098734
STATIC TEMPERATURE RATIO=  1.0729767540973534
POST SHOCK PRESSURE=  2.1617983923708126
POST SHOCK TEMP=  469.47714964437432
POST SHOCK DENSITY= 0.38623091616123378E-03
POST SHOCK VELOCITY=  2734.9545519329265
POST SHOCK AREA=  33.833345109298730
```

POST SHOCK STREAMTUBE HEIGHT= 0.882685758134587259

NCOUNT= 1
REYNOLDS NUM INLET= 331806862.251579821
CF AT INLET= 0.107105669898152579E-02
MACH NUMBER INLET= 2.57486798641474923
MASS FLOW RATE INLET(LBM/S)= 1150.79497939719317
REYNOLDS NUM EXIT= 447882030.799780726
CF AT EXIT= 0.104338929630309201E-02
MACH NUMBER EXIT= 2.49968829265456116
MASS FLOW RATE EXIT= 1150.79497637604453

NCOUNT= 2
REYNOLDS NUM INLET= 331806862.251579821
CF AT INLET= 0.107105669898152579E-02
MACH NUMBER INLET= 2.57486798641474923
MASS FLOW RATE INLET(LBM/S)= 1150.79497939719317
REYNOLDS NUM EXIT= 448318788.613417506
CF AT EXIT= 0.104304079453263561E-02
MACH NUMBER EXIT= 2.50070363430562459
MASS FLOW RATE EXIT= 1150.79497328923497

NCOUNT= 3
REYNOLDS NUM INLET= 331806862.251579821
CF AT INLET= 0.107105669898152579E-02
MACH NUMBER INLET= 2.57486798641474923
MASS FLOW RATE INLET(LBM/S)= 1150.79497939719317
REYNOLDS NUM EXIT= 448323774.473733068
CF AT EXIT= 0.104303681853282958E-02
MACH NUMBER EXIT= 2.50071522046376460
MASS FLOW RATE EXIT= 1150.79497327664200

****

INTERVAL NUMBER= 2

PRINT OUT INPUT DATA
CROSS SECTION AREA
INLET AREA= 33.8333451092987296
EXIT AREA= 35.4143452665071905
CHANNEL DIMENSIONS
INLET CHANNEL HEIGHT= 0.882685758134587259
EXIT CHANNEL HEIGHT= 0.923932827198204853
INLET CHANNEL WIDTH= 38.3299999999999983
EXIT CHANNEL WIDTH= 38.3299999999999983

INITIAL CONDITIONS
MACH NUMBER= 2.57486798641474923
PRESSURE= 2.16179839237081262
TEMPERATURE= 469.477149644374322
DENSITY= 0.386230916161233785E-03
VELOCITY= 2734.95455193292651

X POSITION	MACH NUMBER	PRESSURE	P02/P01	ETA KINETIC
48.50000	2.57487	2.16180	1.00000	1.00000
48.71830	2.57408	2.16180	0.99877	0.99974
48.93660	2.57328	2.16180	0.99755	0.99947
49.15490	2.57249	2.16180	0.99633	0.99921

49.37320	2.57170	2.16180	0.99511	0.99894
49.59150	2.57092	2.16180	0.99389	0.99868
49.80980	2.57013	2.16180	0.99268	0.99842
50.02810	2.56934	2.16180	0.99147	0.99815
50.24640	2.56856	2.16180	0.99027	0.99789
50.46470	2.56777	2.16180	0.98906	0.99763
50.68300	2.56699	2.16180	0.98786	0.99736
50.90130	2.56621	2.16180	0.98667	0.99710
51.11960	2.56543	2.16180	0.98547	0.99684
51.33790	2.56465	2.16180	0.98428	0.99658
51.55620	2.56387	2.16180	0.98310	0.99632
51.77450	2.56309	2.16180	0.98191	0.99606
51.99280	2.56232	2.16180	0.98073	0.99580
52.21110	2.56154	2.16180	0.97955	0.99554
52.42940	2.56077	2.16180	0.97838	0.99527
52.64770	2.55999	2.16180	0.97720	0.99501
52.86600	2.55922	2.16180	0.97604	0.99476
53.08430	2.55845	2.16180	0.97487	0.99450
53.30260	2.55768	2.16180	0.97371	0.99424
53.52090	2.55691	2.16180	0.97254	0.99398
53.73920	2.55615	2.16180	0.97139	0.99372
53.95750	2.55538	2.16180	0.97023	0.99346
54.17580	2.55461	2.16180	0.96908	0.99320
54.39410	2.55385	2.16180	0.96793	0.99294
54.61240	2.55309	2.16180	0.96679	0.99269
54.83070	2.55232	2.16180	0.96564	0.99243
55.04900	2.55156	2.16180	0.96450	0.99217
55.26730	2.55080	2.16180	0.96336	0.99191
55.48560	2.55004	2.16180	0.96223	0.99166
55.70390	2.54928	2.16180	0.96110	0.99140
55.92220	2.54853	2.16180	0.95997	0.99115
56.14050	2.54777	2.16180	0.95884	0.99089
56.35880	2.54701	2.16180	0.95772	0.99063
56.57710	2.54626	2.16180	0.95660	0.99038
56.79540	2.54551	2.16180	0.95548	0.99012
57.01370	2.54475	2.16180	0.95437	0.98987
57.23200	2.54400	2.16180	0.95325	0.98961
57.45030	2.54325	2.16180	0.95215	0.98936
57.66860	2.54250	2.16180	0.95104	0.98911
57.88690	2.54176	2.16180	0.94994	0.98885
58.10520	2.54101	2.16180	0.94883	0.98860
58.32350	2.54026	2.16180	0.94774	0.98834
58.54180	2.53952	2.16180	0.94664	0.98809
58.76010	2.53877	2.16180	0.94555	0.98784
58.97840	2.53803	2.16180	0.94446	0.98759
59.19670	2.53729	2.16180	0.94337	0.98733
59.41500	2.53655	2.16180	0.94228	0.98708
59.63330	2.53581	2.16180	0.94120	0.98683
59.85160	2.53507	2.16180	0.94012	0.98658
60.06990	2.53433	2.16180	0.93904	0.98633
60.28820	2.53359	2.16180	0.93797	0.98607
60.50650	2.53286	2.16180	0.93690	0.98582
60.72480	2.53212	2.16180	0.93583	0.98557
60.94310	2.53139	2.16180	0.93476	0.98532
61.16140	2.53065	2.16180	0.93370	0.98507
61.37970	2.52992	2.16180	0.93264	0.98482
61.59800	2.52919	2.16180	0.93158	0.98457
61.81630	2.52846	2.16180	0.93052	0.98432
62.03460	2.52773	2.16180	0.92947	0.98407
62.25290	2.52700	2.16180	0.92842	0.98382

62.47120	2.52628	2.16180	0.92737	0.98358
62.68950	2.52555	2.16180	0.92632	0.98333
62.90780	2.52482	2.16180	0.92528	0.98308
63.12610	2.52410	2.16180	0.92424	0.98283
63.34440	2.52338	2.16180	0.92320	0.98258
63.56270	2.52265	2.16180	0.92216	0.98234
63.78100	2.52193	2.16180	0.92113	0.98209
63.99930	2.52121	2.16180	0.92010	0.98184
64.21760	2.52049	2.16180	0.91907	0.98159
64.43590	2.51977	2.16180	0.91804	0.98135
64.65420	2.51905	2.16180	0.91702	0.98110
64.87250	2.51834	2.16180	0.91600	0.98086
65.09080	2.51762	2.16180	0.91498	0.98061
65.30910	2.51691	2.16180	0.91396	0.98036
65.52740	2.51619	2.16180	0.91295	0.98012
65.74570	2.51548	2.16180	0.91194	0.97987
65.96400	2.51477	2.16180	0.91093	0.97963
66.18230	2.51406	2.16180	0.90992	0.97938
66.40060	2.51335	2.16180	0.90892	0.97914
66.61890	2.51264	2.16180	0.90792	0.97889
66.83720	2.51193	2.16180	0.90692	0.97865
67.05550	2.51122	2.16180	0.90592	0.97841
67.27380	2.51051	2.16180	0.90492	0.97816
67.49210	2.50981	2.16180	0.90393	0.97792
67.71040	2.50910	2.16180	0.90294	0.97768
67.92870	2.50840	2.16180	0.90195	0.97743
68.14700	2.50770	2.16180	0.90097	0.97719
68.36530	2.50699	2.16180	0.89999	0.97695
68.58360	2.50629	2.16180	0.89901	0.97671
68.80190	2.50559	2.16180	0.89803	0.97646
69.02020	2.50489	2.16180	0.89705	0.97622
69.23850	2.50419	2.16180	0.89608	0.97598
69.45680	2.50350	2.16180	0.89510	0.97574
69.67510	2.50280	2.16180	0.89414	0.97550
69.89340	2.50210	2.16180	0.89317	0.97526
70.11170	2.50141	2.16180	0.89220	0.97502
70.33000	2.50072	2.16180	0.89124	0.97478

X POSITION	TEMPERATURE	DENSITY	VELCTY
48.50000	469.47715	0.0003862	2734.95455
48.71830	469.64196	0.0003861	2734.59248
48.93660	469.80661	0.0003860	2734.23073
49.15490	469.97109	0.0003858	2733.86930
49.37320	470.13541	0.0003857	2733.50818
49.59150	470.29956	0.0003856	2733.14738
49.80980	470.46355	0.0003854	2732.78690
50.02810	470.62737	0.0003853	2732.42673
50.24640	470.79102	0.0003852	2732.06687
50.46470	470.95452	0.0003850	2731.70733
50.68300	471.11784	0.0003849	2731.34810
50.90130	471.28101	0.0003848	2730.98919
51.11960	471.44401	0.0003846	2730.63058
51.33790	471.60685	0.0003845	2730.27229
51.55620	471.76952	0.0003844	2729.91431
51.77450	471.93203	0.0003842	2729.55664
51.99280	472.09438	0.0003841	2729.19929
52.21110	472.25657	0.0003840	2728.84224
52.42940	472.41860	0.0003838	2728.48550
52.64770	472.58046	0.0003837	2728.12907

52.86600	472.74216	0.0003836	2727.77295
53.08430	472.90370	0.0003834	2727.41714
53.30260	473.06509	0.0003833	2727.06163
53.52090	473.22631	0.0003832	2726.70644
53.73920	473.38737	0.0003830	2726.35155
53.95750	473.54827	0.0003829	2725.99696
54.17580	473.70901	0.0003828	2725.64269
54.39410	473.86959	0.0003827	2725.28871
54.61240	474.03001	0.0003825	2724.93504
54.83070	474.19027	0.0003824	2724.58168
55.04900	474.35038	0.0003823	2724.22862
55.26730	474.51032	0.0003821	2723.87587
55.48560	474.67011	0.0003820	2723.52341
55.70390	474.82974	0.0003819	2723.17126
55.92220	474.98922	0.0003817	2722.81942
56.14050	475.14853	0.0003816	2722.46787
56.35880	475.30769	0.0003815	2722.11662
56.57710	475.46669	0.0003814	2721.76568
56.79540	475.62553	0.0003812	2721.41504
57.01370	475.78422	0.0003811	2721.06469
57.23200	475.94276	0.0003810	2720.71465
57.45030	476.10113	0.0003809	2720.36490
57.66860	476.25935	0.0003807	2720.01545
57.88690	476.41742	0.0003806	2719.66631
58.10520	476.57533	0.0003805	2719.31745
58.32350	476.73309	0.0003804	2718.96890
58.54180	476.89069	0.0003802	2718.62064
58.76010	477.04814	0.0003801	2718.27268
58.97840	477.20543	0.0003800	2717.92502
59.19670	477.36257	0.0003799	2717.57765
59.41500	477.51956	0.0003797	2717.23057
59.63330	477.67639	0.0003796	2716.88379
59.85160	477.83307	0.0003795	2716.53730
60.06990	477.98960	0.0003794	2716.19111
60.28820	478.14597	0.0003792	2715.84521
60.50650	478.30219	0.0003791	2715.49961
60.72480	478.45826	0.0003790	2715.15429
60.94310	478.61418	0.0003789	2714.80927
61.16140	478.76995	0.0003787	2714.46454
61.37970	478.92557	0.0003786	2714.12010
61.59800	479.08103	0.0003785	2713.77595
61.81630	479.23634	0.0003784	2713.43209
62.03460	479.39151	0.0003782	2713.08852
62.25290	479.54652	0.0003781	2712.74524
62.47120	479.70138	0.0003780	2712.40225
62.68950	479.85610	0.0003779	2712.05955
62.90780	480.01066	0.0003778	2711.71713
63.12610	480.16508	0.0003776	2711.37501
63.34440	480.31934	0.0003775	2711.03317
63.56270	480.47346	0.0003774	2710.69162
63.78100	480.62743	0.0003773	2710.35035
63.99930	480.78125	0.0003771	2710.00937
64.21760	480.93492	0.0003770	2709.66868
64.43590	481.08844	0.0003769	2709.32827
64.65420	481.24182	0.0003768	2708.98814
64.87250	481.39504	0.0003767	2708.64830
65.09080	481.54813	0.0003765	2708.30874
65.30910	481.70106	0.0003764	2707.96947
65.52740	481.85385	0.0003763	2707.63048
65.74570	482.00649	0.0003762	2707.29177

```
   65.96400      482.15898      0.0003761     2706.95335
   66.18230      482.31133      0.0003760     2706.61521
   66.40060      482.46353      0.0003758     2706.27735
   66.61890      482.61559      0.0003757     2705.93976
   66.83720      482.76750      0.0003756     2705.60246
   67.05550      482.91927      0.0003755     2705.26545
   67.27380      483.07089      0.0003754     2704.92871
   67.49210      483.22237      0.0003752     2704.59225
   67.71040      483.37370      0.0003751     2704.25606
   67.92870      483.52489      0.0003750     2703.92016
   68.14700      483.67593      0.0003749     2703.58454
   68.36530      483.82683      0.0003748     2703.24919
   68.58360      483.97759      0.0003747     2702.91412
   68.80190      484.12820      0.0003745     2702.57933
   69.02020      484.27868      0.0003744     2702.24481
   69.23850      484.42900      0.0003743     2701.91057
   69.45680      484.57919      0.0003742     2701.57661
   69.67510      484.72923      0.0003741     2701.24292
   69.89340      484.87913      0.0003740     2700.90951
   70.11170      485.02889      0.0003738     2700.57637
   70.33000      485.17851      0.0003737     2700.24351
PRESSURE ERROR= 0.74261560671992843 1E-08

OBLIQUE SHOCK HAS BEEN FORMED
SHOCK ANGLE=  30.3583772933689779
MACH NUMBER=  2.15268974490326559
TOTAL PRESSURE RATIO= 0.98512049827205966 4
STATIC PRESSURE RATIO=  1.69695583482102497
STATIC TEMPERATURE RATIO=  1.16810084515798551
POST SHOCK PRESSURE=  3.66847636839768376
POST SHOCK TEMP=  566.737423916152068
POST SHOCK DENSITY= 0.542937873873255723E-03
POST SHOCK VELOCITY=  2512.23524627695571
POST SHOCK AREA=  26.2018310630018512
POST SHOCK STREAMTUBE HEIGHT= 0.683585469945260996


NCOUNT=          1
REYNOLDS NUM INLET=  538461042.696775317
CF AT INLET= 0.109645746716285669E-02
MACH NUMBER INLET=  2.15268974490326559
MASS FLOW RATE INLET(LBM/S)=  1150.79497327664114
REYNOLDS NUM EXIT=  611773862.648332357
CF AT EXIT= 0.108766267753179812E-02
MACH NUMBER EXIT=  2.11202137756772901
MASS FLOW RATE EXIT=  1150.79497289453906

NCOUNT=          2
REYNOLDS NUM INLET=  538461042.696775317
CF AT INLET= 0.109645746716285669E-02
MACH NUMBER INLET=  2.15268974490326559
MASS FLOW RATE INLET(LBM/S)=  1150.79497327664114
REYNOLDS NUM EXIT=  611153462.706054449
CF AT EXIT= 0.108802800474760324E-02
MACH NUMBER EXIT=  2.11104216738588035
MASS FLOW RATE EXIT=  1150.79497197732593

NCOUNT=          3
REYNOLDS NUM INLET=  538461042.696775317
CF AT INLET= 0.109645746716285669E-02
```

MACH NUMBER INLET= 2.15268974490326559
MASS FLOW RATE INLET(LBM/S)= 1150.79497327664114
REYNOLDS NUM EXIT= 611149195.737240553
CF AT EXIT= 0.108803051887133937E-02
MACH NUMBER EXIT= 2.11103542981768899
MASS FLOW RATE EXIT= 1150.79497198254035

****

INTERVAL NUMBER= 3

PRINT OUT INPUT DATA
CROSS SECTION AREA
INLET AREA= 26.2018310630018512
EXIT AREA= 26.9685746464536749
CHANNEL DIMENSIONS
INLET CHANNEL HEIGHT= 0.683585469945260996
EXIT CHANNEL HEIGHT= 0.703589215926263389
INLET CHANNEL WIDTH= 38.3299999999999983
EXIT CHANNEL WIDTH= 38.3299999999999983

INITIAL CONDITIONS
MACH NUMBER= 2.15268974490326559
PRESSURE= 3.66847636839768376
TEMPERATURE= 566.737423916152068
DENSITY= 0.542937873873255723E-03
VELOCITY= 2512.23524627695571

X POSITION	MACH NUMBER	PRESSURE	P02/P01	ETA KINETIC
70.33000	2.15269	3.66848	1.00000	1.00000
70.46000	2.15226	3.66848	0.99932	0.99979
70.59000	2.15183	3.66848	0.99865	0.99958
70.72000	2.15139	3.66848	0.99798	0.99937
70.85000	2.15096	3.66848	0.99730	0.99917
70.98000	2.15053	3.66848	0.99663	0.99896
71.11000	2.15010	3.66848	0.99596	0.99875
71.24000	2.14967	3.66848	0.99529	0.99854
71.37000	2.14924	3.66848	0.99462	0.99834
71.50000	2.14881	3.66848	0.99395	0.99813
71.63000	2.14838	3.66848	0.99328	0.99792
71.76000	2.14795	3.66848	0.99262	0.99771
71.89000	2.14752	3.66848	0.99195	0.99751
72.02000	2.14710	3.66848	0.99129	0.99730
72.15000	2.14667	3.66848	0.99063	0.99709
72.28000	2.14624	3.66848	0.98996	0.99689
72.41000	2.14581	3.66848	0.98930	0.99668
72.54000	2.14539	3.66848	0.98864	0.99647
72.67000	2.14496	3.66848	0.98798	0.99627
72.80000	2.14453	3.66848	0.98732	0.99606
72.93000	2.14411	3.66848	0.98667	0.99585
73.06000	2.14368	3.66848	0.98601	0.99565
73.19000	2.14326	3.66848	0.98535	0.99544
73.32000	2.14283	3.66848	0.98470	0.99524
73.45000	2.14241	3.66848	0.98404	0.99503
73.58000	2.14198	3.66848	0.98339	0.99482
73.71000	2.14156	3.66848	0.98274	0.99462
73.84000	2.14113	3.66848	0.98209	0.99441
73.97000	2.14071	3.66848	0.98144	0.99421
74.10000	2.14029	3.66848	0.98079	0.99400

74.23000	2.13986	3.66848	0.98014	0.99380
74.36000	2.13944	3.66848	0.97949	0.99359
74.49000	2.13902	3.66848	0.97885	0.99339
74.62000	2.13860	3.66848	0.97820	0.99318
74.75000	2.13818	3.66848	0.97756	0.99298
74.88000	2.13775	3.66848	0.97691	0.99278
75.01000	2.13733	3.66848	0.97627	0.99257
75.14000	2.13691	3.66848	0.97563	0.99237
75.27000	2.13649	3.66848	0.97499	0.99216
75.40000	2.13607	3.66848	0.97435	0.99196
75.53000	2.13565	3.66848	0.97371	0.99176
75.66000	2.13523	3.66848	0.97307	0.99155
75.79000	2.13481	3.66848	0.97243	0.99135
75.92000	2.13440	3.66848	0.97180	0.99114
76.05000	2.13398	3.66848	0.97116	0.99094
76.18000	2.13356	3.66848	0.97053	0.99074
76.31000	2.13314	3.66848	0.96989	0.99053
76.44000	2.13272	3.66848	0.96926	0.99033
76.57000	2.13231	3.66848	0.96863	0.99013
76.70000	2.13189	3.66848	0.96800	0.98993
76.83000	2.13147	3.66848	0.96737	0.98972
76.96000	2.13106	3.66848	0.96674	0.98952
77.09000	2.13064	3.66848	0.96611	0.98932
77.22000	2.13023	3.66848	0.96548	0.98912
77.35000	2.12981	3.66848	0.96485	0.98891
77.48000	2.12940	3.66848	0.96423	0.98871
77.61000	2.12898	3.66848	0.96360	0.98851
77.74000	2.12857	3.66848	0.96298	0.98831
77.87000	2.12815	3.66848	0.96236	0.98811
78.00000	2.12774	3.66848	0.96173	0.98790
78.13000	2.12733	3.66848	0.96111	0.98770
78.26000	2.12691	3.66848	0.96049	0.98750
78.39000	2.12650	3.66848	0.95987	0.98730
78.52000	2.12609	3.66848	0.95925	0.98710
78.65000	2.12567	3.66848	0.95864	0.98690
78.78000	2.12526	3.66848	0.95802	0.98670
78.91000	2.12485	3.66848	0.95740	0.98650
79.04000	2.12444	3.66848	0.95679	0.98630
79.17000	2.12403	3.66848	0.95617	0.98610
79.30000	2.12362	3.66848	0.95556	0.98589
79.43000	2.12321	3.66848	0.95495	0.98569
79.56000	2.12280	3.66848	0.95433	0.98549
79.69000	2.12239	3.66848	0.95372	0.98529
79.82000	2.12198	3.66848	0.95311	0.98509
79.95000	2.12157	3.66848	0.95250	0.98489
80.08000	2.12116	3.66848	0.95190	0.98469
80.21000	2.12075	3.66848	0.95129	0.98449
80.34000	2.12034	3.66848	0.95068	0.98430
80.47000	2.11994	3.66848	0.95007	0.98410
80.60000	2.11953	3.66848	0.94947	0.98390
80.73000	2.11912	3.66848	0.94887	0.98370
80.86000	2.11871	3.66848	0.94826	0.98350
80.99000	2.11831	3.66848	0.94766	0.98330
81.12000	2.11790	3.66848	0.94706	0.98310
81.25000	2.11749	3.66848	0.94646	0.98290
81.38000	2.11709	3.66848	0.94586	0.98270
81.51000	2.11668	3.66848	0.94526	0.98250
81.64000	2.11628	3.66848	0.94466	0.98231
81.77000	2.11587	3.66848	0.94406	0.98211
81.90000	2.11547	3.66848	0.94346	0.98191

82.03000	2.11506	3.66848	0.94287	0.98171
82.16000	2.11466	3.66848	0.94227	0.98151
82.29000	2.11426	3.66848	0.94168	0.98132
82.42000	2.11385	3.66848	0.94108	0.98112
82.55000	2.11345	3.66848	0.94049	0.98092
82.68000	2.11305	3.66848	0.93990	0.98072
82.81000	2.11264	3.66848	0.93931	0.98052
82.94000	2.11224	3.66848	0.93872	0.98033
83.07000	2.11184	3.66848	0.93813	0.98013
83.20000	2.11144	3.66848	0.93754	0.97993
83.33000	2.11104	3.66848	0.93695	0.97974

X POSITION	TEMPERATURE	DENSITY	VELCTY
70.33000	566.73742	0.0005429	2512.23525
70.46000	566.84692	0.0005428	2511.97339
70.59000	566.95635	0.0005427	2511.71165
70.72000	567.06571	0.0005426	2511.45004
70.85000	567.17502	0.0005425	2511.18856
70.98000	567.28426	0.0005424	2510.92720
71.11000	567.39343	0.0005423	2510.66596
71.24000	567.50255	0.0005422	2510.40485
71.37000	567.61159	0.0005421	2510.14387
71.50000	567.72058	0.0005420	2509.88301
71.63000	567.82950	0.0005419	2509.62227
71.76000	567.93836	0.0005418	2509.36166
71.89000	568.04716	0.0005417	2509.10117
72.02000	568.15589	0.0005416	2508.84081
72.15000	568.26456	0.0005415	2508.58057
72.28000	568.37317	0.0005414	2508.32045
72.41000	568.48171	0.0005413	2508.06046
72.54000	568.59019	0.0005412	2507.80059
72.67000	568.69861	0.0005411	2507.54084
72.80000	568.80697	0.0005410	2507.28122
72.93000	568.91526	0.0005409	2507.02172
73.06000	569.02349	0.0005408	2506.76234
73.19000	569.13166	0.0005407	2506.50309
73.32000	569.23977	0.0005406	2506.24395
73.45000	569.34781	0.0005404	2505.98495
73.58000	569.45579	0.0005403	2505.72606
73.71000	569.56371	0.0005402	2505.46730
73.84000	569.67157	0.0005401	2505.20866
73.97000	569.77936	0.0005400	2504.95014
74.10000	569.88710	0.0005399	2504.69174
74.23000	569.99477	0.0005398	2504.43347
74.36000	570.10237	0.0005397	2504.17531
74.49000	570.20992	0.0005396	2503.91728
74.62000	570.31741	0.0005395	2503.65937
74.75000	570.42483	0.0005394	2503.40158
74.88000	570.53219	0.0005393	2503.14392
75.01000	570.63949	0.0005392	2502.88637
75.14000	570.74673	0.0005391	2502.62895
75.27000	570.85391	0.0005390	2502.37165
75.40000	570.96102	0.0005389	2502.11447
75.53000	571.06808	0.0005388	2501.85740
75.66000	571.17507	0.0005387	2501.60047
75.79000	571.28200	0.0005386	2501.34365
75.92000	571.38887	0.0005385	2501.08695
76.05000	571.49568	0.0005384	2500.83037
76.18000	571.60243	0.0005383	2500.57391

76.31000	571.70912	0.0005382	2500.31757
76.44000	571.81575	0.0005381	2500.06136
76.57000	571.92231	0.0005380	2499.80526
76.70000	572.02882	0.0005379	2499.54928
76.83000	572.13526	0.0005378	2499.29342
76.96000	572.24165	0.0005377	2499.03768
77.09000	572.34797	0.0005376	2498.78207
77.22000	572.45423	0.0005375	2498.52657
77.35000	572.56043	0.0005374	2498.27119
77.48000	572.66657	0.0005373	2498.01593
77.61000	572.77266	0.0005372	2497.76079
77.74000	572.87868	0.0005371	2497.50576
77.87000	572.98464	0.0005370	2497.25086
78.00000	573.09054	0.0005369	2496.99608
78.13000	573.19638	0.0005368	2496.74141
78.26000	573.30216	0.0005367	2496.48686
78.39000	573.40788	0.0005366	2496.23243
78.52000	573.51354	0.0005365	2495.97812
78.65000	573.61914	0.0005364	2495.72393
78.78000	573.72468	0.0005363	2495.46986
78.91000	573.83016	0.0005362	2495.21590
79.04000	573.93558	0.0005361	2494.96206
79.17000	574.04094	0.0005360	2494.70834
79.30000	574.14624	0.0005359	2494.45474
79.43000	574.25149	0.0005358	2494.20125
79.56000	574.35667	0.0005357	2493.94789
79.69000	574.46179	0.0005356	2493.69464
79.82000	574.56686	0.0005355	2493.44151
79.95000	574.67186	0.0005354	2493.18849
80.08000	574.77680	0.0005353	2492.93559
80.21000	574.88169	0.0005352	2492.68281
80.34000	574.98652	0.0005351	2492.43015
80.47000	575.09129	0.0005351	2492.17760
80.60000	575.19600	0.0005350	2491.92517
80.73000	575.30065	0.0005349	2491.67285
80.86000	575.40524	0.0005348	2491.42065
80.99000	575.50977	0.0005347	2491.16857
81.12000	575.61424	0.0005346	2490.91661
81.25000	575.71866	0.0005345	2490.66476
81.38000	575.82301	0.0005344	2490.41303
81.51000	575.92731	0.0005343	2490.16141
81.64000	576.03155	0.0005342	2489.90991
81.77000	576.13573	0.0005341	2489.65852
81.90000	576.23985	0.0005340	2489.40725
82.03000	576.34392	0.0005339	2489.15610
82.16000	576.44792	0.0005338	2488.90506
82.29000	576.55187	0.0005337	2488.65413
82.42000	576.65576	0.0005336	2488.40333
82.55000	576.75959	0.0005335	2488.15263
82.68000	576.86336	0.0005334	2487.90205
82.81000	576.96707	0.0005333	2487.65159
82.94000	577.07073	0.0005332	2487.40124
83.07000	577.17433	0.0005331	2487.15101
83.20000	577.27787	0.0005330	2486.90089
83.33000	577.38135	0.0005329	2486.65088

PRESSURE ERROR= 0.15710323234016361 3E-08

STREAM-WISE PROFILE POSITION= 83.3299999999999983
LOCAL BOUNDARY LAYER THICKNESS 0.632831400788493870
EXPONENT FOR POWER LAW= 7.00000000000000000

Y POSITION	VELOCITY	TEMPERATURE	DENSITY	MACH NUMBER
0.00000	0.00000	1091.99796	0.0002818	0.00000
0.03164	1637.56624	868.81968	0.0003542	1.13330
0.06328	1808.01971	819.94059	0.0003753	1.28802
0.09492	1915.83920	786.52535	0.0003912	1.39353
0.12657	1996.21561	760.35632	0.0004047	1.47676
0.15821	2060.87540	738.52383	0.0004166	1.54697
0.18985	2115.25797	719.62268	0.0004276	1.60851
0.22149	2162.35586	702.85561	0.0004378	1.66382
0.25313	2204.00072	687.72227	0.0004474	1.71442
0.28477	2241.39932	673.88596	0.0004566	1.76132
0.31642	2275.39091	661.10817	0.0004654	1.80523
0.34806	2306.58392	649.21318	0.0004740	1.84666
0.37970	2335.43415	638.06741	0.0004822	1.88602
0.41134	2362.29234	627.56670	0.0004903	1.92360
0.44298	2387.43443	617.62812	0.0004982	1.95966
0.47462	2411.08163	608.18445	0.0005059	1.99437
0.50627	2433.41408	599.18037	0.0005135	2.02791
0.53791	2454.58058	590.56976	0.0005210	2.06041
0.56955	2474.70548	582.31372	0.0005284	2.09198
0.60119	2493.89384	574.37910	0.0005357	2.12271
0.63283	2512.23525	566.73742	0.0005429	2.15269

LOCAL PROFILE COMPUTATION COMPLETE

AVERAGE CONDITIONS IN SPECIFIED INTERVAL
YMAX= 1.50000000000000000
YMIN= 0.699999999999999997
UAVE= 2512.23524627695571
RHOAVE= 0.5429378738732556 68E-03
TAVE= 566.737423916152068
MACHAVE= 2.15268974490326559
RMDOT (LBM/S/FT)= 35.1363188761237453

SOLUTION COMPLETED

REFERENCES

1. Plencner, R.M.; and C.A. Snyder: The Navy/NASA Engine Program (NNEP89)—A User's Manual. NASA TM–105186, 1991.

2. Anderson, J.D.: Modern Compressible Flow. McGraw-Hill, NY, 1982, p. 466.

3. White, F.M.: *Viscous Fluid Flow*. McGraw-Hill, NY, 1974, p. 725.

4. Schlichting, H.: *Boundary Layer Theory*. McGraw-Hill, NY 1968, p. 747.

Van Driest, E.R.: Turbulent Boundary Layer in Compressible Fluids. J. Aeron. Sci., Vol. 18, 1951, p. 104.

Van Driest, E.R.: Turbulent Boundary Layer on a Cone in a Supersonic Flow at Zero Angle of Attack. J. Aeron. Sci., Vol. 19, 1952, p. 55.

De Chant, L.J.; and Tattar, M.J.: An Analytical Skin Friction and Heat Transfer Formula for Compressible, Internal Flows. NASA CR–191185, 1993.

Shapiro, A.H.: *The Dynamics and Thermodynamics of Compressible Fluid Flow Vol. I.* Ronald Publishing Co., NY, 1953, p. 647.

Young, F.M.: Generalized One-Dimensional, Steady, Compressible Flow. Unpublished, 1992.

Ferziger, J.H.: *Numerical Methods for Engineering Application*. Wiley, NY, 1981, p. 270.

Seddon, J.; and Goldsmith, E.L.: *Intake Aerodynamics*. AIAA, NY, 1985, p. 442.

Liepmann, H.W.; and Roshko, A.: *Elements of Gas Dynamics*. Wiley, NY 1957, p. 439.

Barnhart, P.J.: A Preliminary Design Study of Supersonic Through-Flow Fan Inlets. NASA CR–18224, 1988.

Harloff, G.J.: Personal Communication, 1991.

Crawford, M.E.; and Kays, W.M.: *STAN5—A program for Numerical Computation of Two-Dimensional Internal/External Boundary Layer Flows*. NASA CR–2742, 1976.

Boyce, W.E.; and DiPrima, R.C.: *Elementary Differential Equations and Boundary Value Problems*. Wiley, NY, 1965, p. 582.

Townsend, A.A.: Equilibrium Layers and Wall Turbulence. J. Fluid Mech., Vol. 11, 1961, p. 97.

Spalding, D.B.: Heat Transfer from Turbulent Separated Flows. J. Fluid Mech., Vol. 27, Part I, 1967, pp. 97–109.

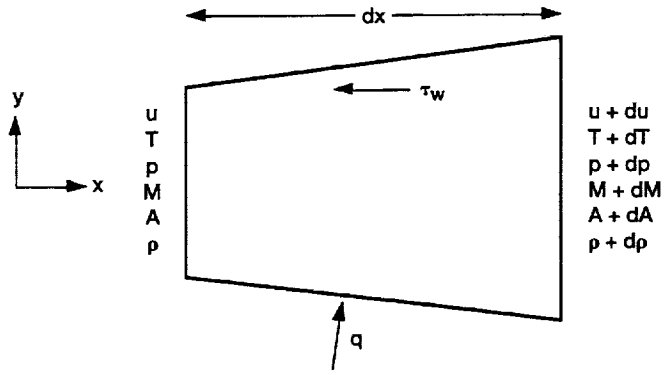

Figure 1.—Quasi-one-dimensional flow field.

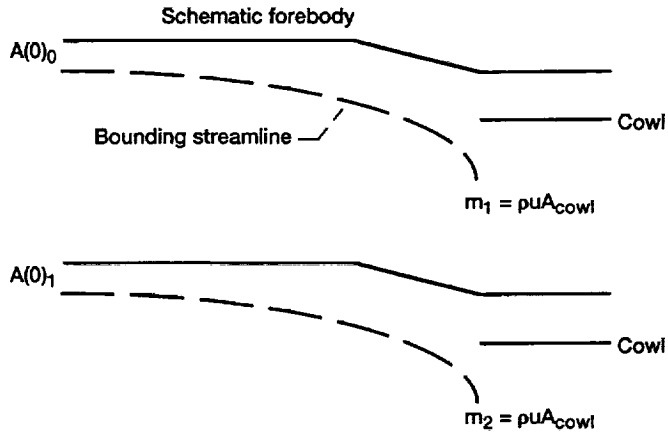

Figure 3.—Capture streamtube iteration process.

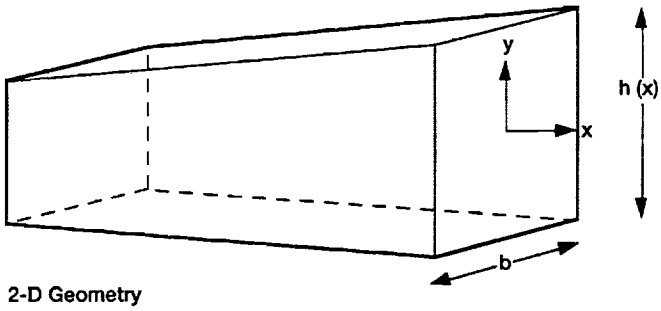

2-D Geometry

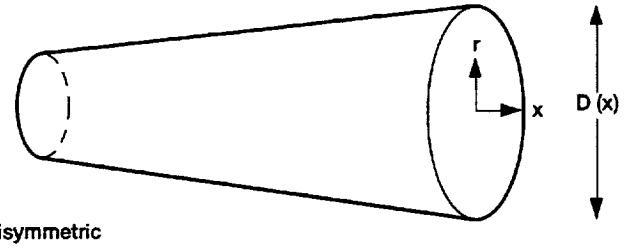

Axisymmetric

Figure 2.—Basic geometry definitions.

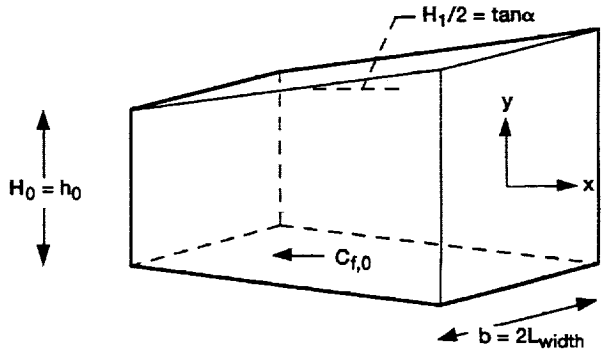

Figure 4.—Variable area duct with friction-flow geometry.

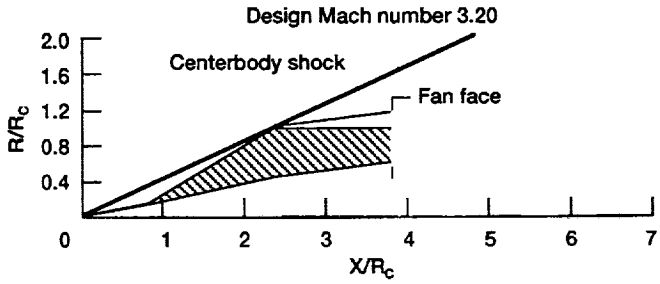

Figure 5.—Supersonic through-flow fan axisymmetric inlet (from Barnhart, 1988).

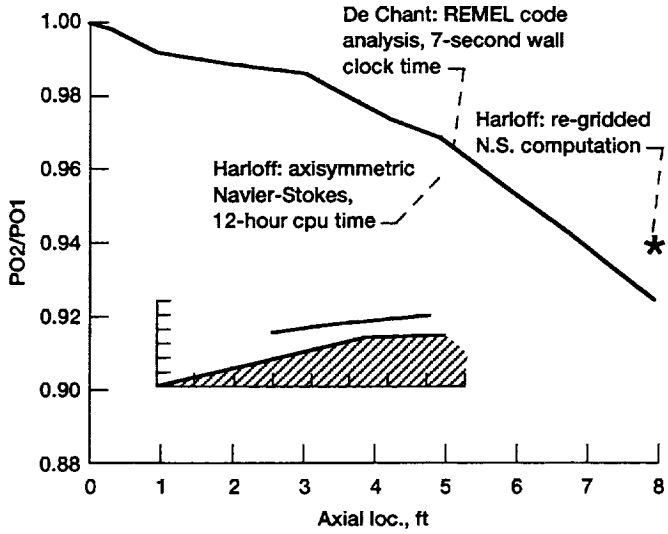

Figure 6.—Supersonic through-flow fan inlet REMEL code versus Navier-Stokes analysis (computational fluid dynamics).

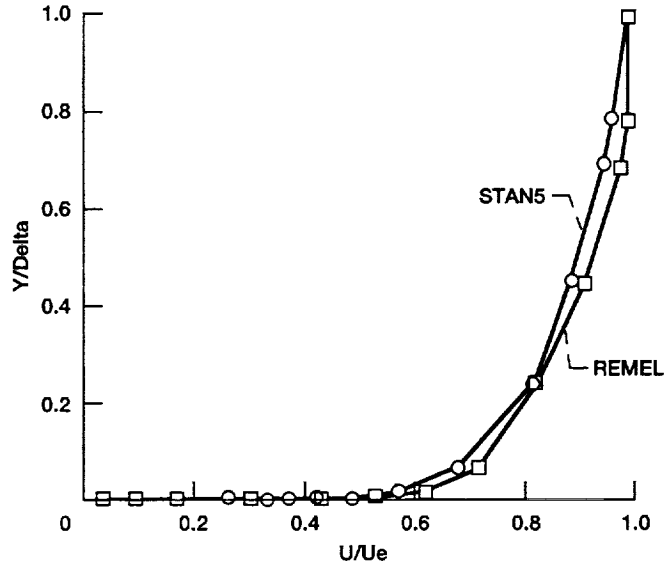

Figure 7.—REMEL code STAN5 (computational fluid dynamics boundary layer) comparison external forebody (flat plate).

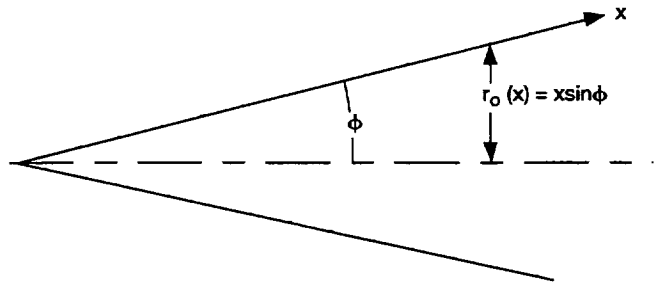

Figure 8.—Conical flow geometry.

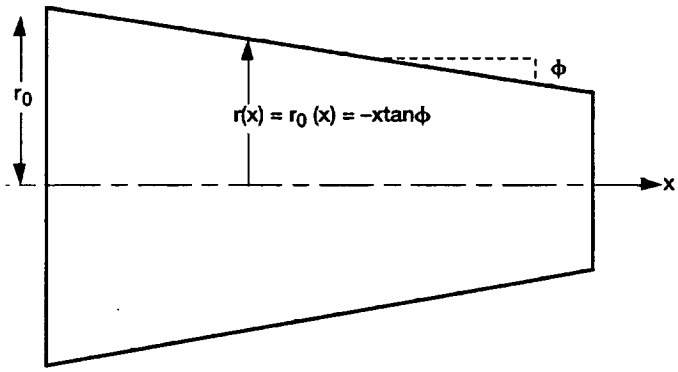

Figure 9.—Conical aft body geometry.

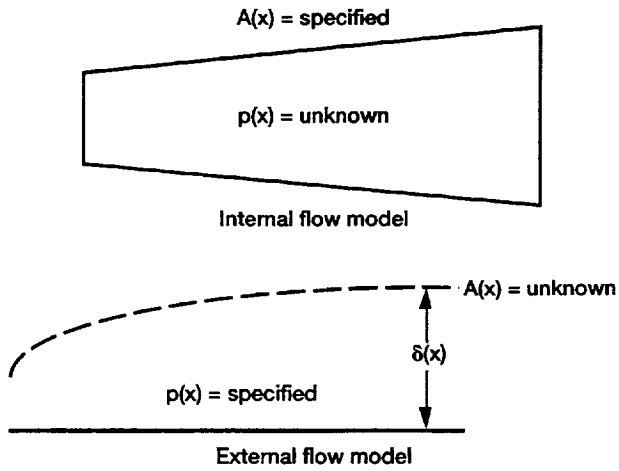

Figure 10.—Internal versus external flow modeling.

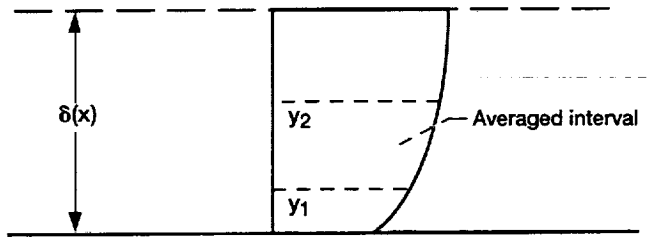

Figure 11.—External flowfield averaging.

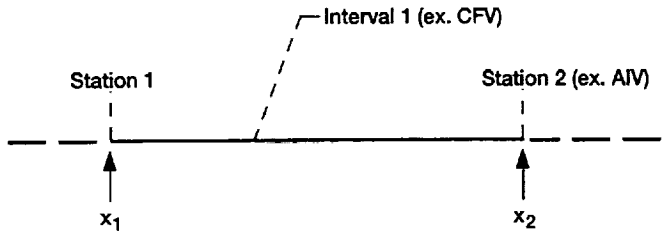

Figure 12.—Station/interval definitions.

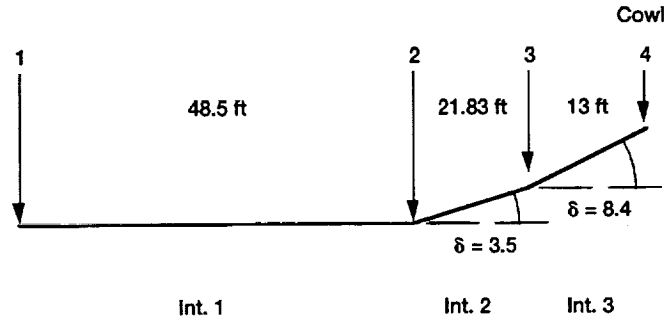

Figure 13.—Multiple ramp, external, two-dimensional forebody.

REPORT DOCUMENTATION PAGE

Form Approved
OMB No. 0704-0188

1. AGENCY USE ONLY (Leave blank)	2. REPORT DATE	3. REPORT TYPE AND DATES COVERED
	November 1994	Final Contractor Report

4. TITLE AND SUBTITLE

An Analysis Code for the Rapid Engineering Estimation of Momentum and Energy Losses (REMEL)

5. FUNDING NUMBERS

WU-505-69-50
C-NAS3-25266

6. AUTHOR(S)

Lawrence J. De Chant

7. PERFORMING ORGANIZATION NAME(S) AND ADDRESS(ES)

Sverdrup Technology, Inc.
Lewis Research Center Group
2001 Aerospace Parkway
Brook Park, Ohio 44142

8. PERFORMING ORGANIZATION REPORT NUMBER

E-8079

9. SPONSORING/MONITORING AGENCY NAME(S) AND ADDRESS(ES)

National Aeronautics and Space Administration
Lewis Research Center
Cleveland, Ohio 44135-3191

10. SPONSORING/MONITORING AGENCY REPORT NUMBER

NASA CR-191178

11. SUPPLEMENTARY NOTES

Lawrence J. De Chant, Sverdrup Technology, Inc., Lewis Research Center Group, Brook Park, Ohio (work funded by NASA Contract NAS3-25266), presently at NYMA, Inc., Engineering Services Division, 2001 Aerospace Parkway, Brook Park, Ohio 44142. Project Manager, John K. Lytle, Aeropropulsion Analysis Office, NASA Lewis Research Center, organization code 2410, (216) 977-7019.

12a. DISTRIBUTION/AVAILABILITY STATEMENT

Unclassified - Unlimited
Subject Category 02

12b. DISTRIBUTION CODE

13. ABSTRACT *(Maximum 200 words)*

Nonideal behavior has traditionally been modeled by defining efficiency (a comparison between actual and isentropic processes), and subsequent specification by empirical or heuristic methods. With the increasing complexity of aeropropulsion system designs, the reliability of these more traditional methods is uncertain. Computational fluid dynamics (CFD) and experimental methods can provide this information but are expensive in terms of human resources, cost, and time. This report discusses an alternative to empirical and CFD methods by applying classical analytical techniques and a simplified flow model to provide rapid engineering estimates of these losses based on steady, quasi-one-dimensional governing equations including viscous and heat transfer terms (estimated by Reynold's analogy). A preliminary verification of REMEL has been compared with full Navier-Stokes (FNS) and CFD boundary layer computations for several high-speed inlet and forebody designs. Current methods compare quite well with more complex method results and solutions compare very well with simple degenerate and asymptotic results such as Fanno flow, isentropic variable area flow, and a newly developed, combined variable area duct with friction flow solution. These solution comparisons may offer an alternative to transitional and CFD-intense methods for the rapid estimation of viscous and heat transfer losses in aeropropulsion systems.

14. SUBJECT TERMS

Inlet recovery prediction; Viscous losses; Heat transfer losses

15. NUMBER OF PAGES

86

16. PRICE CODE

A05

17. SECURITY CLASSIFICATION OF REPORT	18. SECURITY CLASSIFICATION OF THIS PAGE	19. SECURITY CLASSIFICATION OF ABSTRACT	20. LIMITATION OF ABSTRACT
Unclassified	Unclassified	Unclassified	

National Aeronautics and
Space Administration
Lewis Research Center
21000 Brookpark Rd.
Cleveland, OH 44135-3191